Decomposed Linear Dynamical Systems (dLDS) models reveal instantaneous, context-dependent dynamic connectivity in *C. elegans*

Eva Yezerets EYEZERE1@JHU.EDU
Department of Biomedical Engineering
Center for Imaging Science
Johns Hopkins University
Baltimore, MD 21218.

Noga Mudrik NMUDRIK1@JHU.EDU
Department of Biomedical Engineering
Center for Imaging Science
Johns Hopkins University
Baltimore, MD 21218.

Adam S. Charles ADAMSC@JHU.EDU
Department of Biomedical Engineering
Center for Imaging Science
Mathematical Institute for Data Science
Kavli NDI
Johns Hopkins University
Baltimore, MD 21218.

Abstract

Mounting empirical evidence indicates that neural "tuning" can be highly variable within an individual across time and especially across individuals. Furthermore, modulatory effects can change the *relationship* between neurons in the brain as a function of behavioral or other conditions, meaning that the changes in activity (the derivative) may be as important as the activity itself. However, current computational models fail to capture the nonstationarity and variability of neural coding, preventing the quantitative evaluation of these effects, especially during individuals' adaptation to their environments. Here we present a novel way to study the effects of adaptation in one of the most well-studied organisms, *C. elegans*, leveraging recent advances in dynamical systems modeling, specifically decomposed Linear Dynamical Systems (dLDS).Our approach enables the discovery of multiple parallel neural processes on different timescales using a low-dimensional set of linear operators that can be recombined in different ratios. Our model identifies "dynamic connectivity," describing patterns of dynamic neural interactions in time. We use these patterns to identify instantaneous, contextually-dependent, hierarchical roles of neurons; discover the underlying variability of neural representations even under seemingly discrete behaviors; and learn a single aligned latent space underlying multiple individual worms' activity. By analyzing individual worms and neurons, we found evidence that 1) changes in interneuron connectivity mediate efficient task-switching and 2) changes in sensory neuron connectivity show a mechanism of adaptation.

1. Introduction

Neural systems must continuously adapt to the ever-changing and multifacted environments that animals navigate. Such modulation of activity has been observed across species and occurs on timescales from milliseconds to minutes. Understanding how systems modulate their internal dynamics to adapt their computation and match novel experiences is thus critical in learning how the brain flexibly and robustly drives behaviors. However, models of time-varying activity-based population-level interactions remain limited, in part due to the complexity of estimating ever-changing interaction terms in large-scale data [1; 2]. *C. elegans*, whose small size and transparency have enabled scientists to capture its "whole-brain" activity and create a wealth of literature on individual neurons' functions, thus offers a unique opportunity to study the modulation of neural coding.

Using only 302 neurons, *C. elegans* can pirouette, navigate mazes, adapt to stimuli, and even learn associations [1; 3; 4; 5; 6]. These sensorimotor and cognitive processes all occur in parallel with other homeostatic functions. *C. elegans* is also an incredibly well-mapped organism. The anatomical connectome and proposed functions for almost all of its 302 neurons are available [7; 8; 9; 10; 11]. While the time-averaged neural activity required to execute its complex repertoire of behaviors appears as a stable connectome, the anatomical scaffold alone is insufficient to understand the mechanisms that *C. elegans* implements. Analysis over time within one animal [12] or between animals [12; 13; 14] reveals variability in *C. elegans* population neural coding. This is not noise; this variability is *required* for adaptation and reflects worm individuality in behavioral tendencies.

Recent work has revealed that the diversity of signaling mechanisms and timescales in *C. elegans* may be the reason why the stationary, i.e., time-averaged, anatomical connectome doesn't tell the full story. Randi *et al.* 2023 [11] showed a number of discrepancies between the functional connections recorded from pairs of neurons and the activity predicted based on the anatomical path lengths between them [11]. Moreover, the connectome of long-distance chemical messengers (e.g., neuropeptides) is being mapped [15; 16], and its concordance with the anatomical connectome appears limited, or at least complex [1; 17]. For one, *C. elegans* neurons can communicate both with and without traditional action potentials—consider the nociceptor ASH, which can generate graded responses to stimuli. Action potentials in the traditional sense are not required for signaling from ASH to AVA, a key interneuron [18]. Instead, synaptic communication is predominantly based on graded potentials. For another, pairs of cells can communicate with each other on multiple timescales, from milliseconds across gap junctions, to seconds for action potentials, to minutes across gap junctions again, with neuromodulators concurrently playing a role on the timescale of seconds to minutes. For example, these overlapping timescales of signaling are present in the defecation-related pacemaker signal [19; 20].

It is particularly difficult to map function onto the *C. elegans* anatomical connectome because direct, synaptic signaling and long-distance chemical messengers may operate on similar timescales to each other in this species [11]. Therefore, either a multi-hop connection directly across neurons or a neuropeptide could reasonably implement a seconds-long functional response that is relevant to a seconds-timescale behavior. Moreover, multiple processes happen on overlapping timescales in *C. elegans*, including homeostatic processes such as managing energy levels and attention [21], and even its most clearly annotated neural pathways are used in slightly different ratios throughout behavioral motifs [22]. All of these factors contribute to the challenge of determining each neuron's function in *C. elegans*, even if those functions *were* stable and universal across worms and conditions.

However, *C. elegans* also generates *nonstationary* cognitive processes and behaviors. In fact, Atanas *et al.* 2023 [23] showed that 20 to 30% of *C. elegans* neurons changed their behavior encodings between the first and second halves of a single recording period, either via gain modulation, changes in tuning, or simply changing which behaviors they encoded. These encodings are also known to be context-dependent, e.g., the AIA neuron's sensory-context-dependent role in roaming vs. dwelling behavior depending on food in the environment [24]; BAG's behavioral-context-dependent role in self-produced (reafferent) oxygen sensing [25]; RIM's context-dependent role in mechanosensation

during turns vs. other behaviors [26]; AWC's context-dependent role in deciding whether the worm will be attracted to an odor, or will avoid it [27]; and context-dependent differences in nervous system-wide sensory-interneuron-motor interactions during male-hermaphrodite *C. elegans* mating [28]. The mechanisms governing these internal neural states seem to be largely neuromodulatory [29], as opposed to purely synaptic, thus requiring neural population-level analysis. In particular, the context-dependent roles of interneurons are especially difficult to pin down — existing models do not have the granularity to describe their complex and changing roles in neural encoding.

Moreover, the species has demonstrated associative and non-associative learning (e.g., habituation, sensitization) [30; 31] via chemosensation, mechanosensation, and proprioception, with short-term memory shown to persist over minutes [4] and long-term memory over hours [6] to up to a day [32; 33; 34]. Because learning can occur over the course of a minutes-long trial in this species, stationary functional connectomes averaged across trials are meaningful for understanding the general functions of certain networks of neurons, but they are insufficient for understanding how neurons create behavioral changes over the seconds-to-minutes timescale.

Finally, even without nonstationarity, behaviors that appear stereotyped are not completely so; each worm's neural dynamics are unique [13; 14]. For example, some worms simply tend to roam more than other worms do [13], and worms can also develop these differences throughout development [12].

To address these gaps in mechanistic understanding, multiple groups have characterized aspects of *C. elegans*' stationary functional connectome [11; 15]. For example, recent work has described functional connectivity modes via principal component analysis (PCA) [23], and has used topologically motivated analyses [35] to conclude that the redundancy and flexibility of *C. elegans* neural circuitry means that only perturbing certain hub neurons has a significant impact on function. Moreover, another recent PCA-based linear time-invariant low-dimensional manifold model of *C. elegans* [36] showed that behavior-related brain states have wide-reaching effects across the *C. elegans* nervous system, creating global brain states that hierarchically gate neuron activity and allow for distributed coding. These examples show the mechanistic insights about *C. elegans* neural coding that can be derived time-averaged models.

However, to track *time-varying* relationships between cognitive states or processes both within and across individuals, we need dynamical systems models. Such models reinterpret high-dimensional time series data, such as neural population activity, as noisy manifestations of underlying, lower-dimensional processes that evolve within certain constraints in the state space, e.g., on a manifold. The manifold can be shared across individuals, representing a common functional landscape of cognitive processes. The evolution between latent states can be described by trajectories, i.e., dynamics. With such a model, it is possible to represent latent functional states at each time point and map those back to the neural activity patterns for each subject to examine dynamic connectivity.

To date, time-varying models of *C. elegans* neural dynamics have primarily employed switching linear dynamical systems (SLDS) [37; 38; 39]. Such models assign a single, discrete state to each time point or time window, but the states are nonstationary, unlike in dynamic mode decomposition, for example [40]. SLDS models are locally linear and hierarchical, with continuous latent states being controlled by discrete overall neural population states. These have shown strong concordance between model-inferred neural states and experimentally-labelled behavioral states. However, such models are limited by the assumption that the entire neural population is experiencing the same overall state, and that these overall states transition abruptly from one to the other.

A non-switching, nonlinear model of *C. elegans* also found whole-worm neural dynamics reflecting two primary behavior states, forward and reverse crawling, as two loops on a low-dimensional manifold [14]. This model successfully predicts neural activity and behavior across individuals. However, the authors acknowledged that the worms had a high degree of individuality, both in terms of which neurons were identified in each recording and in terms of their behavior and utilization of neurons to execute similar behaviors. Because the gross behaviors could be decoded from almost any individual neuron with some fidelity, it was possible to build a shared dynamics model across worms. Moreover, this model is nonlinear, which makes its components and their interactions

less interpretable than a linear model. Thus, there remains a need for linear models that do not abstract away from worm individuality in order to help researchers understand the mechanisms of how individual worms adjust their neural activity and connectivity in order to adapt to their environments, or even to learn.

Not all dynamical systems models capture time-varying dynamics. A linear time-invariant model [41] demonstrated the value of anatomical-connectome-constrained models in recapitulating the expected effects of optogenetically stimulating one neuron at a time and recording from other neurons. This paper claimed that while multi-hop, indirect, extrasynaptic connections do exist in the worm, the effects of single neurons on the system are well-modeled using what we know about *C. elegans* synaptic connections. However, this paper's definitions of function, causality, and anatomical connectivity are time-averaged. While interpretable due to linearity and the anatomical-connectome-based restrictions on the weights, these constraints prevent the model from accounting for adaptation and learning, which also relies on extrasynaptic signaling.

We address these gaps in available modeling frameworks with our recently developed decomposed linear dynamical systems (dLDS) model (Fig. 1; more details in Section 2.1 and Methods Section 6.1). dLDS allows for locally linear, nonstationary dynamics that can be active simultaneously in different continuous ratios, and that can transition continuously without such hierarchical state constraints [42]. The coefficients that describe the time-varying utilization of these dynamics can show differences between instances of a behavior within a trial while still containing decodable information about behavior-related latent neural processes. The dynamics operators (DOs) themselves describe relationships between latent neural processes that can be mapped back to functional relationships between neurons. Furthermore, these operators can be linearly recombined in different ratios, as regulated by a set of coefficients that capture when different dynamics turn on and to what extent, enabling the modeling of gradual transitions in neural dynamic connectivity throughout behavior.

In addition, we present an across-worm aligned[1] extension of dLDS. Worms may not only exhibit individuality in their behavior and neural encodings of behavior and internal states, but also have slightly different recorded neurons, trial durations, experimental conditions, and frequencies, durations, and qualities of performed behaviors. In order to identify shared vs. individual mechanisms of neural signaling across worms, it is necessary to have a common framework or space of operators for comparing them.

Using dLDS models learned for individual *C. elegans* (per-worm) models and the across-worm aligned model extension we develop here, we discover the dynamic (i.e., nonstationary, anatomy-unconstrained functional) connectivity maps from learned DOs. These maps represent dynamic connections beyond anatomy or one-to-one direct stimulation-induced stationary functional connections and reveal key nonstationary properties of neurons in *C. elegans*. For one, the dynamic connectivity maps reveal how stereotyped discrete behavior has a neural basis that, while patterned, is also variable across repetitions of the same behavior and across individuals. We further show that our model's decomposition of the dynamics underlying these maps disentangles concurrent processes within a trial, such as adaptation to varying aversive oxygen levels while performing a repetitive behavior.

This variability in latent neural dynamics underlying discrete behavioral states can highlight functional networks related to latent neural processes that can be otherwise difficult to observe, isolate, and test. These difficulties arise because such circuits can be the result of internal processes separate from the measured behavior and environmental variables, or because they reflect those variables indirectly, e.g., in the form of intermediary computations bridging sensing and behavior. In other words, even when activity levels of a neuron look similar across behaviors, the dynamic connectivity of those neurons with the rest of the network differs, indicating new roles for neurons with and without known functions. We are thus able to characterize the dynamic roles of interneurons such as AVFR,

1. We use the term "aligned" in this paper to mean that the latent states are inferred across individuals such that they have shared relationships with each other, i.e., a shared set of dynamics operators. We do not refer to "alignment" in the machine learning sense of alignment to human values [43].

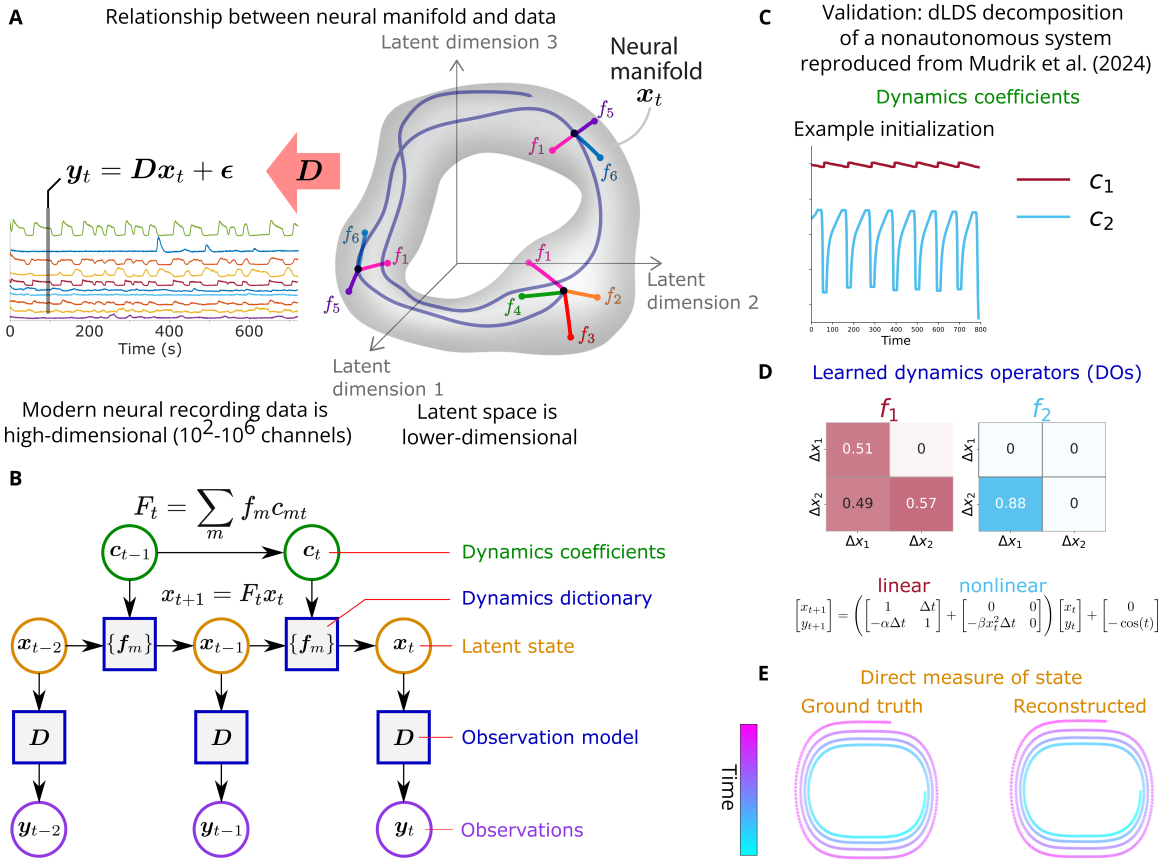

Figure 1: **Modeling latent manifolds from neuroimaging data.A:** Recorded neural activity $\boldsymbol{y}$ relates to latent neural states on the manifold $\boldsymbol{x}$ via observation model (matrix) $\boldsymbol{D}$. Neural dynamics (trajectories) on the manifold operate in the tangent space. These linear operators can be summed linearly. The manifold depicted here is an illustration; we do not constrain the model to a particular manifold, nor do we define a particular manifold in the process of learning the dLDS model. **B:** Graphical model depicting the relationships between data $\boldsymbol{y}$ and model parameters from time point to time point (dynamics coefficients $\boldsymbol{c}$, DO dictionary of matrices $\boldsymbol{f}$, latent states $\boldsymbol{x}$, and observation model $\boldsymbol{D}$). Dynamics coefficients $\boldsymbol{c}$ describe DO use over time. **C-E:** Example of a dLDS decomposition of a nonautonomous dynamical system - the Duffing oscillator, reproduced from [42]. dLDS can recover the activity of a simple nonautonomous system (**E**) using dynamics coefficients (**C**) dynamics operators (**D**) that represent its linear and nonlinear components.

RIS, and RIGL, which show evidence of different dynamic encodings when modulated strongly by sensory vs. motor information, as well as the sensory BAG neurons, the motor neuron RMED, and the interneuron/motor neuron SABD, which strongly reflect both behavior and stimulation state and the interactions between their levels. These results complement and extend the extensive study of stationary properties of neurons in *C. elegans*, bringing a new analysis of their nonstationary properties.

2. Results

2.1 dLDS model architecture

Our analysis builds on the recently developed decomposed linear dynamical systems (dLDS) formulation [42], which is a dynamical systems model whose learned parameters reflect latent, concurrent neural processes through a generative model. In dLDS, the observed neural fluorescence $\boldsymbol{y}_t$ at time t is modeled by latent states $\boldsymbol{x}_t$ through a linear generative model, i.e.,

$$\boldsymbol{y}_t = \boldsymbol{D}\boldsymbol{x}_t, \tag{1}$$

where $\boldsymbol{D}$ describes to what extent each latent dimension represents each recorded trace. Specifically, each column of $\boldsymbol{D}$ contains a consistantly co-active group of neurons representative of one latent dimension (a single entry of $\boldsymbol{x}_t$). In dLDS, we assume a constant latent state representation $\boldsymbol{D}$ for each individual worm. dLDS then models the brain dynamics as a dynamical system over the latent state $\boldsymbol{x}_t$.

Two key aspects drive the form of the dynamical systems model in dLDS: the need to capture concurrent processes, and the need to capture time-varying changes to the network interations. The former aims to model the fact that independent systems, such as sensory and motor networks, can be independently recruited. The latter aims to model adaptation via neuromodulation as an implicit change in the network behavior. To capture these effects, dLDS models the trajectory of the latent state as a time-varying linear dynamical system, i.e.,

$$\boldsymbol{x}_t = \boldsymbol{F}_t\boldsymbol{x}_{t-1}, \tag{2}$$

where the time varying linear system $\boldsymbol{F}_t$ is modeled as a linear combination of stereotyped interconnection patterns that drive the full dynamics. Specifically,

$$\boldsymbol{F}_t = \sum_{m=1}^{M} \boldsymbol{f}_m c_{mt}, \tag{3}$$

where the set of M dynamics operators $\{\boldsymbol{f}_m\}_{m=1,\ldots,M}$ are system properties (i.e., patterns of interconnection between neurons that are reused) and the coefficients c_{mt} represent when different interconnections drive the neural dynamics at each time t (i.e., when $c_{mt} \neq 0$) and how much influence they have. To induce greater interpretability and independence in terms of the use of different interconnectivity patterns over time, we further assume that the c_{mt} coefficients are mostly zero at each time-step, i.e., the temporally local dynamics are most heavily driven by only few connectivity patterns. We refer to the set of $\{\boldsymbol{f}_m\}_{m=1,\ldots,M}$ operators as dynamics operators (DOs) and $c_{mt} \neq 0$ as dynamics coefficients.

In other words, the vocabulary of the dLDS model consists of DOs, and the grammar that regulates how they work together to generate latent neural states consists of the dynamics coefficients. Then, we use $\boldsymbol{D}$ to translate from the language of latent states to the language of observable neural activity.

We fit the DOs in a data-driven way through an expectation maximization algorithm that approximates the Maximum Likelihood of the data given the DOs $\{\boldsymbol{f}_m\}_{m=1,\ldots,M}$ and the latent

state representation $\boldsymbol{D}$. The learning procedure strongly resembles an iterative dictionary learning optimization which iterates between updating estimates for the unknown variables $\boldsymbol{x}_t$ and $\boldsymbol{c}_t$, and updating the estimates for the model parameters $\{\boldsymbol{f}_m\}_{m=1,\ldots,M}$ and $\boldsymbol{D}$ (for more details, see Section 6.1). Experimental model reconstruction performance and parameters are explained in detail in Tables 1 and 2.

Validation: **dLDS characterizes the dynamics of nonautonomous dynamical systems:** To validate dLDS, we demonstrate its ability to capture nonlinear behavior on a simulated dynamical system modulated by an external driving force. Specifically, we tested dLDS on the Duffing oscillator, a classic example of a nonlinear, nonautonomous dynamical system. The Duffing oscillator is characterized by the second-order differential equation,

$$\dot{y} + \delta y + \alpha x + \beta x^3 = \gamma \cos(\omega t), \tag{4}$$

which generates a dynamical system that can be both damped and driven. In this version of the equation, $y = \dot{x}$, which leads to a discrete-time matrix version of the Duffing equation as

$$\begin{bmatrix} x_{t+1} \\ y_{t+1} \end{bmatrix} = \left(\begin{bmatrix} 1 & \Delta t \\ -\alpha \Delta t & 1 \end{bmatrix} + \begin{bmatrix} 0 & 0 \\ -\beta x_t^2 \Delta t & 0 \end{bmatrix} \right) \begin{bmatrix} x_t \\ y_t \end{bmatrix} + \begin{bmatrix} 0 \\ \gamma \cos(t) \end{bmatrix}. \tag{5}$$

Our prior work [42] demonstrated that, across initializations, dLDS can recover a Duffing oscillator's behavior and coefficients. Specifically, the dynamics operators learned by dLDS separated out the linear (DO 1) and nonlinear (DO 2) components of the discrete-time version of the Duffing equation (e.g., an example reproduced from [42] for $\gamma = -1$ is shown in Fig. 1) Thus, dLDS recovers a meaningful decomposition of this nonautonomous dynamical system. Additional demonstrations of dLDS on Lorenz attractors, Fitz Hugh Nagumo models, and other examples can be found in Mudrik *et al.* 2024 [42].

2.2 Assessment and validation of dLDS fits to *C. elegans* dynamics

We applied the dLDS model to *C. elegans* calcium imaging data from Kato *et al.* 2015 [3]. This dataset was collected from 12 worms (Table 3). Five of the worms experienced hyperoxia for 18 minutes (NoStim trials) to spontaneously elicit a pirouetting behavior, i.e., a sequence of forward crawling, turns, and reverse crawling. Seven of the worms were exposed to hyperoxia (21% oxygen) for the first half of the experiment, and alternating bouts of hypo- and hyperoxia (4% vs. 21% oxygen) for the second half in order to entrain the pirouettes to the oxygen levels (Stim trials). Approximately 100 calcium traces, imaged at 3 Hz, were identified from the imaging data per worm. Of these traces, only approximately 40 were labeled as originating from one or more known neurons, some with multiple neurons per trace and with some neurons appearing as labels for multiple traces. Moreover, once the protocol was established, the calcium imaging recordings were actually performed in immobilized worms.

Despite this limitation of immobilization [22], [3] also provided expert labels for the discrete fictive pirouetting behavioral states by inferring their behavior from the activity of key neurons. These were coarse-grained for the Stim experiments (1: 'FWD' forward crawling, 2: 'REV' reverse crawling, 3: 'REVSUS' sustained reverse crawling, 4: 'TURN' post reversal turn) and fine-grained for the NoStim experiments (1: 'FWD' forward crawling, 2: 'SLOW' forward slowing, 3: 'DT' dorsal post reversal turn, 4: 'VT' ventral post reversal turn, 5: 'REV1' reverse crawling, 6: 'REV2' reverse crawling, 7: 'REVSUS' sustained reverse crawling, 'NOSTATE' - ambiguous). We then applied dLDS to each individual worm's normalized (dF/F) traces.

We fit the dLDS model to each worm's neural activity, using 10 dynamical operators and 10 latent states (see Section 6.1). We first validate that dLDS learns meaningful representations of the *C. elegans* dynamics by comparing the temporal and spatial statistics to known properties.

We can make inferences about the features of systems that generate that neural activity, and therefore the behavior, using the interpretable locally-linear properties (i.e., that the dynamics at each

time point and the latent generative model are linear) of the dLDS model. All neurally-generated variables should be encoded in neural activity, representing a noisy version of discrete behavioral states. Therefore, the learned model parameters should reflect quantitative information such as speed of movement or modulation in response to sensory stimuli, as well as other background cognitive processes, e.g., hunger, wakefulness, etc. We thus test dLDS's capabilities to capture these simultaneously active neural processes and variables by characterizing the dynamics of *C. elegans* neural activity.

The dLDS DO coefficients $\boldsymbol{c}$ reflect the utilization of DOs to generate latent neural states. Qualitatively, we observed that, for each worm, the same coefficients appeared in similar patterns ("motifs") during the same *C. elegans* behaviors. These combinations of latent processes were discrete in that similar sets of DOs appeared every time. However, the DOs were also continuous because they appeared in slightly different ratios, which changed gradually over time or shifted in response to environmental variables such as stimulation protocols without switching completely. We also successfully decoded behavior states from the dynamics coefficients (see t-SNE and Isomap clustering by behavior states and linear discriminant analysis classification by behavior states in Figure 2, Supplementary Figures 1, 2, and 3).

To observe these behavior-related encodings in the DO coefficients $\boldsymbol{c}$ more quantitatively, we performed clustering analyses using t-distributed stochastic neighbor embedding (t-SNE) and Isomap, and classification vs. behavioral states using Support Vector Machine (SVM) models. Thus, from the dLDS DO utilization coefficients $\boldsymbol{c}$ and from their first derivative $\frac{d\boldsymbol{c}}{dt}$, it was possible to decode the behavioral state labels inferred by Kato *et al.* 2015 [3] (Fig. 2 - Stim Worm 1 and NoStim Worm 1 shown in detail; Isomap for $\boldsymbol{c}$ only for all others, Supplementary Figs. 1, 2, 3)[2]. By clustering and coloring by behavioral states, t-SNE appears to show a continuum from forward to backward crawling (DO coefficients' first derivative $\frac{d\boldsymbol{c}}{dt}$), while Isomap embedding reveals a ring-like structure from state to state (with additional loops) in the coefficients and a spoke-like structure in the first derivative. Via linear discriminant analysis, it is also possible to classify at least the two major behavioral states from the DO coefficients alone (Fig. 2 - Stim Worm 1 and NoStim Worm 1). The observations above were similar when decoding from the latent states $\boldsymbol{x}$. In Sections 2.3, 2.4, and 6.3 and Supplementary Figures 4, 5, 6, and 7, we also investigated the behavioral and environmental context-dependent differences in DO utilization and what the DOs mean in the neural space.

2.3 *Novel capabilities:* dLDS identifies instantaneous dynamic connectivity between neurons

Having found evidence that the DO coefficients reflect behaviorally-relevant, continuous patterns in the neural activity, we then set out to quantify how the DOs themselves affect the neural activity and connectivity. Given that dLDS DOs transition smoothly (e.g., Fig. 3, Supplementary Figs. 8, 9, 10, 11, 12, 13), it is important to understand which neurons corresponding to those DOs are active and correlated at each time point in order to interpret the gradual effects of these DOs. This is even more important because these smooth transitions might reflect gradual changes in neural activity during or between behavioral states or other time-varying factors, such as oxygen levels. We created dynamic connectivity maps that can tie latent states and dynamics operators back to the neural space by simulating the effects of any linear combination of DOs at any time point (or the effects when applied to an impulse function of latent states). The dynamic connectivity maps essentially capture the correlational structure of an equivalent linear time-invariant system with the dynamics coefficients c_{mt} frozen for all time (see Methods Section 6.4). By tracking how the dynamic connectivity maps change over time with the changes in c_{mt}, we can track the dynamic networks active across all the recorded neurons.

As described in Section 2.2, the results abounded with occurrences of repeated motifs of simultaneously active DOs (often corresponding to behavior states) that appeared similarly but in slightly

2. There is some bias due to the base rates of forward and reverse crawling vs. relatively short bouts of turning.

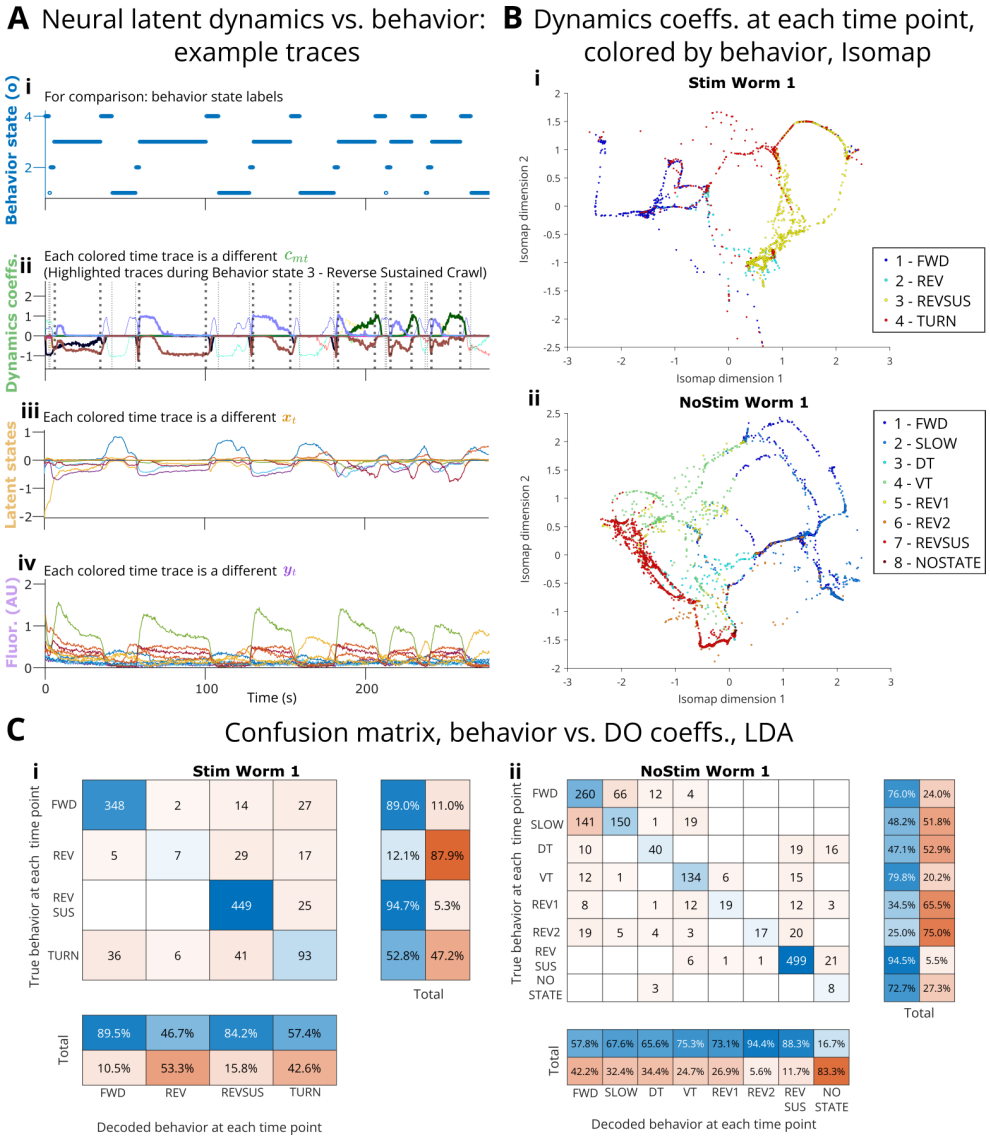

Figure 2: **Model coefficients vs. behavior. A:** Sample of time traces of behavior, dynamics (DO) coefficients, latent states, and fluorescence data. textbfB, C Behavior decoding from dynamics coefficients for Stim Worm 1 and NoStim Worm 1. Behavior labels: Stim 1 FWD forward crawling, 2 TURN post-reversal turn, 3 REV reverse crawling, 4 REVSUS sustained reverse crawling; NoStim 1 FWD forward crawling, 2 SLOW forward slowing, 3 DT dorsal post-reversal turn, 4 VT ventral post-reversal turn, 5 REV1 and 6 REV2 reverse crawling, 7 REVSUS reverse sustained crawling, 8 NOSTATE ambiguous. **B.i, B.ii:** Isomap finds a ring-like 2D embedding of the DO coefficients themselves, well clustered by behavior state (more examples in Supplementary Figs. 1, 2, 3). Each dot represents a time point in DO coefficient trace; see Section 6.1 and Table 3 for model parameter settings and counts. While biased toward the two behavior states with the highest base rates (1-FWD and 3-REVSUS in Stim, 1-FWD and 7-REVSUS in NoStim), linear discriminant analysis (LDA, **C.i, C.ii**) achieved high decoding performance on the DO coefficients.

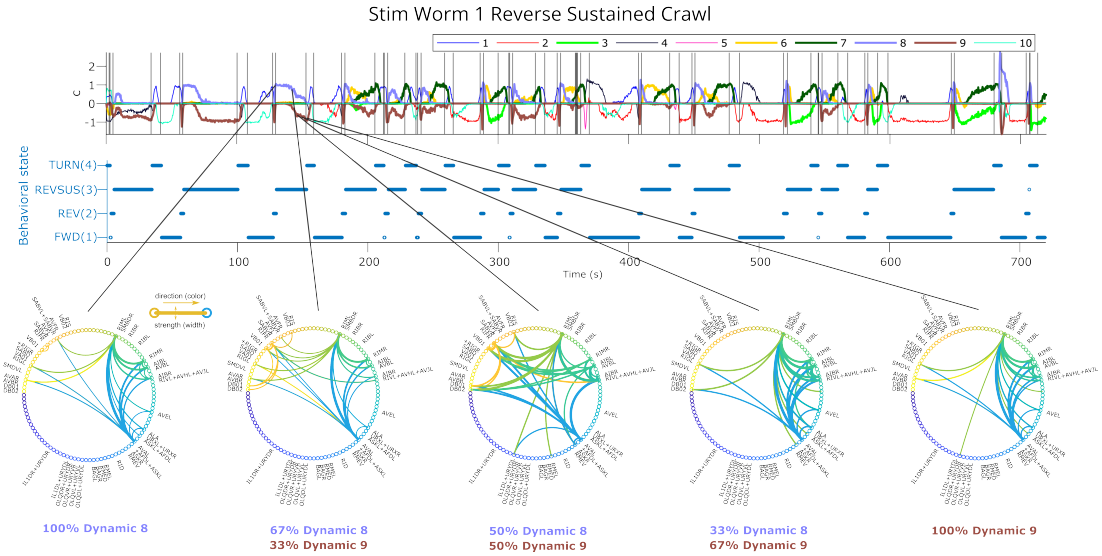

Figure 3: **Continuous transition between DOs during behavior.** DOs 8 and 9 in Stim Worm 1 are active during behavior state 3 (REVSUS). As DO 8 transitions to DO 9, connectivity between a core set of interneurons and the sensory neurons as well as motor neurons evolves in terms of which neurons are involved as well as in terms of strength and quantity. Here we show these two DOs linearly combined in different ratios, from 100% DO 8, to 67% DO 8 and 33% DO 9, all the way to 100% DO 9. We show the connection strengths (above a theshold) in the circle graphs in the right column, with a large percentage of neurons unlabelled.

different ratios at different times throughout the trial and also gradually evolved during the course of a behavior state. In Figure 3, we show a generative example of the effects of different ratios of two DOs in combination. These two DOs appeared in combination during reverse sustained crawling in Stim Worm 1, but did not merely turn on when the reverse sustained crawling behavior started and turn off when it ended — their dynamics coefficients increased and decreased in magnitude gradually throughout the behavior. We see a small, gradual transition in which neurons participate most strongly as we move from one operator to another — for example, the SABV neurons and RIFR, cholinergic motor/interneurons [44], become less connected and less active. This suggests that while most of the circuit participating in this behavior stays constant throughout the behavior, gradual changes at the neuron interaction level might also occur throughout the course of the behavior. Such continuous changes to the latent dynamics throughout behavior states are perhaps needed to generate preparation to change to the next behavior or other internal processes.

2.4 *Biological findings:* Dynamics learned from dLDS help identify dynamic roles for interneurons and connectivity adaptation for sensory neurons

In order to study how different classes of neurons (sensory, motor, and interneurons) use dynamic encoding to generate behavior in a changing environment, we used dLDS to reconstruct individual neurons' estimated activity and connectivity from time point to time point throughout the trial. Given the alternating hypoxia/hyperoxia oxygen stimulation protocol (second half of the Stim experiments), we investigated if and how some DO coefficients were different in the two halves of the Stim experiments, how the differently-utilized DOs might feature oxygen-sensing neurons in their corresponding dynamic connectivity maps, and how interneurons reflect behavior and stimulation.

We found that most of the neurons studied, in terms of activity and connectivity to and from the neuron, had a significant relationship with stimulation state, behavior state, and the interaction of the two. Thus, we observed that we could recover global behavior- or stimulation-related low-dimensional manifold states, similar to the global manifold gating effects reported by Fieseler *et al.* 2025 [36], i.e., there do appear to be some global brain states that strongly modulate the activity of a broad range of neurons. However, dLDS does not have to time-average across such brain states; we can observe instantaneous dynamics for each neuron and observe how its connectivity creates or responds to such brain states.

Digging deeper, each neuron class shows different patterns in the ways each uses its connectivity to fulfill its functions. First, connections to and from the oxygen-sensing BAG neurons (Fig. 4) were strongest during acute hypoxia and are fairly system-wide, which was to be expected given their known oxygen-sensing function. Importantly, these connections can adapt over time, using different neurons, not just less activity, as the worm habituates to hypoxia. Sensory neurons were also shown to be sensitive to motor information, which recent experimental work has shown is related to reafferent perception [25; 36].

In comparison, connections to and from the RMED motor neuron (Fig. 5) were more stable throughout the experiment. However, these connections were also correlated both with bouts of pirouetting and with hypoxia. In fact, there were qualitatively different patterns and strengths of RMED inputs ("connectivity to") depending on behavior state and hypoxia leading to RMED operating in two separate (positive vs. negative) regimes during most of the trial vs. during hypoxia. These context-dependent dynamics might even indicate a hierarchy between the standard pirouetting behavior and the hypoxia "alert" overriding it.

Finally, we show an example interneuron, AVFR, whose function is less clear from the literature — unsurprisingly, it is more difficult to classify interneurons' roles because they exist between sensory and motor neurons and seem to account for internal computation. While the noisy motor and interneurons were not as well-reconstructed as the BAG neurons, we saw a distinct pattern of behavior-dependent connectivity, interspersed with what seems to be an overriding hypoxia alert, as in the motor neuron. Importantly, the connectivity completely changed for short periods of time during hypoxia - the interneuron changed its connectivity, and thus its function, over time to relay information to different circuits, rather than always using the same mixed selectivity, irrespective of task variables. Thus, we can use dLDS dynamic connectivity to describe at each time step how even an interneuron's role in its circuits is evolving.

2.4.1 BAGL and BAGR neurons and their circuits

The BAG neurons are known to be involved in sensing increased carbon dioxide or decreased oxygen [44; 5; 45], making this pair of neurons a natural candidate for evaluating how sensory neurons can use their connectivity to adapt and habituate to changes in their environment. We put forward two possible hypotheses: all DOs might feature BAG relatively equally in order to make them all accommodate for the change in experimental conditions while creating the stereotyped behaviors, regardless of which half of the experiment they were in; or some DOs might feature BAG more strongly in a nonstationary way, possibly to account for hypoxia, separating out the underlying BAG-dependent circuits that are simultaneously active with the circuits that produce the stereotyped behaviors that persist throughout the experiment. This second hypothesis could not be explored with a switched linear dynamical system, where only one operator would represent each state at each time point.

What we found was even more nuanced and supports recent reports of the context-dependent function of BAG [25]. We observed that, while at the start of the alternating hypoxia/hyperoxia protocol (second half of the Stim experiments), there was a large spike in BAG activity, this was followed by smaller spikes. This led us to investigate whether the relationship between earlier and later BAG activity was merely a quantitative difference in *activity* of the same neurons, or whether

habituation, and changes to *connectivity*, were leading to different responses to hypoxia over time. Using instantaneous dynamic connectivity, we quantitatively showed evidence of the latter. When hypoxia starts (around 360 s), BAG connectivity was strong to a large range of sensory, motor, and interneurons. Later in the trial, when hypoxia occurred again, connections from BAG were still present, but some of this sensory role shifted from external sensing (from BAG) to internal sensing (e.g., proprioceptive/motor neurons VB and DB).

Furthermore, based on the proportions of connectivity maps that most strongly featured the BAG neurons across the Stim worms, we found evidence that the BAG-featuring DOs were used in a nonstationary way throughout the experiments, potentially in relation to the alternating hypoxia/hyperoxia levels (Section 6.5, Table 4, Supplementary Figs. 14, 15, 16, 17, 18, 19, 20, 21, 22, 23, 24, 25, 26, 27, 28, 29, 30). We also observed that BAG-featuring DOs were only up to approximately half of the DOs active during the two major behavioral states (forward crawling and reverse sustained crawling), potentially with context-dependent bias toward one or the other major behavioral state. This indicates that there might be multiple interrelated but distinct circuits, some of which are BAG-related and some of which are more specific to generating the behaviors, that are active simultaneously, and that dLDS can separate them.

These results were supported by χ^2, ANOVA, and MANOVA tests (Sections 5, 6, 7) on the reconstructed activity and connectivity, in a hierarchical way: at a low threshold for "active" or "connected", the BAG neurons were more significantly influenced by behavior states, but at a high threshold, the stimulation protocol's effects on their activity and connectivity were significant, which aligns with the visual patterns in Figure 4 and Supplementary Figure 31.

2.4.2 RMED neuron

For comparison, we identified another forward crawling-biased neuron, RMED, a motor neuron with limited function documentation in the WormAtlas [44]. [46] proposed that the RME neurons regulate the amplitude of head-bending during locomotion. RMED-featuring DOs also showed some nonstationarity but were generally utilized in a more balanced way between halves of the experiment than the BAG neurons (Section 6.8, Table 8, Supplementary Figs. 14, 15, 16, 17, 18, 19, 20, 21, 22, 23, 24, 25, 26, 27, 28, 29, 30).

To further complicate the story, the χ^2 tests of RMED only showed significant relationships between the connectivity to and from RMED and stimulation state or behavior, even though these are clear visually (Fig. 5 - Stim Worm 1 as an example), but they did show a consistently significant relationship between RMED reconstructed activity and both stimulation and behavior. As with BAGL and BAGR, the ANOVA results showed significant effects of behavior and usually significant effects of the stimulation setting. A possible mechanistic interpretation of the significant stimulation effects is that RMED appears to play a more direct role in sensorimotor circuits than otherwise previously indicated, and plays a different role during strong sensory signaling. Moreover, this degree of variability in terms of how RMED contributes to generating behavior could be another example of worm individuality, as shown in Figure 1D in [14].

2.4.3 Other neurons for comparison: AVFR, RIGL, RIS, SABD

We selected four interneurons—AVFR, RIGL, RIS, and SABD—for further analysis based both on their limited function documentation in the Worm Atlas [44] and on the consistency with which they were uniquely and distinctly labelled across the 7 worms (AVFR in all 7, RIS in worms 1-6, RIGL in worms 2,3,4, and 6, and SABD in worm 1; See Fig. 6 and Supplementary Figs. 32, 33 for the activity and connectivity of the Stim Worm 1 neurons). Through an ANOVA analysis, we observed significant effects of oxygen stimulation on AVFR, RIS, and RIGL reconstructed activity in most of the worms (Table 6) but persistently significant effects on connectivity across all of the worms (Table 7).

Considering the example of the interneuron AVFR (Fig. 6), we saw evidence of how these behavior and stimulation effects play out differently compared to sensory and motor neurons, and that dynamic encoding of behavior in this interneuron really depended on the overall, dynamic state of the animal.

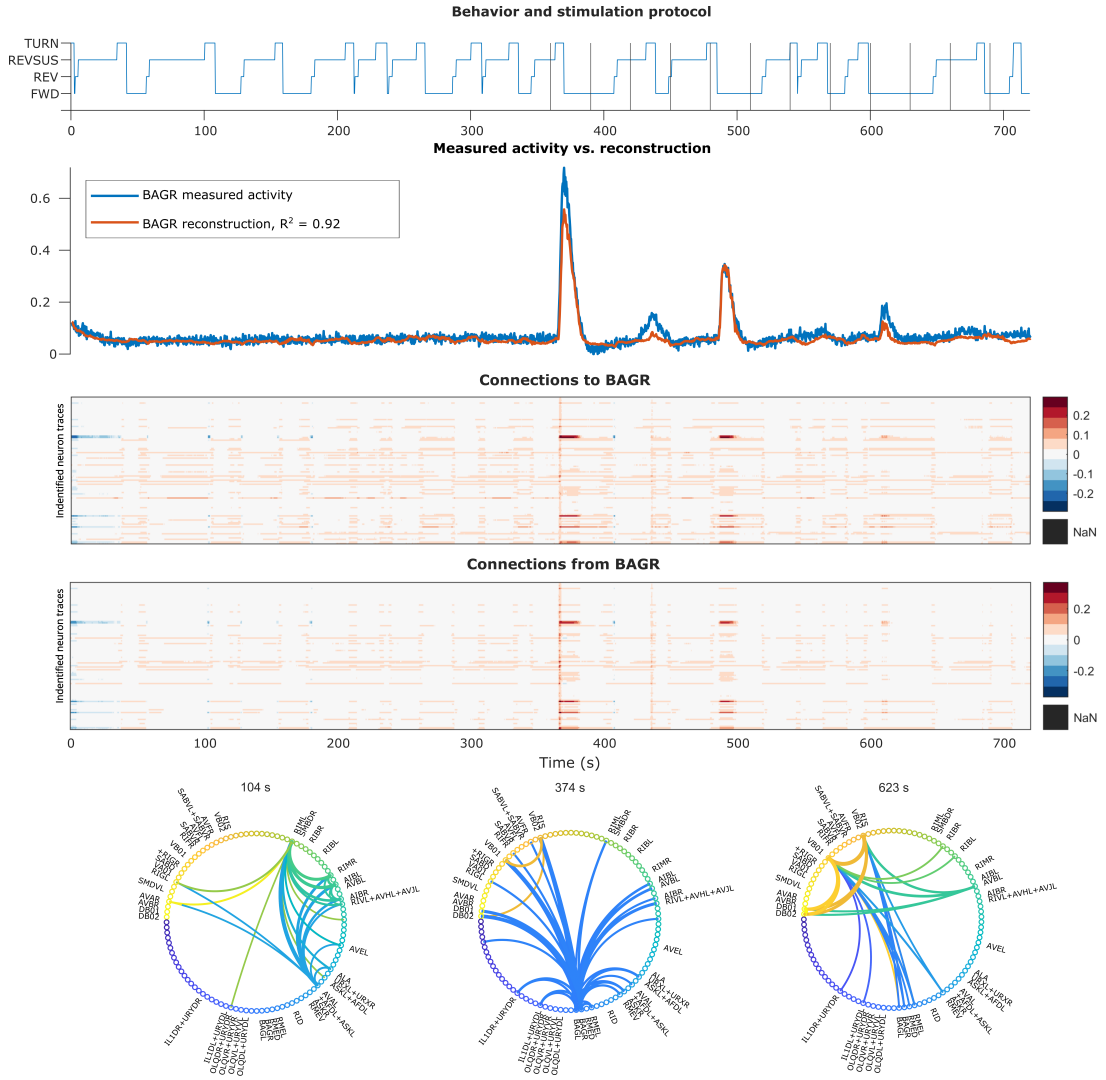

Figure 4: **Reconstructed activity and dynamic connectivity to and from BAGR. Top:** behavior state labels, with vertical lines indicating switches in the oxygen stimulation protocol. **Second from top:** measured BAGR activity vs. reconstructed BAGR activity ($\hat{y}$). **Third and fourth from top:** dynamic connectivity to vs. from BAGR at each time point. **Bottom row:** instantaneous dynamic connectivity maps at time points of strong BAGR connectivity before and during hypoxia. While BAGR sent out strong connections during the first bout of hypoxia, its connections shifted more strongly to motor/proprioceptive neurons in later bouts.

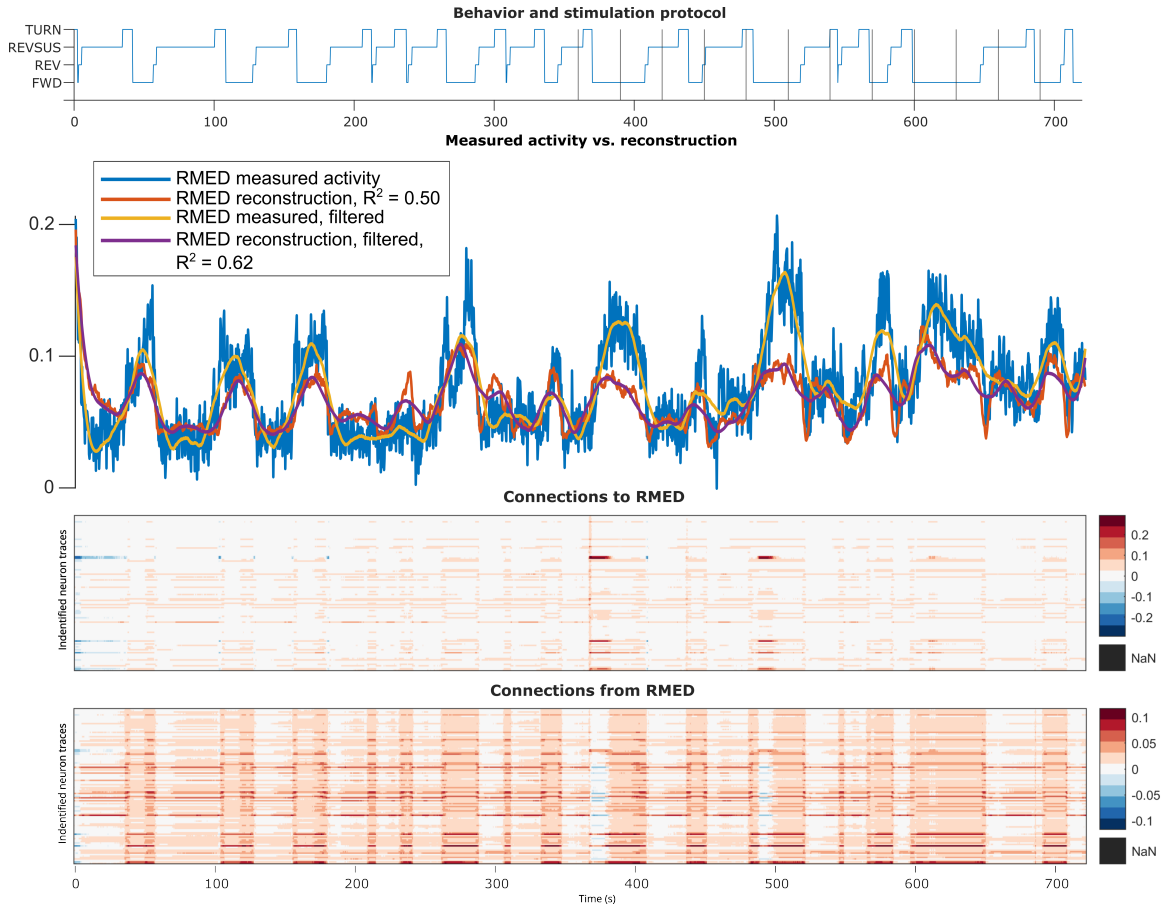

Figure 5: **Stim Worm 1 RMED motor neuron reconstructed activity and connectivity.**

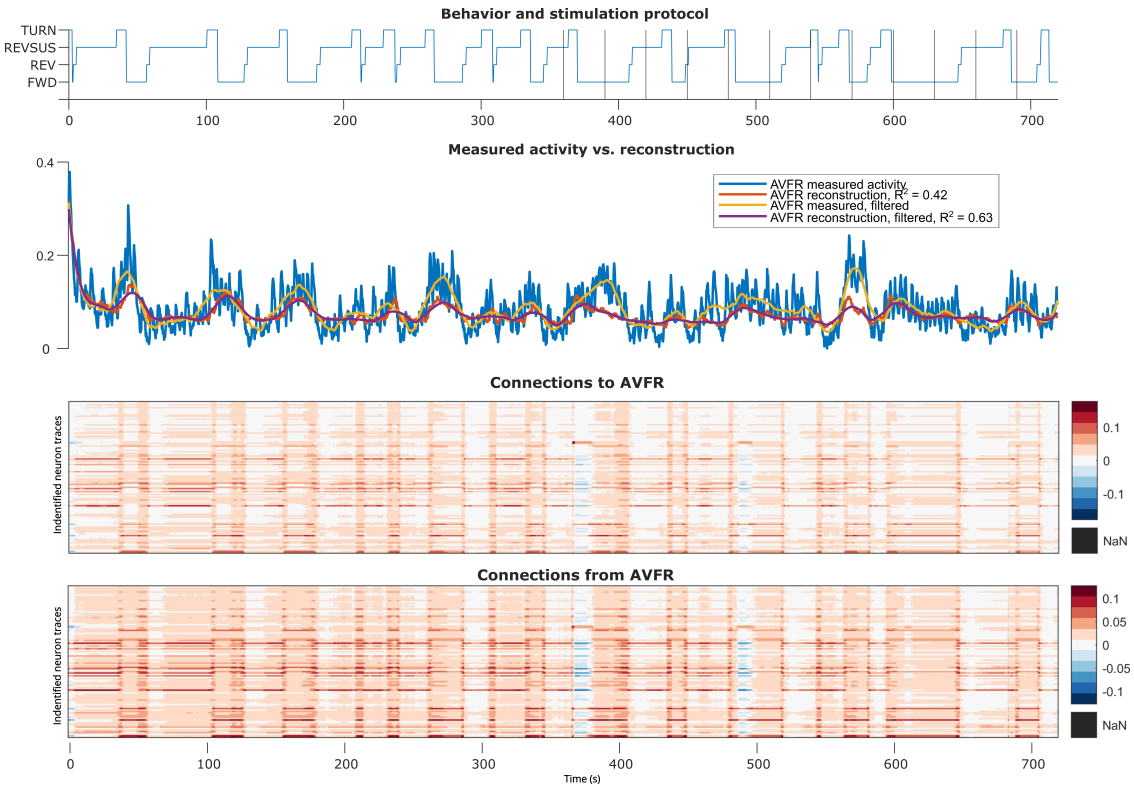

Figure 6: **Stim Worm 1 AVFR interneuron reconstructed activity and connectivity.**

Whereas the connectivity to and from sensory neuron BAGR was somewhat correlated with behavior and was strongly correlated with sensory information (Fig. 4), AVFR's connectivity appeared to correlate strongly with behavior cycles, but transitioned into a different regime (negative values) during the acute hypoxia periods, where connectivity to and from AVFR was also strongly influenced by the stimulation. Likewise, whereas the connectivity to motor neuron RMED was hierarchically correlated to behavior state and stimulation state but strongly sent out behavior-related connectivity, the connectivity to and from interneuron AVFR was strongly correlated to both behavior and stimulation. Thus, we can hypothesize that AVFR participates strongly in relaying both sensory and motor information, and can dynamically change functional regimes.

2.5 *Validation:* dLDS dynamic connectivity maps identify novel connections compared to stationary anatomical and functional connectivity atlases

While the *C. elegans* anatomical connectome has been available for over a decade [7], questions remain as to context-dependent functions, nonlinear relationships, and differences between individuals in terms of how those neurons work together. More recently, the pairwise stationary functional connectome has been mapped by stimulating each neuron and observing the responses of every other neuron individually [11]. Along with greater understanding of the role of long-range neuropeptide signaling [15; 17], this functional connectome work has revealed novel relationships that are not mediated by direct synapses.

Using dLDS, we investigated dynamic connectivity, which we define as the graph where each vertex is a single neuron and each edge from nodes i to j is the directional local influence of neuron i

on neuron j. As dLDS is a nonstationary model, this definition of connectivity allows each edge to be time-varying and to capture the changes in network structure across behaviors. Moreover, the ability of dLDS to represent nonlinear dynamics can further capture effects such as two or more neurons needing to be active to activate another downstream neuron (AND gate)—an effect that cannot be determined from one-to-one stationary functional connectomes.

We compared the dynamic connections found by the subset of *C. elegans* head neurons recorded in this dataset to the aforementioned anatomical and functional connectomes. The magnitudes of dynamic connections that were also found in the respective reference were kept positive (red), while connections that were unique to the dLDS model were given a negative coefficient (blue). We observed that, across the Stim and NoStim worms, a majority of the connections identified by dLDS did not match those in the anatomical or functional connectivity reference atlases, although some connections did (Supplementary Figs. 34, 35, 36, 37). These dLDS-only connections could be avenues for future exploration.

2.6 *Novel capabilities:* dLDS enables the alignment of latent manifolds across individuals

Per-worm models are useful for characterizing the dynamics of individual worms and even show some commonalities in terms of the dynamic connectivity maps across worms corresponding to different behavioral states or environmental variables. However, we wanted to investigate how a *shared* latent neural manifold might reflect more general principles of dynamic connectivity across worms. We modified dLDS to learn one set of DOs across all 7 Stim worms, with an individual observation matrix for each worm, resulting in one aligned model per worm (Fig. 7). We kept all the same hyperparameters as for the individual models, with the exception of allowing 70 DOs (thus permitting the possibility of 10 completely unique operators per worm).

We found that, while the aligned models' inferred DO coefficients were sparser than the total possible number of DOs, they were usually less sparse than the per-worm models (Supplementary Figs. 8, 9, 13); this was as expected, given that we did not scale up the sparsity hyperparameters for this larger model.

We also investigated whether each DO had a different "meaning" in terms of neuron-space dynamic connectivity in each worm, since each worm had a different projection out from the latent space (i.e., the per-worm representations $\boldsymbol{D}$). (e.g., DO 29 in Supplementary Figs. 38,39,40, 41, 42, 43, 44, and correlations between DOs vs. coefficients in Supplementary Figs. 45, 46). We thus tested whether the aligned DOs were washing out any structure, splitting up dynamic connectivity maps in space, or subdividing the activity of the per-worm operators in time, reflecting nonstationarity in a finer-grained way. By tallying features of the aligned DO dynamic connectivity maps (e.g., BAG and RMED participation), we observed that the aligned model operators shared key dynamic connectivity map features with the per-worm models. Therefore, even though the aligned model DOs used the same directions on the shared manifold to generate different connectivity maps, the aligned DOs overall for each worm still captured important and similar trends in which neurons were coactive and the relationships between them through time (e.g., Supplementary Figs. 38,39,40, 41, 42, 43, 44). We also observed smooth transitions in the middle of behavioral states in the aligned models, reminiscent of those in the per-worm models. This led us to reject the hypothesis that the aligned model with 70 DOs was washing out structure entirely.

Then, for each pair of per-worm and aligned DO coefficient traces, we calculated the probability of the intersection of their activity divided by the activity of one of the two DOs (e.g., Stim Worm 1, Supplementary Fig. 47). We saw a marked asymmetry: each aligned DO represented a small percentage of a per-worm DO utilization probability, but whenever an aligned DO was active, it was strongly coactive with at least one per-worm DO, and sometimes multiple. This indicated that the aligned DOs split up the per-worm DOs utilization patterns in time, as well as subdividing and reusing in multiple ways the dynamic connectivity maps associated with the per-worm DOs. In

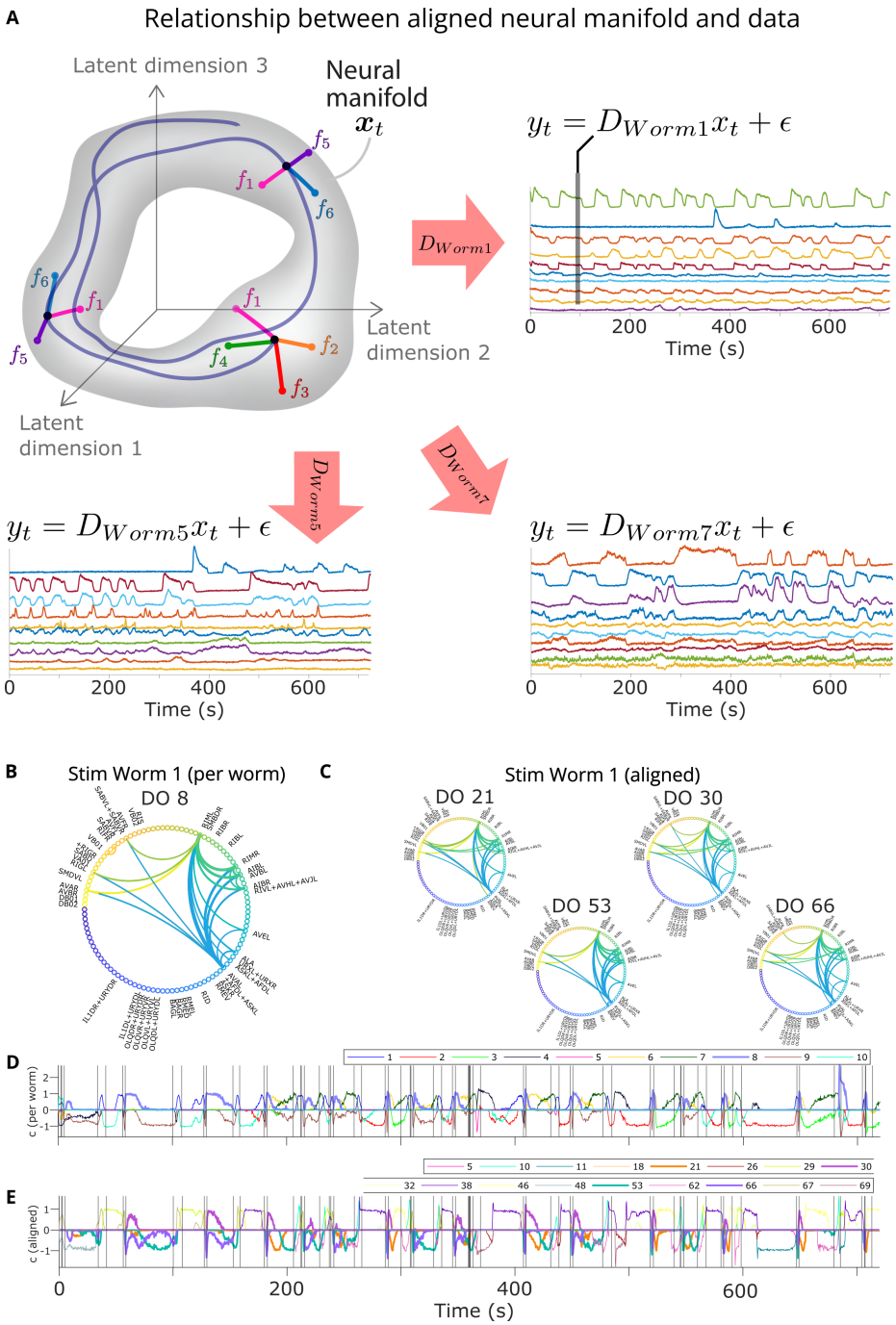

Figure 7: **Aligned latent manifold and Stim Worm 1 example. A:** We learn a shared set of DOs and latent dimensions, but a unique observation matrix and set of latent states and DO coefficients for each worm. **B,C:** We compare the connectivity maps for DO 8 in the per-worm model and the aligned DOs that co-occur with it. **D,E:** The DO coefficients themselves.

conclusion, when aligning dynamics across individuals using dLDS, model size can have an impact on how key dynamics are split up and represented, but the key dynamics will still be decipherable and will still represent key latent neural processes such that shared activity patterns across individuals are preserved.

3. Discussion, Limitations, and Future Work

In this work, we study the time-varying and contextual nature of *C. elegans* neural function. We focused on the novel characterization afforded by recent advances in time-varying dyanmical systems estimation—decomposed linear dynamical systems (dLDS)—to identify instantaneous "dynamic connectivity" that was able to track changing functional connections across behaviors. The decomposed nature of (dLDS) was able to uncover simultaneous neural processes, the dynamic operators (DOs) where each DO represents one fundament set of interconnections that ebb, flow, and combine to represent the complex nature of moment-by-moment neural dynamics across the full imaged population. We found that the DOs strongly corresponded to either specific motor or sensory tasks, and recombined in different ways across trials and across individuals to capture a diverse set of nonstationary interactions.

A key contribution is the combination of the instantaneous nature of our modeling framework with an interpretable locally linear dynamics model. These properties enabled us to define the dynamic connectivity, i.e., the moment-by-moment directional interactions between the full set of neurons. By interpreting directional dynamics in the latent state via their effects in the natural neural space, we reveal evidence that changes in instantaneous, dynamic connectivity can be the mechanism for sensory neuron adaptation and interneuron function across multiple circuits and task variables.

In general, understanding context-dependent functions or nonlinear relationships between neurons has been a challenging endeavor in systems neuroscience. Specifically, context-dependent relationships can overlay and interact with context-independent operators, interacting in ways that would be impossible to unravel in current RNNs or switched dynamical systems. We demonstrate that exploring the neural interactions through the dLDS dynamic connectivity maps across behavioral states or conditions can reveal these context-dependent functions or nonlinear relationships. Using the dLDS-derived dynamic connectivity, we identified many novel connections not mapped by direct anatomical synapses or one-to-one functional connections, emphasizing the possibility that neurons also communicate indirectly and nonlinearly with other neurons (e.g., as AND, OR, XOR gates, etc.). Moreover, we developed an extension to dLDS that allows latent neural processes to be aligned across individuals. This model extension enables greater generalizability of the learned models.

Our analysis' unique perspective results in the following findings:

- **Neurons can have dynamic functional roles in circuits, rather than a single or stable function or set of functions:** All of the neurons highlighted in this paper (sensory neurons BAGL and BAGR, interneurons AVFR, RIGL, RIS, interneuron/motor neuron SABD, and motor neuron RMED) are active and connected in both a behavioral and environmental context-dependent way.

- **Changes in interneuron connectivity mediate efficient task-switching:** Some interneurons (e.g., AVFR) may rapidly change their connectivity in different regimes based on the task-related sensory vs. motor information they receive, without obvious changes to their activity levels. While this looks like mixed selectivity when time-averaged, instantaneous dynamic connectivity shows that they act as relay stations that may rapidly switch connectivity regimes, instead. Thus, these highly connected neurons can efficiently reuse their connections to relay information from different circuits. In general, principles of efficient interneuron connectivity and task-selective function are an important question because interneurons are highly connected and they only constitute 27% of the *C. elegans* nervous system [47] and only 20-30% of primate cortical neurons [48].

- **Changes in sensory neuron connectivity show a mechanism of adaptation:** Sensory neurons (e.g., BAG) may change their dynamic connectivity to adapt to stimuli over time, first signaling broadly to many neurons, and then signaling more to a small number of connected interneurons, motor neurons and proprioceptive neurons. Moreover, using the connectivity strengths at each time point, we can quantitatively measure the connectivity shift from external sensing to proprioception as the worm adapts to the experimental protocol.

- **Worm individuality must be modeled to understand adaptation:** Despite the many features shared by these worms, their similar responses to stimuli, and the similar reconstruction performance achieved by the per-worm and aligned dLDS models, the data were nevertheless not identical, and no aligned model used the dynamic connectivity in the same way. We posit that these individual differences are *not* noise; they are essential to understand worm adaptation to their environments. Worm individuality and adaptation (or even learning) is supported by prior work [4; 6; 12; 13; 14; 30; 31; 32; 33; 34].

These findings based on the Kato 2015 data [3] can also lead to new avenues for experimentation. Contextual time-varying neural connectivity patterns across individuals during adaptation can be further investigated across species with perturbation experiments, e.g., using a mixture of new protocols and optical stimulation.

Taken together, our results show that dLDS can be used to reveal a detailed story of lower-dimensional latent neural processes such as sensation that are hierarchically overlaid on those latent neural processes regulating motor behavior states, and the complex roles of interneurons in between. We can use dLDS to gain insight into internal cognitive processes that are otherwise difficult to disentangle. Our analysis complements prior and concurrent work to show, in a data-driven way without time-averaging across behavioral or experimental conditions, that distributed coding in *C. elegans* instantaneously changes to create behavior-related neural activity, and that the connections effecting these changes adapt throughout a trial, even across outwardly similar behaviors.

While not explored in this study due to the confounding variable of behavior base rates potentially impacting nonstationarity in addition to environmental variables, it is possible that the amplitude of DO coefficients might reflect habituation or sensitization to a sensory stimulus, evidence accumulation, a change in wakefulness or attention, etc. Future attempts at applying dLDS to neural data to interpret quantitative differences in the DO coefficients would also benefit from detailed, quantitative measures of behavior and environment variables.

More generally, dLDS complements the space of current models by enabling both interpretability and expressivity. Switched LDS models can model nonstationary processes in terms of temporally local linear systems, but only one system can be active at a time. dLDS enables the flexibility to put together a combination of linear operators, which allows us to track continuously varying changes in the network even with single behavioral bouts. Moreover, it allows the modeling of simultaneous parallel processes, such as if an animal is monitoring for potential threats while also navigating its environment for food—or in our case turning while being puffed with oxygen.

4. Data and Code Availability

The code for both the discrete and the continuous models can be found at `https://github.com/dLDS-Decomposed-Linear-Dynamics`. The code used to run the *C. elegans* data can be found at `https://github.com/dLDS-Decomposed-Linear-Dynamics/dLDS-Discrete-Matlab-Model`. The discrete code can also be pip-installed using the **dLDS-discrete** Python package, as described in `https://pypi.org/project/dLDS-discrete-2022/`.

The *C. elegans* calcium imaging data that support the findings of this study are available in the "Kato2015 whole brain imaging data" repository with the identifier `http://dx.doi.org/10.17605/osf.io/2395t` [3; 49].

The SSM Python package from the Linderman lab was used to run rSLDS [50].

The code for generating the circular dynamic connectivity graphs is available from the MATLAB File Exchange [51].

5. Acknowledgments

EY and ASC were supported in part by NSF CAREER award 2340338 and NM was supported by a Kavli Fellowship. We would like to acknowledge Sue Ann Koay for the original version of the manifold illustration in Figure 1 and Francesco Randi for the advice on how to use the Leifer Lab repositories. We would further like to thank Andrew Gordus for his helpful review of our paper and literature recommendations, our reviewers for their guidance, and Olya Hakobyan, Esther Whang, and Matthew Creamer for their comments on our manuscript.

6. Methods

6.1 Decomposed Linear Dynamical Systems (dLDS)

In our framework [42], we rely on the neural manifold hypothesis, that is that neural activity comes from an underlying low-dimensional space that evolves characteristically in time via trajectories, which we call dynamics. We observe neural activity during behavior as neural time series traces $\boldsymbol{y} \in \mathbb{R}$, which are modeled as a linear function of the latent neural states $\boldsymbol{x}$ via the observation matrix $\boldsymbol{D}$. (Note that here we define a neural latent "state" as a larger process in the brain that can occur simultaneously with other processes, as opposed to one whole-brain or whole-animal state at a time.) If trajectories in latent space are a useful model of neural processes, it is necessary to understand them as traversing a manifold. If we look at the tangent space at each latent state time point, we can break down the dynamics trajectories into a linear combination of operators G in continuous time. However, the matrix exponential becomes cumbersome to compute with even a small number of dimensions, so we use the discrete time approximation of this model to work with real neural data.

dLDS uses an expectation maximization algorithm to alternate between jointly inferring the latent states $\boldsymbol{x}$ and the dynamics coefficients $\boldsymbol{c}$, and updating the randomly initialized dynamics dictionary $\boldsymbol{F}$ and observation matrix $\boldsymbol{D}$ via projected gradient descent. Inputs from the user are just the neural activity $\boldsymbol{y}$ and some parameters, including the hypothesized latent dimensionality and number of operators, as well as some regularization terms for sparsity and smoothness of the latent states and dynamics (Table 2). Sparsity is important because it helps with interpretability – it constrains the model to use a small number of linear operators to represent each time point.

1. Randomly initialize $\boldsymbol{F}$ and $\boldsymbol{D}$.

2. Infer $\boldsymbol{x}$ and $\boldsymbol{c}$ via LASSO (Equations 6 and 7):

$$\boldsymbol{x}_t = \boldsymbol{F}_t \boldsymbol{x}_{t-1} = \sum_{m=1}^{M} c_{mt} \boldsymbol{f}_m \boldsymbol{x}_{t-1} = \sum_{m=1}^{M} [\boldsymbol{f}_m \boldsymbol{x}_{t-1}] c_{mt} = \widetilde{\boldsymbol{F}_t} \boldsymbol{c}_t, \tag{6}$$

$$\widehat{\boldsymbol{x}}_t, \widehat{\boldsymbol{c}}_t = \arg\min_{\boldsymbol{x}_t, \boldsymbol{c}_t} \Bigg[\|\boldsymbol{y_t} - \boldsymbol{D}\boldsymbol{x}_t\|_2^2 + \lambda_0 \left\| \boldsymbol{x}_t - \widetilde{\boldsymbol{F}}_t \boldsymbol{c}_t \right\|_2^2 + \lambda_1 \|\boldsymbol{x}_t\|_1 + \lambda_2 \|\boldsymbol{c}_t\|_1 + \lambda_3 \|\boldsymbol{c}_t - \widehat{\boldsymbol{c}}_{t-1}\|_2^2 \Bigg]. \tag{7}$$

3. Update $\boldsymbol{D}$ and $\boldsymbol{F}$ via projected gradient descent (Equations 8, 9):

$$\widehat{\boldsymbol{D}} \leftarrow \Pi_{C_D}(\boldsymbol{D} - \eta_D \nabla_{\boldsymbol{D}} \sum_{t=1}^{T} (\boldsymbol{y}_t - \boldsymbol{D}\boldsymbol{x}_t)^2) = \Pi_{C_D}(\boldsymbol{D} + \eta_D \sum_{t=1}^{T} (\boldsymbol{y}_t - \boldsymbol{D}\boldsymbol{x}_t)\boldsymbol{x}_t^T)), \tag{8}$$

$$\begin{aligned} \widehat{\boldsymbol{f}}_m &\leftarrow \Pi_{C_{f_m}} \left(\widehat{\boldsymbol{f}}_m - \eta_f \nabla_{f_m} \sum_{t=2}^{T} \left\| \boldsymbol{x}_t - \sum_{m=1}^{M} \boldsymbol{c}_{mt} \boldsymbol{f}_m \boldsymbol{x}_{t-1} \right\|_2^2 \right) && (9) \\ &= \Pi_{C_{f_m}} \left(\widehat{\boldsymbol{f}}_m + \eta_f \sum_{t=2}^{T} \left(\boldsymbol{c}_{mt} \left(\boldsymbol{x}_t - \widetilde{\boldsymbol{F}}_t \boldsymbol{c}_t \right) \boldsymbol{x}_{t-1}^T \right) \right). && (10) \end{aligned}$$

4. Repeat steps 2 and 3 until $\boldsymbol{D}$ and $\boldsymbol{F}$ each converge.

In the aligned model, we modify this procedure by inferring and storing $\boldsymbol{x}$,$\boldsymbol{c}$, and $\boldsymbol{D}$ separately for each worm on each update iteration, whereas $\boldsymbol{F}$ is updated using a cell array containing the data from all of the worms, essentially concatenated as one trial after another.

We applied dLDS to each worm delta fluorescence trace individually on the CIS cluster. Preprocessing was minimal - negative values (up to 3% of each trace) were set to 0 because calcium-based imaging is a non-negative measure of activity. All values were scaled between 0 and 1 (maximum fluorescence value per worm) to promote even reconstruction performance.

Model type	Protocol	Worm number	R^2
Per-worm	Stim	1	0.86
		2	0.78
		3	0.83
		4	0.79
		5	0.79
		6	0.81
		7	0.7
Aligned	Stim	1	0.87
		2	0.84
		3	0.85
		4	0.82
		5	0.75
		6	0.8
		7	0.83
Per-worm	NoStim	1	0.85
		2	0.86
		3	0.81
		4	0.85
		5	0.77

Table 1: **dLDS performance in terms of R^2.**

We first ran 3000 iterations of dLDS and observed that after 500 iterations, all of the models achieved change in $\boldsymbol{D}$ and change in $\boldsymbol{F}$ on the order of 10^{-3}. $\boldsymbol{D}$ and $\boldsymbol{F}$ were stored and used to perform inference one last time after dynamics learning to obtain the latent states ($\boldsymbol{x}$) and dynamics coefficients (c). The number of latent dimensions and dynamics were initialized heuristically as

10 because there were 4-8 behavioral states labelled and because the median number of dynamics active at a time converged to 3-8 with a range of dimensionalities (6, 8, 10, 20), so an intermediate value (10) was chosen in favor of the smallest stable number of coefficients without artificially constraining the median number of active coefficients at any given time (Table 2). Similarly, a range of regularization parameters was explored (from near 0 to greater than 1) before settling on the fairly strong regularization for the smoothness of the states and coefficients. Since $\boldsymbol{D}$ and $\boldsymbol{F}$ are randomly initialized, multiple examples were generated for three of the worms and compared visually.

Parameter	Meaning	How to set	*C. elegans* parameters (per-worm models)
nF	number of dynamics operators (DOs)	First set to 2x the number of PCs required for 95% variance explained. Then decrease until the median number of active dynamics coefficients starts decreasing. (Goal: minimize the number of DOs while maintaining the inherent dimensionality of the data.) Alternative heuristic: use the number of known behavioral states as a benchmark and double it to get the starting point for the number of DOs, and then start decreasing from there.	10
N	number of latent dimensions	Set approximately equal to nF	10
lambda_val	regularization: sparsity of states (x)	Increase to reduce the number of states active at the same time (moderately sensitive)	0.1
lambda_history	regularization: smoothness of states (x)	Increase to encourage states to change smoothly from time point to time point (less sensitive)	0.9
lambda_b	regularization: sparsity of dynamics coefficients (c)	Increase to reduce the number of DOs active at the same time (sensitive)	0.01
lambda_historyb	regularization: smoothness of dynamics coefficients (c)	Increase to encourage DO coefficients to change smoothly from time point to time point	0

Table 2: **Meaning of key dLDS parameters, heuristics for setting them, and settings used for *C. elegans* models.**

rSLDS was also run for 500 iterations on each worm with 10 latent dimensions and 4 output states for the Stim worms (or 8 for the NoStim worms).

For the reconstructions (Table 1), the product of D with the latent states was rescaled back to the original dF/F range (R^2 between 0.7 and 0.9 for each of the worms). The dynamics coefficients

were also compared in terms of their utilization during the experimental settings of the experiment (histograms) and during various behavioral states.

6.2 *C. elegans* data

C. elegans calcium imaging data was obtained from [49] (Table 3).

Condition	Worm	Duration (s)	Time points	Recorded traces	Labelled with one or more neurons	Oxygen level switch times (s)	Behavior states
Stim	1	720	2198	107	45	every 30 s starting at 360 until the end	4
	2		2017	122	44		
	3		2197	124	40		
	4		2018	134	55		
	5		2201	123	48		
	6		2017	151	44		
	7		2019	146	51		
NoStim	1	1080	3137	109	34	N/A	8
	2		3134	107	44		
	3		3059	131	33		
	4		3311	126	48		
	5		3021	129	49		

Table 3: ***C. elegans* data characteristics.**

6.3 Validation: Decoding other variables from dLDS outputs

We validated the decoding of other additional variables, such as speed or oxygen concentration, from the DO coefficients or latent states. First, we trained an SVM to predict nonstationarity, i.e., whether individual time points were in the first or second half of the trial based on either 1) the DO coefficients ("c vals") or 2) the latent states ("x vals") at only that time point. These SVMs correctly classified at 85% mean accuracy for the DO coefficients and 87% mean accuracy for the latent states (Supplementary Figs. 4, 5). However, we saw slightly decreased mean accuracy (84% for the DO coefficients, 85% for the latent states) in the prediction of precise oxygen levels (detailed stimulation times in the Stim experiments only, rather than first half vs. second half), where 4% oxygen times were primarily misclassified as 21% oxygen (Supplementary Fig. 6). This is not entirely surprising, as it is not possible to change the oxygen concentration in a chamber uniformly and instantaneously, and the base rate of 21% oxygen exposure was higher in these experiments. Despite these confounds, the latent states and DO coefficients are clearly nonstationary between the two halves of all the Stim experiments and 4 out of the 5 NoStim experiments in a way that an SVM can decode (Supplementary Figs. 4, 5). Since nonstationarity was also observed in the NoStim worms, dLDS may be picking up on nonstationarity in the data not only due to the oxygen protocol, but also likely due to other time-dependent factors.

As far as classifying speed (forward crawling vs. forward slowing), SVMs trained on either the DO coefficients or the latent state values were also successful (mean accuracy: 83% for the DO coefficients, 82% for the latent states), but were mostly biased toward the forward slowing states (Supplementary Fig. 7). Overall, we found, qualitatively and quantitatively, that the DO coefficients do encode features of the latent neural states that reflect both the discrete and continuous nature of the behaviors they generate.

6.4 Computing dynamic connectivity

In this paper we feature dynamic connectivity maps based on neuron location in the *C. elegans* head, which also show time-averaged simulated activity of the neurons of interest. We also use circular dynamic connectivity graphs [51] that only show connections, without activity.

6.4.1 Connectivity mapped to *C. elegans* head

Each labelled neural trace was matched to a three-dimensional location in the worm and a class, as labelled by [11]. The connections between neurons were calculated as a covariance matrix between traces (from rows to columns). Recall that in a latent dynamics model where $\boldsymbol{y}_t = \boldsymbol{D}\boldsymbol{x}_t$, $\boldsymbol{D}$ is the mapping from the latent space to the ambient (e.g., neural recording) space. In typical connectivity maps, the system (i.e., $\boldsymbol{F} = \sum_{m=1}^{M} \boldsymbol{f}_m \boldsymbol{c}_m$) is considered stationary, but because of the time-varying DO coefficients $\boldsymbol{c}_t$ in dLDS, the system can be modeled in a time-dependent way. Our dynamic connectivity maps can show not only the dynamic (i.e., time-varying) connectivity (via lines between neurons), but also the reconstructed time-averaged or instantaneous activity of those neurons (via neuron opacity) resulting from that particular linear combination of DOs. For any linear combination of DOs $\boldsymbol{F}$, the correlations in the ambient space of an equivalent linear time-invariant dynamical system are calculated as $\boldsymbol{D} * \boldsymbol{F} * \boldsymbol{D}^T$. To produce the time-averaged simulated fluorescence values $\hat{\boldsymbol{x}}$ generated only by a particular combination of DOs of interest, simulated latent states were calculated by applying an impulse function (vector of ones) to the combined DO $\boldsymbol{F}$, taking the dot product iteratively for 500 time points, and then taking the mean reconstructed neural activity for each neuron. To produce stable combined DOs, $\boldsymbol{F}$ was rescaled to unit norm (after linearly combining the component DOs, but before applying the impulse function). Then the simulated latent states were multiplied by $\boldsymbol{D}$ to produce the simulated fluorescence.

The dynamic connectivity maps were produced for only the labelled traces (less than 50% of the recorded traces). If multiple neurons were present in that trace, the activity of that trace was plotted redundantly in each of the locations associated with the corresponding component neurons. The simulated fluorescences plotted were the mean for each trace. Strong thresholding on both the fluorescence values and the connectivity was performed to declutter the plotting - i.e., only the strongest 0.1-0.5% of connections are shown. Thresholding was also performed on the automatic neuron trace labels so that the strongest activity and strongest connections were labelled.

6.4.2 Circular connectivity graphs

The circular connectivity graphs [51] are another way of visualizing the dynamic connectivity, without spatial information or information about neuron activity. The lines go from source to target neuron (or neuron combination, or unlabelled trace). The color of each line denotes its source.

6.5 BAGL/R dynamic connectivity tally

For each behavior or experimental condition context analyzed, the corresponding active DO traces were visually selected for each worm model. Then a dynamic connectivity map was made for each trace, and the presence of key neurons was tallied across those maps, both in terms of their appearance in DOs across worms and whether they appeared in each worm model (Tables 4, 8).

Table 4 is a tally of strong connectivity with or activity in BAGL and/or BAGR across the worms' dynamic connectivity maps for each DO.

In the per-worm models, BAGL and BAGR were strongly present in DOs that were only active in the second half of the trials (alternative oxygen levels) in more than half of the worms and in DOs that were mostly active in the second half in more than a third of the worms (Supplementary Figs. 16, 19, Table 4). Furthermore, they were present in *none* of the operators that were exclusively or mostly in the first half (Supplementary Figs. 21, 24).

subset	per-worm DOs	worms	aligned DOs	worms
Stim FWD	11/31	7/7	24/46	7/7
Stim REVSUS	3/36	2/7	10/54	3/7
Stim only 1st half	0/3	0/7	1/6	1/7
Stim mostly 1st half	0/11	0/7	2/8	1/7
Stim mostly 2nd half	4/8	3/7	3/9	3/7
Stim only 2nd half	8/9	5/7	13/20	6/7
Stim sign flip between halves	1/3	1/7	1/1	1/7

Table 4: **Tally of BAGR or BAGL presence in dynamic connectivity maps across conditions**.

We also observed that BAGL and BAGR were not evenly used between behavioral states; DOs featuring BAGL/R utilized during forward crawling were present in all 7 Stim worms (Fig. 27), but only during reverse sustained crawling in 2 out of 7 worms (Fig. 30). This brings up the question of whether BAGL/R activity and connectivity is dependent on behavioral context. This bias of BAG-featuring DOs toward forward crawling could be a result of the base rates of those two behavioral states, which were biased toward forward crawling in the second half of the experiments, indicating that BAGL/R utilization is independent of behavior and is simply more present during forward crawling because forward crawling occurred more often during hypoxia. However, the bias of BAG-featuring DOs toward forward crawling states could indicate context-dependent BAG utilization. This also called into question whether nonstationarity generally was a side effect of when forward crawling was occurring.

6.6 χ^2 tests

In order to test the independence of individual neuron activity and connectivity levels (on/off) from categorical variables such as oxygen stimulation settings and behavior states, we conducted χ^2 tests [52] for each Stim worm per-worm model (Table 5). The null hypothesis of the χ^2 test is that there is no difference in expected value of the observed variable (in our case, reconstructed activity or connectivity) between groups (behavior states, stimulation states - in the stim half of the trial or not, or a detailed readout of either of those categories). Rejecting the null hypothesis reflects a significant difference in observed vs. expected values, indicating that that category significantly impacts the observed values. Most tests were found to be significant, even when the alpha value for rejection was set at an extremely conservative 9e-5, based on a Bonferroni correction from 0.05 by the number of tests per worm.

First, we compared behavior states to stimulation levels and found that the stimulation times significantly impacted the behavior states in most of the worms, which validates the idea that the stimulation protocol could be used to entrain worm behavior (see "bhv" and "FWD" vs. "stimTimes" and "stimTimesDetailed" in Table 5). For most of the 7 Stim worms, in terms of reconstructed activity ($\hat{y}$), at a weak threshold for "active" (above median value), both BAGL and BAGR were influenced by state 3 (REVSUS), but at a strong threshold (median plus 3 standard deviations), BAGL was most influenced by state 1 (FWD). At both levels, they were most active during the second half of the experiments (alternating oxygen stimulation protocol ("Stim"= 1)). The stimulation protocol results and the strong threshold results align with the visual observations from the connectivity maps above, which only showed the strongest activity levels and connections. As far as the connections to and from BAGR and BAGL, the χ^2 test results were inconclusive as far as whether they were dependent on stimulation protocol state at the lower threshold for "connected", but at the higher threshold, connectivity to and from BAGR and BAGR in most worms significantly interacted with both the stimulation protocol states and behavior states.

Stim worm	variable 1	variable 2	p value	max level	df	Q
1	bhv	AVFRconnFrom	0.153422	3	3	5.264503
2	bhv	AVFRconnFrom	0.852213	1	3	0.788512
3	bhv	AVFRconnFrom	0.86671	1	3	0.727532
4	bhv	AVFRconnFrom	0.007016	3	3	12.1099
5	bhv	AVFRconnFrom	0.004201	3	3	13.21129
6	bhv	AVFRconnFrom	0.821141	3	3	0.917755
7	bhv	AVFRconnFrom	0.760397	3	3	1.169215
1	FWD	AVFRconnFrom	0.455954	2	1	0.555808
2	FWD	AVFRconnFrom	0.374551	1	1	0.788512
3	FWD	AVFRconnFrom	0.393684	1	1	0.727532
4	FWD	AVFRconnFrom	0.521763	2	1	0.410406
5	FWD	AVFRconnFrom	0.104907	2	1	2.629308
6	FWD	AVFRconnFrom	0.552443	2	1	0.352958
7	FWD	AVFRconnFrom	0.390819	2	1	0.736392
1	Stim	AVFRconnFrom	0.3172	2	1	1.000455
2	Stim	AVFRconnFrom	0.316951	2	1	1.001489
3	Stim	AVFRconnFrom	0.31698	2	1	1.001367
4	Stim	AVFRconnFrom	0.317191	2	1	1.000496
5	Stim	AVFRconnFrom	0.045206	2	1	4.010926
6	Stim	AVFRconnFrom	0.316951	2	1	1.001489
7	Stim	AVFRconnFrom	0.31743	1	1	0.999505
1	StimDetailed	AVFRconnFrom	0.563378	1	1	0.33389
2	StimDetailed	AVFRconnFrom	0.56322	1	1	0.33416
3	StimDetailed	AVFRconnFrom	0.56468	1	1	0.331666
4	StimDetailed	AVFRconnFrom	0.563349	1	1	0.333939
5	StimDetailed	AVFRconnFrom	0.247926	1	1	1.334952
6	StimDetailed	AVFRconnFrom	0.56322	1	1	0.33416
7	StimDetailed	AVFRconnFrom	0.563477	1	1	0.333719
1	bhv	AVFRconnFrom3	0.002175	3	3	14.61688
2	bhv	AVFRconnFrom3	1.53E-09	1	3	43.96989
3	bhv	AVFRconnFrom3	6.80E-05	1	3	21.91259
4	bhv	AVFRconnFrom3	0	3	3	233.665
5	bhv	AVFRconnFrom3	5.67E-09	3	3	41.29154
6	bhv	AVFRconnFrom3	0	3	3	164.9716
7	bhv	AVFRconnFrom3	2.91E-09	3	3	42.6603
1	FWD	AVFRconnFrom3	0.004727	2	1	7.981118
2	FWD	AVFRconnFrom3	1.30E-09	1	1	36.81344
3	FWD	AVFRconnFrom3	0.182261	1	1	1.779094
4	FWD	AVFRconnFrom3	0	2	1	123.5084
5	FWD	AVFRconnFrom3	0.004898	2	1	7.916752
6	FWD	AVFRconnFrom3	0	2	1	84.89804
7	FWD	AVFRconnFrom3	1.27E-07	2	1	27.90499
1	Stim	AVFRconnFrom3	2.68E-13	1	1	53.43277
2	Stim	AVFRconnFrom3	1.57E-13	2	1	54.48424
3	Stim	AVFRconnFrom3	0.999273	2	1	8.30E-07
4	Stim	AVFRconnFrom3	0	1	1	117.9731
5	Stim	AVFRconnFrom3	0.000511	2	1	12.07675
6	Stim	AVFRconnFrom3	0	1	1	235.9593
7	Stim	AVFRconnFrom3	7.01E-12	2	1	47.02587
1	StimDetailed	AVFRconnFrom3	1.19E-05	1	1	19.17793

2	StimDetailed	AVFRconnFrom3	2.01E-05	1	1	18.17941
3	StimDetailed	AVFRconnFrom3	0.996217	1	1	2.25E-05
4	StimDetailed	AVFRconnFrom3	2.73E-05	1	1	17.59624
5	StimDetailed	AVFRconnFrom3	0.044977	1	1	4.019492
6	StimDetailed	AVFRconnFrom3	2.22E-16	1	1	67.06295
7	StimDetailed	AVFRconnFrom3	7.42E-05	1	1	15.70119
1	bhv	AVFRconnFromNeg	0	1	3	99.65838
2	bhv	AVFRconnFromNeg	NaN	1	3	NaN
3	bhv	AVFRconnFromNeg	NaN	1	3	NaN
4	bhv	AVFRconnFromNeg	NaN	1	3	NaN
5	bhv	AVFRconnFromNeg	1.41E-07	4	3	34.70232
6	bhv	AVFRconnFromNeg	NaN	1	3	NaN
7	bhv	AVFRconnFromNeg	NaN	1	3	NaN
1	FWD	AVFRconnFromNeg	0	1	1	75.76626
2	FWD	AVFRconnFromNeg	NaN	1	1	NaN
3	FWD	AVFRconnFromNeg	NaN	1	1	NaN
4	FWD	AVFRconnFromNeg	NaN	1	1	NaN
5	FWD	AVFRconnFromNeg	0.007082	2	1	7.252064
6	FWD	AVFRconnFromNeg	NaN	1	1	NaN
7	FWD	AVFRconnFromNeg	NaN	1	1	NaN
1	Stim	AVFRconnFromNeg	1.54E-10	2	1	40.98106
2	Stim	AVFRconnFromNeg	NaN	1	1	NaN
3	Stim	AVFRconnFromNeg	NaN	1	1	NaN
4	Stim	AVFRconnFromNeg	NaN	1	1	NaN
5	Stim	AVFRconnFromNeg	2.02E-08	1	1	31.47144
6	Stim	AVFRconnFromNeg	NaN	1	1	NaN
7	Stim	AVFRconnFromNeg	NaN	1	1	NaN
5	StimDetailed	AVFRconnFromNeg	0.00121	1	1	10.4746
7	StimDetailed	AVFRconnFromNeg	NaN	1	1	NaN
1	bhv	AVFRconnFromNeg3	8.88E-16	1	3	73.21871
2	bhv	AVFRconnFromNeg3	NaN	1	3	NaN
3	bhv	AVFRconnFromNeg3	NaN	1	3	NaN
4	bhv	AVFRconnFromNeg3	NaN	1	3	NaN
5	bhv	AVFRconnFromNeg3	NaN	1	3	NaN
6	bhv	AVFRconnFromNeg3	NaN	1	3	NaN
7	bhv	AVFRconnFromNeg3	NaN	1	3	NaN
1	FWD	AVFRconnFromNeg3	1.67E-15	1	1	63.47413
2	FWD	AVFRconnFromNeg3	NaN	1	1	NaN
3	FWD	AVFRconnFromNeg3	NaN	1	1	NaN
4	FWD	AVFRconnFromNeg3	NaN	1	1	NaN
5	FWD	AVFRconnFromNeg3	NaN	1	1	NaN
6	FWD	AVFRconnFromNeg3	NaN	1	1	NaN
7	FWD	AVFRconnFromNeg3	NaN	1	1	NaN
1	Stim	AVFRconnFromNeg3	1.62E-10	2	1	40.88402
2	Stim	AVFRconnFromNeg3	NaN	1	1	NaN
3	Stim	AVFRconnFromNeg3	NaN	1	1	NaN
4	Stim	AVFRconnFromNeg3	NaN	1	1	NaN
5	Stim	AVFRconnFromNeg3	NaN	1	1	NaN
6	Stim	AVFRconnFromNeg3	NaN	1	1	NaN
7	Stim	AVFRconnFromNeg3	NaN	1	1	NaN

5	StimDetailed	AVFRconnFromNeg3	NaN	1	1	NaN
7	StimDetailed	AVFRconnFromNeg3	NaN	1	1	NaN
1	bhv	AVFRconnFromPos	0.153422	3	3	5.264503
2	bhv	AVFRconnFromPos	0.852213	1	3	0.788512
3	bhv	AVFRconnFromPos	0.86671	1	3	0.727532
4	bhv	AVFRconnFromPos	0.007016	3	3	12.1099
5	bhv	AVFRconnFromPos	0.004201	3	3	13.21129
6	bhv	AVFRconnFromPos	0.821141	3	3	0.917755
7	bhv	AVFRconnFromPos	0.760397	3	3	1.169215
1	FWD	AVFRconnFromPos	0.455954	2	1	0.555808
2	FWD	AVFRconnFromPos	0.374551	1	1	0.788512
3	FWD	AVFRconnFromPos	0.393684	1	1	0.727532
4	FWD	AVFRconnFromPos	0.521763	2	1	0.410406
5	FWD	AVFRconnFromPos	0.104907	2	1	2.629308
6	FWD	AVFRconnFromPos	0.552443	2	1	0.352958
7	FWD	AVFRconnFromPos	0.390819	2	1	0.736392
1	Stim	AVFRconnFromPos	0.3172	2	1	1.000455
2	Stim	AVFRconnFromPos	0.316951	2	1	1.001489
3	Stim	AVFRconnFromPos	0.31698	2	1	1.001367
4	Stim	AVFRconnFromPos	0.317191	2	1	1.000496
5	Stim	AVFRconnFromPos	0.045206	2	1	4.010926
6	Stim	AVFRconnFromPos	0.316951	2	1	1.001489
7	Stim	AVFRconnFromPos	0.31743	1	1	0.999505
1	StimDetailed	AVFRconnFromPos	0.563378	1	1	0.33389
2	StimDetailed	AVFRconnFromPos	0.56322	1	1	0.33416
3	StimDetailed	AVFRconnFromPos	0.56468	1	1	0.331666
4	StimDetailed	AVFRconnFromPos	0.563349	1	1	0.333939
5	StimDetailed	AVFRconnFromPos	0.247926	1	1	1.334952
6	StimDetailed	AVFRconnFromPos	0.56322	1	1	0.33416
7	StimDetailed	AVFRconnFromPos	0.563477	1	1	0.333719
1	bhv	AVFRconnFromPos3	0.028315	3	3	9.074636
2	bhv	AVFRconnFromPos3	1.53E-09	1	3	43.96989
3	bhv	AVFRconnFromPos3	6.80E-05	1	3	21.91259
4	bhv	AVFRconnFromPos3	0	3	3	233.665
5	bhv	AVFRconnFromPos3	5.67E-09	3	3	41.29154
6	bhv	AVFRconnFromPos3	0	3	3	164.9716
7	bhv	AVFRconnFromPos3	2.91E-09	3	3	42.6603
1	FWD	AVFRconnFromPos3	0.687188	2	1	0.162147
2	FWD	AVFRconnFromPos3	1.30E-09	1	1	36.81344
3	FWD	AVFRconnFromPos3	0.182261	1	1	1.779094
4	FWD	AVFRconnFromPos3	0	2	1	123.5084
5	FWD	AVFRconnFromPos3	0.004898	2	1	7.916752
6	FWD	AVFRconnFromPos3	0	2	1	84.89804
7	FWD	AVFRconnFromPos3	1.27E-07	2	1	27.90499
1	Stim	AVFRconnFromPos3	0	1	1	81.07336
2	Stim	AVFRconnFromPos3	1.57E-13	2	1	54.48424
3	Stim	AVFRconnFromPos3	0.999273	2	1	8.30E-07
4	Stim	AVFRconnFromPos3	0	1	1	117.9731
5	Stim	AVFRconnFromPos3	0.000511	2	1	12.07675
6	Stim	AVFRconnFromPos3	0	1	1	235.9593

7	Stim	AVFRconnFromPos3	7.01E-12	2	1	47.02587
1	StimDetailed	AVFRconnFromPos3	0.154357	1	1	2.028655
2	StimDetailed	AVFRconnFromPos3	2.01E-05	1	1	18.17941
3	StimDetailed	AVFRconnFromPos3	0.996217	1	1	2.25E-05
4	StimDetailed	AVFRconnFromPos3	2.73E-05	1	1	17.59624
5	StimDetailed	AVFRconnFromPos3	0.044977	1	1	4.019492
6	StimDetailed	AVFRconnFromPos3	2.22E-16	1	1	67.06295
7	StimDetailed	AVFRconnFromPos3	7.42E-05	1	1	15.70119
1	bhv	AVFRconnTo	0.153422	3	3	5.264503
2	bhv	AVFRconnTo	0.852213	1	3	0.788512
3	bhv	AVFRconnTo	0.86671	1	3	0.727532
4	bhv	AVFRconnTo	0.007016	3	3	12.1099
5	bhv	AVFRconnTo	0.004201	3	3	13.21129
6	bhv	AVFRconnTo	0.821141	3	3	0.917755
7	bhv	AVFRconnTo	0.760397	3	3	1.169215
1	FWD	AVFRconnTo	0.455954	2	1	0.555808
2	FWD	AVFRconnTo	0.374551	1	1	0.788512
3	FWD	AVFRconnTo	0.393684	1	1	0.727532
4	FWD	AVFRconnTo	0.521763	2	1	0.410406
5	FWD	AVFRconnTo	0.104907	2	1	2.629308
6	FWD	AVFRconnTo	0.552443	2	1	0.352958
7	FWD	AVFRconnTo	0.390819	2	1	0.736392
1	Stim	AVFRconnTo	0.3172	2	1	1.000455
2	Stim	AVFRconnTo	0.316951	2	1	1.001489
3	Stim	AVFRconnTo	0.31698	2	1	1.001367
4	Stim	AVFRconnTo	0.317191	2	1	1.000496
5	Stim	AVFRconnTo	0.045206	2	1	4.010926
6	Stim	AVFRconnTo	0.316951	2	1	1.001489
7	Stim	AVFRconnTo	0.31743	1	1	0.999505
1	StimDetailed	AVFRconnTo	0.563378	1	1	0.33389
2	StimDetailed	AVFRconnTo	0.56322	1	1	0.33416
3	StimDetailed	AVFRconnTo	0.56468	1	1	0.331666
4	StimDetailed	AVFRconnTo	0.563349	1	1	0.333939
5	StimDetailed	AVFRconnTo	0.247926	1	1	1.334952
6	StimDetailed	AVFRconnTo	0.56322	1	1	0.33416
7	StimDetailed	AVFRconnTo	0.563477	1	1	0.333719
1	bhv	AVFRconnTo3	0.003414	3	3	13.65503
2	bhv	AVFRconnTo3	0.852213	1	3	0.788512
3	bhv	AVFRconnTo3	0.86671	1	3	0.727532
4	bhv	AVFRconnTo3	0.007016	3	3	12.1099
5	bhv	AVFRconnTo3	0.004201	3	3	13.21129
6	bhv	AVFRconnTo3	0.821141	3	3	0.917755
7	bhv	AVFRconnTo3	0.760397	3	3	1.169215
1	FWD	AVFRconnTo3	0.109545	2	1	2.560777
2	FWD	AVFRconnTo3	0.374551	1	1	0.788512
3	FWD	AVFRconnTo3	0.393684	1	1	0.727532
4	FWD	AVFRconnTo3	0.521763	2	1	0.410406
5	FWD	AVFRconnTo3	0.104907	2	1	2.629308
6	FWD	AVFRconnTo3	0.552443	2	1	0.352958
7	FWD	AVFRconnTo3	0.390819	2	1	0.736392

1	Stim	AVFRconnTo3	1.88E-08	1	1	31.61775
2	Stim	AVFRconnTo3	0.316951	2	1	1.001489
3	Stim	AVFRconnTo3	0.31698	2	1	1.001367
4	Stim	AVFRconnTo3	0.317191	2	1	1.000496
5	Stim	AVFRconnTo3	0.045206	2	1	4.010926
6	Stim	AVFRconnTo3	0.316951	2	1	1.001489
7	Stim	AVFRconnTo3	0.31743	1	1	0.999505
1	StimDetailed	AVFRconnTo3	0.000571	1	1	11.86984
2	StimDetailed	AVFRconnTo3	0.56322	1	1	0.33416
3	StimDetailed	AVFRconnTo3	0.56468	1	1	0.331666
4	StimDetailed	AVFRconnTo3	0.563349	1	1	0.333939
5	StimDetailed	AVFRconnTo3	0.247926	1	1	1.334952
6	StimDetailed	AVFRconnTo3	0.56322	1	1	0.33416
7	StimDetailed	AVFRconnTo3	0.563477	1	1	0.333719
1	bhv	AVFRconnToNeg	1.28E-12	1	3	58.41645
2	bhv	AVFRconnToNeg	NaN	1	3	NaN
3	bhv	AVFRconnToNeg	NaN	1	3	NaN
4	bhv	AVFRconnToNeg	NaN	1	3	NaN
5	bhv	AVFRconnToNeg	2.43E-13	4	3	61.79254
6	bhv	AVFRconnToNeg	NaN	1	3	NaN
7	bhv	AVFRconnToNeg	NaN	1	3	NaN
1	FWD	AVFRconnToNeg	3.85E-10	1	1	39.18842
2	FWD	AVFRconnToNeg	NaN	1	1	NaN
3	FWD	AVFRconnToNeg	NaN	1	1	NaN
4	FWD	AVFRconnToNeg	NaN	1	1	NaN
5	FWD	AVFRconnToNeg	0.006517	2	1	7.401417
6	FWD	AVFRconnToNeg	NaN	1	1	NaN
7	FWD	AVFRconnToNeg	NaN	1	1	NaN
1	Stim	AVFRconnToNeg	2.45E-05	2	1	17.80395
2	Stim	AVFRconnToNeg	NaN	1	1	NaN
3	Stim	AVFRconnToNeg	NaN	1	1	NaN
4	Stim	AVFRconnToNeg	NaN	1	1	NaN
5	Stim	AVFRconnToNeg	6.97E-06	1	1	20.20175
6	Stim	AVFRconnToNeg	NaN	1	1	NaN
7	Stim	AVFRconnToNeg	NaN	1	1	NaN
5	StimDetailed	AVFRconnToNeg	0.009514	1	1	6.723726
5	StimDetailed	AVFRconnToNeg	0.009514	1	1	6.723726
7	StimDetailed	AVFRconnToNeg	NaN	1	1	NaN
7	StimDetailed	AVFRconnToNeg	NaN	1	1	NaN
1	bhv	AVFRconnToNeg3	1.87E-10	1	3	48.2618
2	bhv	AVFRconnToNeg3	NaN	1	3	NaN
3	bhv	AVFRconnToNeg3	NaN	1	3	NaN
4	bhv	AVFRconnToNeg3	NaN	1	3	NaN
5	bhv	AVFRconnToNeg3	NaN	1	3	NaN
6	bhv	AVFRconnToNeg3	NaN	1	3	NaN
7	bhv	AVFRconnToNeg3	NaN	1	3	NaN
1	FWD	AVFRconnToNeg3	7.39E-09	1	1	33.42869
2	FWD	AVFRconnToNeg3	NaN	1	1	NaN
3	FWD	AVFRconnToNeg3	NaN	1	1	NaN
4	FWD	AVFRconnToNeg3	NaN	1	1	NaN

5	FWD	AVFRconnToNeg3	NaN	1	1	NaN
6	FWD	AVFRconnToNeg3	NaN	1	1	NaN
7	FWD	AVFRconnToNeg3	NaN	1	1	NaN
1	Stim	AVFRconnToNeg3	9.48E-06	2	1	19.6139
2	Stim	AVFRconnToNeg3	NaN	1	1	NaN
3	Stim	AVFRconnToNeg3	NaN	1	1	NaN
4	Stim	AVFRconnToNeg3	NaN	1	1	NaN
5	Stim	AVFRconnToNeg3	NaN	1	1	NaN
6	Stim	AVFRconnToNeg3	NaN	1	1	NaN
7	Stim	AVFRconnToNeg3	NaN	1	1	NaN
5	StimDetailed	AVFRconnToNeg3	NaN	1	1	NaN
5	StimDetailed	AVFRconnToNeg3	NaN	1	1	NaN
7	StimDetailed	AVFRconnToNeg3	NaN	1	1	NaN
7	StimDetailed	AVFRconnToNeg3	NaN	1	1	NaN
1	bhv	AVFRconnToPos	0.153422	3	3	5.264503
2	bhv	AVFRconnToPos	0.852213	1	3	0.788512
3	bhv	AVFRconnToPos	0.86671	1	3	0.727532
4	bhv	AVFRconnToPos	0.007016	3	3	12.1099
5	bhv	AVFRconnToPos	0.004201	3	3	13.21129
6	bhv	AVFRconnToPos	0.821141	3	3	0.917755
7	bhv	AVFRconnToPos	0.760397	3	3	1.169215
1	FWD	AVFRconnToPos	0.455954	2	1	0.555808
2	FWD	AVFRconnToPos	0.374551	1	1	0.788512
3	FWD	AVFRconnToPos	0.393684	1	1	0.727532
4	FWD	AVFRconnToPos	0.521763	2	1	0.410406
5	FWD	AVFRconnToPos	0.104907	2	1	2.629308
6	FWD	AVFRconnToPos	0.552443	2	1	0.352958
7	FWD	AVFRconnToPos	0.390819	2	1	0.736392
1	Stim	AVFRconnToPos	0.3172	2	1	1.000455
2	Stim	AVFRconnToPos	0.316951	2	1	1.001489
3	Stim	AVFRconnToPos	0.31698	2	1	1.001367
4	Stim	AVFRconnToPos	0.317191	2	1	1.000496
5	Stim	AVFRconnToPos	0.045206	2	1	4.010926
6	Stim	AVFRconnToPos	0.316951	2	1	1.001489
7	Stim	AVFRconnToPos	0.31743	1	1	0.999505
1	StimDetailed	AVFRconnToPos	0.563378	1	1	0.33389
2	StimDetailed	AVFRconnToPos	0.56322	1	1	0.33416
3	StimDetailed	AVFRconnToPos	0.56468	1	1	0.331666
4	StimDetailed	AVFRconnToPos	0.563349	1	1	0.333939
5	StimDetailed	AVFRconnToPos	0.247926	1	1	1.334952
6	StimDetailed	AVFRconnToPos	0.56322	1	1	0.33416
7	StimDetailed	AVFRconnToPos	0.563477	1	1	0.333719
1	bhv	AVFRconnToPos3	0.000329	3	3	18.61041
2	bhv	AVFRconnToPos3	0.852213	1	3	0.788512
3	bhv	AVFRconnToPos3	0.86671	1	3	0.727532
4	bhv	AVFRconnToPos3	0.007016	3	3	12.1099
5	bhv	AVFRconnToPos3	0.004201	3	3	13.21129
6	bhv	AVFRconnToPos3	0.821141	3	3	0.917755
7	bhv	AVFRconnToPos3	0.760397	3	3	1.169215
1	FWD	AVFRconnToPos3	0.071189	2	1	3.2554

2	FWD	AVFRconnToPos3	0.374551	1	1	0.788512
3	FWD	AVFRconnToPos3	0.393684	1	1	0.727532
4	FWD	AVFRconnToPos3	0.521763	2	1	0.410406
5	FWD	AVFRconnToPos3	0.104907	2	1	2.629308
6	FWD	AVFRconnToPos3	0.552443	2	1	0.352958
7	FWD	AVFRconnToPos3	0.390819	2	1	0.736392
1	Stim	AVFRconnToPos3	2.75E-07	1	1	26.41767
2	Stim	AVFRconnToPos3	0.316951	2	1	1.001489
3	Stim	AVFRconnToPos3	0.31698	2	1	1.001367
4	Stim	AVFRconnToPos3	0.317191	2	1	1.000496
5	Stim	AVFRconnToPos3	0.045206	2	1	4.010926
6	Stim	AVFRconnToPos3	0.316951	2	1	1.001489
7	Stim	AVFRconnToPos3	0.31743	1	1	0.999505
1	StimDetailed	AVFRconnToPos3	0.000394	1	1	12.55972
2	StimDetailed	AVFRconnToPos3	0.56322	1	1	0.33416
3	StimDetailed	AVFRconnToPos3	0.56468	1	1	0.331666
4	StimDetailed	AVFRconnToPos3	0.563349	1	1	0.333939
5	StimDetailed	AVFRconnToPos3	0.247926	1	1	1.334952
6	StimDetailed	AVFRconnToPos3	0.56322	1	1	0.33416
7	StimDetailed	AVFRconnToPos3	0.563477	1	1	0.333719
1	bhv	AVFRyhat	0	1	3	803.8678
2	bhv	AVFRyhat	0	1	3	828.4552
3	bhv	AVFRyhat	0	1	3	605.7794
4	bhv	AVFRyhat	0	1	3	501.9176
5	bhv	AVFRyhat	0	1	3	177.3765
6	bhv	AVFRyhat	0	1	3	351.3449
7	bhv	AVFRyhat	0	3	3	170.6179
1	FWD	AVFRyhat	0	1	1	664.3134
2	FWD	AVFRyhat	0	1	1	812.1669
3	FWD	AVFRyhat	0	1	1	507.6664
4	FWD	AVFRyhat	0	2	1	220.561
5	FWD	AVFRyhat	0	1	1	146.3624
6	FWD	AVFRyhat	0	2	1	215.9023
7	FWD	AVFRyhat	0	2	1	91.51452
1	Stim	AVFRyhat	0.015033	1	1	5.912648
2	Stim	AVFRyhat	0.640085	2	1	0.218631
3	Stim	AVFRyhat	1.11E-16	1	1	68.16997
4	Stim	AVFRyhat	0	1	1	315.5619
5	Stim	AVFRyhat	0.359371	1	1	0.840091
6	Stim	AVFRyhat	4.04E-06	1	1	21.24404
7	Stim	AVFRyhat	4.44E-16	2	1	65.98585
1	StimD	AVFRyhat	0.076264	1	1	3.142771
2	StimD	AVFRyhat	4.61E-10	1	1	38.83551
3	StimD	AVFRyhat	2.60E-05	1	1	17.69038
4	StimD	AVFRyhat	0	1	1	214.5263
5	StimD	AVFRyhat	2.14E-08	1	1	31.36274
6	StimD	AVFRyhat	0.055553	1	1	3.665423
7	StimD	AVFRyhat	0.33529	1	1	0.928359
1	bhv	AVFRyhat3	4.20E-06	3	3	27.69767
2	bhv	AVFRyhat3	0.367791	1	3	3.158747

3	bhv	AVFRyhat3	0.16415	1	3	5.10668
4	bhv	AVFRyhat3	8.86E-13	4	3	59.16692
5	bhv	AVFRyhat3	0	4	3	100.8311
6	bhv	AVFRyhat3	0	4	3	118.5279
7	bhv	AVFRyhat3	0	4	3	123.8975
1	FWD	AVFRyhat3	0.00546	2	1	7.720573
2	FWD	AVFRyhat3	0.075521	1	1	3.158747
3	FWD	AVFRyhat3	0.023834	1	1	5.10668
4	FWD	AVFRyhat3	0.042318	2	1	4.122455
5	FWD	AVFRyhat3	0.012274	2	1	6.270887
6	FWD	AVFRyhat3	0.011365	2	1	6.40728
7	FWD	AVFRyhat3	0.011078	2	1	6.452826
1	Stim	AVFRyhat3	1.01E-07	1	1	28.36129
2	Stim	AVFRyhat3	0.045393	2	1	4.003976
3	Stim	AVFRyhat3	0.008021	1	1	7.02877
4	Stim	AVFRyhat3	0.001524	1	1	10.0498
5	Stim	AVFRyhat3	0.000612	2	1	11.73917
6	Stim	AVFRyhat3	2.01E-05	1	1	18.1801
7	Stim	AVFRyhat3	0.0003	1	1	13.07129
1	StimD	AVFRyhat3	0.002094	1	1	9.465236
2	StimD	AVFRyhat3	0.247275	1	1	1.338634
3	StimD	AVFRyhat3	0.127063	1	1	2.328024
4	StimD	AVFRyhat3	0.067027	1	1	3.354362
5	StimD	AVFRyhat3	2.35E-11	2	1	44.65795
6	StimD	AVFRyhat3	0.013781	1	1	6.066039
7	StimD	AVFRyhat3	0.0367	1	1	4.364296
1	bhv	BAGLconnFrom	0.153422	3	3	5.264503
2	bhv	BAGLconnFrom	0.852213	1	3	0.788512
3	bhv	BAGLconnFrom	0.86671	1	3	0.727532
4	bhv	BAGLconnFrom	0.133764	3	3	5.582888
5	bhv	BAGLconnFrom	0.008364	3	3	11.73084
6	bhv	BAGLconnFrom	0	3	3	268.1857
7	bhv	BAGLconnFrom	0.760397	3	3	1.169215
1	FWD	BAGLconnFrom	0.455954	2	1	0.555808
2	FWD	BAGLconnFrom	0.374551	1	1	0.788512
3	FWD	BAGLconnFrom	0.393684	1	1	0.727532
4	FWD	BAGLconnFrom	0.364824	2	1	0.821219
5	FWD	BAGLconnFrom	0.069782	2	1	3.288132
6	FWD	BAGLconnFrom	0	2	1	108.096
7	FWD	BAGLconnFrom	0.390819	2	1	0.736392
1	Stim	BAGLconnFrom	0.3172	2	1	1.000455
2	Stim	BAGLconnFrom	0.316951	2	1	1.001489
3	Stim	BAGLconnFrom	0.31698	2	1	1.001367
4	Stim	BAGLconnFrom	0.157093	2	1	2.001984
5	Stim	BAGLconnFrom	0.025115	2	1	5.01594
6	Stim	BAGLconnFrom	0	2	1	306.7129
7	Stim	BAGLconnFrom	0.31743	1	1	0.999505
1	StimDetailed	BAGLconnFrom	0.563378	1	1	0.33389
2	StimDetailed	BAGLconnFrom	0.56322	1	1	0.33416
3	StimDetailed	BAGLconnFrom	0.56468	1	1	0.331666

4	StimDetailed	BAGLconnFrom	0.413676	1	1	0.66821
5	StimDetailed	BAGLconnFrom	0.196332	1	1	1.66945
6	StimDetailed	BAGLconnFrom	0	1	1	102.339
7	StimDetailed	BAGLconnFrom	0.563477	1	1	0.333719
1	bhv	BAGLconnFrom3	0.035457	3	3	8.578265
2	bhv	BAGLconnFrom3	4.44E-16	1	3	74.58049
3	bhv	BAGLconnFrom3	0	3	3	785.8092
4	bhv	BAGLconnFrom3	0	3	3	315.0905
5	bhv	BAGLconnFrom3	0	1	3	306.5793
6	bhv	BAGLconnFrom3	0	1	3	726.7748
7	bhv	BAGLconnFrom3	0	1	3	125.6072
1	FWD	BAGLconnFrom3	0.174965	2	1	1.839876
2	FWD	BAGLconnFrom3	3.19E-12	1	1	48.57108
3	FWD	BAGLconnFrom3	0	2	1	784.0925
4	FWD	BAGLconnFrom3	0	2	1	312.3635
5	FWD	BAGLconnFrom3	0	1	1	253.808
6	FWD	BAGLconnFrom3	0	1	1	378.5621
7	FWD	BAGLconnFrom3	0	1	1	90.66841
1	Stim	BAGLconnFrom3	0.068785	2	1	3.311777
2	Stim	BAGLconnFrom3	9.64E-11	2	1	41.89223
3	Stim	BAGLconnFrom3	0	1	1	77.18278
4	Stim	BAGLconnFrom3	0	2	1	124.9179
5	Stim	BAGLconnFrom3	0	2	1	420.0473
6	Stim	BAGLconnFrom3	0	2	1	136.8379
7	Stim	BAGLconnFrom3	0	2	1	511.749
1	StimDetailed	BAGLconnFrom3	0	1	1	76.3616
2	StimDetailed	BAGLconnFrom3	0.000185	1	1	13.97792
3	StimDetailed	BAGLconnFrom3	3.35E-13	1	1	52.99006
4	StimDetailed	BAGLconnFrom3	0	1	1	444.1357
5	StimDetailed	BAGLconnFrom3	0	2	1	853.7878
6	StimDetailed	BAGLconnFrom3	0	1	1	111.7575
7	StimDetailed	BAGLconnFrom3	0	1	1	405.762
1	bhv	BAGLconnFromNeg	0.069563	3	3	7.074426
2	bhv	BAGLconnFromNeg	NaN	1	3	NaN
3	bhv	BAGLconnFromNeg	NaN	1	3	NaN
4	bhv	BAGLconnFromNeg	NaN	1	3	NaN
5	bhv	BAGLconnFromNeg	5.45E-09	2	3	41.37183
6	bhv	BAGLconnFromNeg	NaN	1	3	NaN
7	bhv	BAGLconnFromNeg	NaN	1	3	NaN
1	FWD	BAGLconnFromNeg	0.441856	2	1	0.591456
2	FWD	BAGLconnFromNeg	NaN	1	1	NaN
3	FWD	BAGLconnFromNeg	NaN	1	1	NaN
4	FWD	BAGLconnFromNeg	NaN	1	1	NaN
5	FWD	BAGLconnFromNeg	0.160333	2	1	1.971084
6	FWD	BAGLconnFromNeg	NaN	1	1	NaN
7	FWD	BAGLconnFromNeg	NaN	1	1	NaN
1	Stim	BAGLconnFromNeg	5.28E-07	1	1	25.15744
2	Stim	BAGLconnFromNeg	NaN	1	1	NaN
3	Stim	BAGLconnFromNeg	NaN	1	1	NaN
4	Stim	BAGLconnFromNeg	NaN	1	1	NaN

5	Stim	BAGLconnFromNeg	0.082915	1	1	3.006826
6	Stim	BAGLconnFromNeg	NaN	1	1	NaN
7	Stim	BAGLconnFromNeg	NaN	1	1	NaN
5	StimDetailed	BAGLconnFromNeg	0.317127	1	1	1.000758
7	StimDetailed	BAGLconnFromNeg	NaN	1	1	NaN
1	bhv	BAGLconnFromNeg3	3.59E-13	3	3	61.00187
2	bhv	BAGLconnFromNeg3	NaN	1	3	NaN
3	bhv	BAGLconnFromNeg3	NaN	1	3	NaN
4	bhv	BAGLconnFromNeg3	NaN	1	3	NaN
5	bhv	BAGLconnFromNeg3	NaN	1	3	NaN
6	bhv	BAGLconnFromNeg3	NaN	1	3	NaN
7	bhv	BAGLconnFromNeg3	NaN	1	3	NaN
1	FWD	BAGLconnFromNeg3	4.11E-13	2	1	52.5879
2	FWD	BAGLconnFromNeg3	NaN	1	1	NaN
3	FWD	BAGLconnFromNeg3	NaN	1	1	NaN
4	FWD	BAGLconnFromNeg3	NaN	1	1	NaN
5	FWD	BAGLconnFromNeg3	NaN	1	1	NaN
6	FWD	BAGLconnFromNeg3	NaN	1	1	NaN
7	FWD	BAGLconnFromNeg3	NaN	1	1	NaN
1	Stim	BAGLconnFromNeg3	0	1	1	117.7325
2	Stim	BAGLconnFromNeg3	NaN	1	1	NaN
3	Stim	BAGLconnFromNeg3	NaN	1	1	NaN
4	Stim	BAGLconnFromNeg3	NaN	1	1	NaN
5	Stim	BAGLconnFromNeg3	NaN	1	1	NaN
6	Stim	BAGLconnFromNeg3	NaN	1	1	NaN
7	Stim	BAGLconnFromNeg3	NaN	1	1	NaN
5	StimDetailed	BAGLconnFromNeg3	NaN	1	1	NaN
7	StimDetailed	BAGLconnFromNeg3	NaN	1	1	NaN
1	bhv	BAGLconnFromPos	0.153422	3	3	5.264503
2	bhv	BAGLconnFromPos	0.852213	1	3	0.788512
3	bhv	BAGLconnFromPos	0.86671	1	3	0.727532
4	bhv	BAGLconnFromPos	0.133764	3	3	5.582888
5	bhv	BAGLconnFromPos	6.90E-05	3	3	21.88323
6	bhv	BAGLconnFromPos	0	3	3	268.1857
7	bhv	BAGLconnFromPos	0.760397	3	3	1.169215
1	FWD	BAGLconnFromPos	0.455954	2	1	0.555808
2	FWD	BAGLconnFromPos	0.374551	1	1	0.788512
3	FWD	BAGLconnFromPos	0.393684	1	1	0.727532
4	FWD	BAGLconnFromPos	0.364824	2	1	0.821219
5	FWD	BAGLconnFromPos	0.031831	2	1	4.607581
6	FWD	BAGLconnFromPos	0	2	1	108.096
7	FWD	BAGLconnFromPos	0.390819	2	1	0.736392
1	Stim	BAGLconnFromPos	0.3172	2	1	1.000455
2	Stim	BAGLconnFromPos	0.316951	2	1	1.001489
3	Stim	BAGLconnFromPos	0.31698	2	1	1.001367
4	Stim	BAGLconnFromPos	0.157093	2	1	2.001984
5	Stim	BAGLconnFromPos	0.008021	2	1	7.028718
6	Stim	BAGLconnFromPos	0	2	1	306.7129
7	Stim	BAGLconnFromPos	0.31743	1	1	0.999505
1	StimDetailed	BAGLconnFromPos	0.563378	1	1	0.33389

2	StimDetailed	BAGLconnFromPos	0.56322	1	1	0.33416
3	StimDetailed	BAGLconnFromPos	0.56468	1	1	0.331666
4	StimDetailed	BAGLconnFromPos	0.413676	1	1	0.66821
5	StimDetailed	BAGLconnFromPos	0.126141	1	1	2.33936
6	StimDetailed	BAGLconnFromPos	0	1	1	102.339
7	StimDetailed	BAGLconnFromPos	0.563477	1	1	0.333719
1	bhv	BAGLconnFromPos3	0.530963	3	3	2.205007
2	bhv	BAGLconnFromPos3	4.44E-16	1	3	74.58049
3	bhv	BAGLconnFromPos3	0	3	3	785.8092
4	bhv	BAGLconnFromPos3	0	3	3	315.0905
5	bhv	BAGLconnFromPos3	0	1	3	306.5793
6	bhv	BAGLconnFromPos3	0	1	3	726.7748
7	bhv	BAGLconnFromPos3	0	1	3	125.6072
1	FWD	BAGLconnFromPos3	0.36935	2	1	0.805851
2	FWD	BAGLconnFromPos3	3.19E-12	1	1	48.57108
3	FWD	BAGLconnFromPos3	0	2	1	784.0925
4	FWD	BAGLconnFromPos3	0	2	1	312.3635
5	FWD	BAGLconnFromPos3	0	1	1	253.808
6	FWD	BAGLconnFromPos3	0	1	1	378.5621
7	FWD	BAGLconnFromPos3	0	1	1	90.66841
1	Stim	BAGLconnFromPos3	0.006857	2	1	7.310053
2	Stim	BAGLconnFromPos3	9.64E-11	2	1	41.89223
3	Stim	BAGLconnFromPos3	0	1	1	77.18278
4	Stim	BAGLconnFromPos3	0	2	1	124.9179
5	Stim	BAGLconnFromPos3	0	2	1	420.0473
6	Stim	BAGLconnFromPos3	0	2	1	136.8379
7	Stim	BAGLconnFromPos3	0	2	1	511.749
1	StimDetailed	BAGLconnFromPos3	0	1	1	82.61539
2	StimDetailed	BAGLconnFromPos3	0.000185	1	1	13.97792
3	StimDetailed	BAGLconnFromPos3	3.35E-13	1	1	52.99006
4	StimDetailed	BAGLconnFromPos3	0	1	1	444.1357
5	StimDetailed	BAGLconnFromPos3	0	2	1	853.7878
6	StimDetailed	BAGLconnFromPos3	0	1	1	111.7575
7	StimDetailed	BAGLconnFromPos3	0	1	1	405.762
1	bhv	BAGLconnTo	0.153422	3	3	5.264503
2	bhv	BAGLconnTo	0.852213	1	3	0.788512
3	bhv	BAGLconnTo	0.86671	1	3	0.727532
4	bhv	BAGLconnTo	0.007016	3	3	12.1099
5	bhv	BAGLconnTo	0.004201	3	3	13.21129
6	bhv	BAGLconnTo	0	3	3	91.45084
7	bhv	BAGLconnTo	0.760397	3	3	1.169215
1	FWD	BAGLconnTo	0.455954	2	1	0.555808
2	FWD	BAGLconnTo	0.374551	1	1	0.788512
3	FWD	BAGLconnTo	0.393684	1	1	0.727532
4	FWD	BAGLconnTo	0.521763	2	1	0.410406
5	FWD	BAGLconnTo	0.104907	2	1	2.629308
6	FWD	BAGLconnTo	3.02E-09	2	1	35.17096
7	FWD	BAGLconnTo	0.390819	2	1	0.736392
1	Stim	BAGLconnTo	0.3172	2	1	1.000455
2	Stim	BAGLconnTo	0.316951	2	1	1.001489

3	Stim	BAGLconnTo	0.31698	2	1	1.001367
4	Stim	BAGLconnTo	0.317191	2	1	1.000496
5	Stim	BAGLconnTo	0.045206	2	1	4.010926
6	Stim	BAGLconnTo	0	2	1	99.79453
7	Stim	BAGLconnTo	0.31743	1	1	0.999505
1	StimDetailed	BAGLconnTo	0.563378	1	1	0.33389
2	StimDetailed	BAGLconnTo	0.56322	1	1	0.33416
3	StimDetailed	BAGLconnTo	0.56468	1	1	0.331666
4	StimDetailed	BAGLconnTo	0.563349	1	1	0.333939
5	StimDetailed	BAGLconnTo	0.247926	1	1	1.334952
6	StimDetailed	BAGLconnTo	7.91E-09	1	1	33.29781
7	StimDetailed	BAGLconnTo	0.563477	1	1	0.333719
1	bhv	BAGLconnTo3	0	3	3	82.77762
2	bhv	BAGLconnTo3	0.852213	1	3	0.788512
3	bhv	BAGLconnTo3	1.49E-07	1	3	34.59181
4	bhv	BAGLconnTo3	0	3	3	344.1666
5	bhv	BAGLconnTo3	0	1	3	469.5483
6	bhv	BAGLconnTo3	0	1	3	1256.707
7	bhv	BAGLconnTo3	0	3	3	174.5673
1	FWD	BAGLconnTo3	1.68E-14	2	1	58.88097
2	FWD	BAGLconnTo3	0.374551	1	1	0.788512
3	FWD	BAGLconnTo3	2.54E-08	1	1	31.03315
4	FWD	BAGLconnTo3	0	2	1	342.8264
5	FWD	BAGLconnTo3	0	1	1	449.5595
6	FWD	BAGLconnTo3	0	1	1	756.9948
7	FWD	BAGLconnTo3	0	2	1	173.9562
1	Stim	BAGLconnTo3	0.403364	1	1	0.698274
2	Stim	BAGLconnTo3	0.316951	2	1	1.001489
3	Stim	BAGLconnTo3	0.236329	1	1	1.402361
4	Stim	BAGLconnTo3	0.003525	2	1	8.51377
5	Stim	BAGLconnTo3	0	2	1	659.1007
6	Stim	BAGLconnTo3	2.34E-09	2	1	35.66844
7	Stim	BAGLconnTo3	0	2	1	130.3942
1	StimDetailed	BAGLconnTo3	4.44E-13	1	1	52.43667
2	StimDetailed	BAGLconnTo3	0.56322	1	1	0.33416
3	StimDetailed	BAGLconnTo3	0.00449	1	1	8.074173
4	StimDetailed	BAGLconnTo3	0	1	1	109.5453
5	StimDetailed	BAGLconnTo3	0	2	1	560.7455
6	StimDetailed	BAGLconnTo3	0.010911	1	1	6.479725
7	StimDetailed	BAGLconnTo3	1.67E-10	1	1	40.82013
1	bhv	BAGLconnToNeg	0.000985	3	3	16.29781
2	bhv	BAGLconnToNeg	NaN	1	3	NaN
3	bhv	BAGLconnToNeg	NaN	1	3	NaN
4	bhv	BAGLconnToNeg	NaN	1	3	NaN
5	bhv	BAGLconnToNeg	4.99E-10	3	3	46.26315
6	bhv	BAGLconnToNeg	NaN	1	3	NaN
7	bhv	BAGLconnToNeg	2.04E-10	1	3	48.09132
1	FWD	BAGLconnToNeg	0.002475	2	1	9.158899
2	FWD	BAGLconnToNeg	NaN	1	1	NaN
3	FWD	BAGLconnToNeg	NaN	1	1	NaN

4	FWD	BAGLconnToNeg	NaN	1	1	NaN
5	FWD	BAGLconnToNeg	3.86E-10	2	1	39.18124
6	FWD	BAGLconnToNeg	NaN	1	1	NaN
7	FWD	BAGLconnToNeg	0.111068	1	1	2.53896
1	Stim	BAGLconnToNeg	4.60E-12	1	1	47.85242
2	Stim	BAGLconnToNeg	NaN	1	1	NaN
3	Stim	BAGLconnToNeg	NaN	1	1	NaN
4	Stim	BAGLconnToNeg	NaN	1	1	NaN
5	Stim	BAGLconnToNeg	2.79E-10	1	1	39.81288
6	Stim	BAGLconnToNeg	NaN	1	1	NaN
7	Stim	BAGLconnToNeg	3.37E-08	2	1	30.48267
5	StimDetailed	BAGLconnToNeg	0.064316	1	1	3.422428
5	StimDetailed	BAGLconnToNeg	0.064316	1	1	3.422428
7	StimDetailed	BAGLconnToNeg	0	2	1	91.29716
7	StimDetailed	BAGLconnToNeg	0	2	1	91.29716
1	bhv	BAGLconnToNeg3	1.04E-12	3	3	58.83325
2	bhv	BAGLconnToNeg3	NaN	1	3	NaN
3	bhv	BAGLconnToNeg3	NaN	1	3	NaN
4	bhv	BAGLconnToNeg3	NaN	1	3	NaN
5	bhv	BAGLconnToNeg3	8.62E-14	4	3	63.90237
6	bhv	BAGLconnToNeg3	NaN	1	3	NaN
7	bhv	BAGLconnToNeg3	NaN	1	3	NaN
1	FWD	BAGLconnToNeg3	1.20E-12	2	1	50.47947
2	FWD	BAGLconnToNeg3	NaN	1	1	NaN
3	FWD	BAGLconnToNeg3	NaN	1	1	NaN
4	FWD	BAGLconnToNeg3	NaN	1	1	NaN
5	FWD	BAGLconnToNeg3	0.010248	2	1	6.591271
6	FWD	BAGLconnToNeg3	NaN	1	1	NaN
7	FWD	BAGLconnToNeg3	NaN	1	1	NaN
1	Stim	BAGLconnToNeg3	0	1	1	118.8466
2	Stim	BAGLconnToNeg3	NaN	1	1	NaN
3	Stim	BAGLconnToNeg3	NaN	1	1	NaN
4	Stim	BAGLconnToNeg3	NaN	1	1	NaN
5	Stim	BAGLconnToNeg3	0.001535	2	1	10.03652
6	Stim	BAGLconnToNeg3	NaN	1	1	NaN
7	Stim	BAGLconnToNeg3	NaN	1	1	NaN
5	StimDetailed	BAGLconnToNeg3	3.99E-08	2	1	30.15519
5	StimDetailed	BAGLconnToNeg3	3.99E-08	2	1	30.15519
7	StimDetailed	BAGLconnToNeg3	NaN	1	1	NaN
7	StimDetailed	BAGLconnToNeg3	NaN	1	1	NaN
1	bhv	BAGLconnToPos	0.153422	3	3	5.264503
2	bhv	BAGLconnToPos	0.852213	1	3	0.788512
3	bhv	BAGLconnToPos	0.86671	1	3	0.727532
4	bhv	BAGLconnToPos	0.007016	3	3	12.1099
5	bhv	BAGLconnToPos	1.19E-11	3	3	53.87812
6	bhv	BAGLconnToPos	0	3	3	91.45084
7	bhv	BAGLconnToPos	0.760397	3	3	1.169215
1	FWD	BAGLconnToPos	0.455954	2	1	0.555808
2	FWD	BAGLconnToPos	0.374551	1	1	0.788512
3	FWD	BAGLconnToPos	0.393684	1	1	0.727532

4	FWD	BAGLconnToPos	0.521763	2	1	0.410406
5	FWD	BAGLconnToPos	0.020803	2	1	5.343192
6	FWD	BAGLconnToPos	3.02E-09	2	1	35.17096
7	FWD	BAGLconnToPos	0.390819	2	1	0.736392
1	Stim	BAGLconnToPos	0.3172	2	1	1.000455
2	Stim	BAGLconnToPos	0.316951	2	1	1.001489
3	Stim	BAGLconnToPos	0.31698	2	1	1.001367
4	Stim	BAGLconnToPos	0.317191	2	1	1.000496
5	Stim	BAGLconnToPos	8.30E-07	2	1	24.28664
6	Stim	BAGLconnToPos	0	2	1	99.79453
7	Stim	BAGLconnToPos	0.31743	1	1	0.999505
1	StimDetailed	BAGLconnToPos	0.563378	1	1	0.33389
2	StimDetailed	BAGLconnToPos	0.56322	1	1	0.33416
3	StimDetailed	BAGLconnToPos	0.56468	1	1	0.331666
4	StimDetailed	BAGLconnToPos	0.563349	1	1	0.333939
5	StimDetailed	BAGLconnToPos	0.004468	1	1	8.083296
6	StimDetailed	BAGLconnToPos	7.91E-09	1	1	33.29781
7	StimDetailed	BAGLconnToPos	0.563477	1	1	0.333719
1	bhv	BAGLconnToPos3	3.33E-16	3	3	75.11481
2	bhv	BAGLconnToPos3	0.852213	1	3	0.788512
3	bhv	BAGLconnToPos3	1.49E-07	1	3	34.59181
4	bhv	BAGLconnToPos3	0	3	3	344.1666
5	bhv	BAGLconnToPos3	0	1	3	469.5483
6	bhv	BAGLconnToPos3	0	1	3	1256.707
7	bhv	BAGLconnToPos3	0	3	3	174.5673
1	FWD	BAGLconnToPos3	6.11E-15	2	1	60.85144
2	FWD	BAGLconnToPos3	0.374551	1	1	0.788512
3	FWD	BAGLconnToPos3	2.54E-08	1	1	31.03315
4	FWD	BAGLconnToPos3	0	2	1	342.8264
5	FWD	BAGLconnToPos3	0	1	1	449.5595
6	FWD	BAGLconnToPos3	0	1	1	756.9948
7	FWD	BAGLconnToPos3	0	2	1	173.9562
1	Stim	BAGLconnToPos3	0.482755	2	1	0.492633
2	Stim	BAGLconnToPos3	0.316951	2	1	1.001489
3	Stim	BAGLconnToPos3	0.236329	1	1	1.402361
4	Stim	BAGLconnToPos3	0.003525	2	1	8.51377
5	Stim	BAGLconnToPos3	0	2	1	659.1007
6	Stim	BAGLconnToPos3	2.34E-09	2	1	35.66844
7	Stim	BAGLconnToPos3	0	2	1	130.3942
1	StimDetailed	BAGLconnToPos3	3.11E-15	1	1	62.16386
2	StimDetailed	BAGLconnToPos3	0.56322	1	1	0.33416
3	StimDetailed	BAGLconnToPos3	0.00449	1	1	8.074173
4	StimDetailed	BAGLconnToPos3	0	1	1	109.5453
5	StimDetailed	BAGLconnToPos3	0	2	1	560.7455
6	StimDetailed	BAGLconnToPos3	0.010911	1	1	6.479725
7	StimDetailed	BAGLconnToPos3	1.67E-10	1	1	40.82013
1	bhv	BAGLyhat	0	3	3	150.0971
2	bhv	BAGLyhat	0	1	3	246.4557
3	bhv	BAGLyhat	0	3	3	1205.009
4	bhv	BAGLyhat	0	3	3	401.6204

5	bhv	BAGLyhat	0	1	3	119.0088
6	bhv	BAGLyhat	5.92E-13	3	3	59.98423
7	bhv	BAGLyhat	0	1	3	85.96362
1	FWD	BAGLyhat	0.082548	2	1	3.014013
2	FWD	BAGLyhat	0	2	1	130.3386
3	FWD	BAGLyhat	0	2	1	1091.556
4	FWD	BAGLyhat	0	2	1	327.1118
5	FWD	BAGLyhat	5.00E-15	2	1	61.26463
6	FWD	BAGLyhat	0.000592	2	1	11.80111
7	FWD	BAGLyhat	1.82E-10	2	1	40.65017
1	Stim	BAGLyhat	1.80E-09	2	1	36.18016
2	Stim	BAGLyhat	4.44E-16	2	1	66.05092
3	Stim	BAGLyhat	0.000431	2	1	12.39183
4	Stim	BAGLyhat	0	2	1	214.551
5	Stim	BAGLyhat	0	2	1	681.7921
6	Stim	BAGLyhat	0	2	1	715.1217
7	Stim	BAGLyhat	0	2	1	203.5076
1	StimDetailed	BAGLyhat	0	1	1	108.9882
2	StimDetailed	BAGLyhat	0.028008	1	1	4.827558
3	StimDetailed	BAGLyhat	0	1	1	170.6217
4	StimDetailed	BAGLyhat	0	1	1	495.1841
5	StimDetailed	BAGLyhat	0	1	1	468.7295
6	StimDetailed	BAGLyhat	0	1	1	522.5093
7	StimDetailed	BAGLyhat	0	1	1	394.984
1	bhv	BAGLyhat3	1.57E-14	1	3	67.36783
2	bhv	BAGLyhat3	6.66E-16	4	3	73.78761
3	bhv	BAGLyhat3	0	1	3	106.9087
4	bhv	BAGLyhat3	0.000121	3	3	20.71101
5	bhv	BAGLyhat3	0	4	3	101.5347
6	bhv	BAGLyhat3	0	1	3	132.938
7	bhv	BAGLyhat3	0	1	3	97.04037
1	FWD	BAGLyhat3	1.44E-14	1	1	59.17059
2	FWD	BAGLyhat3	0.001411	2	1	10.19115
3	FWD	BAGLyhat3	0.190523	1	1	1.713573
4	FWD	BAGLyhat3	0.445287	2	1	0.582621
5	FWD	BAGLyhat3	0.798675	2	1	0.065056
6	FWD	BAGLyhat3	0	1	1	123.0829
7	FWD	BAGLyhat3	1.69E-11	1	1	45.29808
1	Stim	BAGLyhat3	6.88E-15	2	1	60.6274
2	Stim	BAGLyhat3	0.004616	2	1	8.023896
3	Stim	BAGLyhat3	1.11E-16	2	1	69.04463
4	Stim	BAGLyhat3	0	2	1	82.21867
5	Stim	BAGLyhat3	1.25E-11	2	1	45.89751
6	Stim	BAGLyhat3	0	2	1	79.97684
7	Stim	BAGLyhat3	0	2	1	94.29243
1	StimDetailed	BAGLyhat3	0	2	1	181.6617
2	StimDetailed	BAGLyhat3	0.998059	1	1	5.92E-06
3	StimDetailed	BAGLyhat3	0	2	1	208.4596
4	StimDetailed	BAGLyhat3	0	2	1	246.3304
5	StimDetailed	BAGLyhat3	0	2	1	137.9012

6	StimDetailed	BAGLyhat3	0	2	1	239.693
7	StimDetailed	BAGLyhat3	0	2	1	265.9205
1	bhv	BAGRconnFrom	0.153422	3	3	5.264503
2	bhv	BAGRconnFrom	0.852213	1	3	0.788512
3	bhv	BAGRconnFrom	0.86671	1	3	0.727532
4	bhv	BAGRconnFrom	0.133764	3	3	5.582888
5	bhv	BAGRconnFrom	0.004201	3	3	13.21129
6	bhv	BAGRconnFrom	0	3	3	102.6272
7	bhv	BAGRconnFrom	0.760397	3	3	1.169215
1	FWD	BAGRconnFrom	0.455954	2	1	0.555808
2	FWD	BAGRconnFrom	0.374551	1	1	0.788512
3	FWD	BAGRconnFrom	0.393684	1	1	0.727532
4	FWD	BAGRconnFrom	0.364824	2	1	0.821219
5	FWD	BAGRconnFrom	0.104907	2	1	2.629308
6	FWD	BAGRconnFrom	3.33E-10	2	1	39.46928
7	FWD	BAGRconnFrom	0.390819	2	1	0.736392
1	Stim	BAGRconnFrom	0.3172	2	1	1.000455
2	Stim	BAGRconnFrom	0.316951	2	1	1.001489
3	Stim	BAGRconnFrom	0.31698	2	1	1.001367
4	Stim	BAGRconnFrom	0.157093	2	1	2.001984
5	Stim	BAGRconnFrom	0.045206	2	1	4.010926
6	Stim	BAGRconnFrom	0	2	1	111.9906
7	Stim	BAGRconnFrom	0.31743	1	1	0.999505
1	StimDetailed	BAGRconnFrom	0.563378	1	1	0.33389
2	StimDetailed	BAGRconnFrom	0.56322	1	1	0.33416
3	StimDetailed	BAGRconnFrom	0.56468	1	1	0.331666
4	StimDetailed	BAGRconnFrom	0.413676	1	1	0.66821
5	StimDetailed	BAGRconnFrom	0.247926	1	1	1.334952
6	StimDetailed	BAGRconnFrom	9.79E-10	1	1	37.36721
7	StimDetailed	BAGRconnFrom	0.563477	1	1	0.333719
1	bhv	BAGRconnFrom3	7.59E-08	3	3	35.97162
2	bhv	BAGRconnFrom3	0.861703	1	3	0.748663
3	bhv	BAGRconnFrom3	0	3	3	798.0366
4	bhv	BAGRconnFrom3	0	3	3	394.8619
5	bhv	BAGRconnFrom3	0	1	3	292.6434
6	bhv	BAGRconnFrom3	0	1	3	673.6905
7	bhv	BAGRconnFrom3	0	1	3	80.29296
1	FWD	BAGRconnFrom3	1.50E-06	2	1	23.14471
2	FWD	BAGRconnFrom3	0.865917	1	1	0.028509
3	FWD	BAGRconnFrom3	0	2	1	796.9195
4	FWD	BAGRconnFrom3	0	2	1	391.6893
5	FWD	BAGRconnFrom3	0	1	1	239.5775
6	FWD	BAGRconnFrom3	0	1	1	330.378
7	FWD	BAGRconnFrom3	1.07E-13	1	1	55.22841
1	Stim	BAGRconnFrom3	1.44E-15	1	1	63.77727
2	Stim	BAGRconnFrom3	0.156888	2	1	2.003971
3	Stim	BAGRconnFrom3	0	1	1	83.96648
4	Stim	BAGRconnFrom3	0	2	1	85.08102
5	Stim	BAGRconnFrom3	0	2	1	404.9418
6	Stim	BAGRconnFrom3	0	2	1	118.7458

7	Stim	BAGRconnFrom3	0	2	1	573.3883
1	StimDetailed	BAGRconnFrom3	1.56E-07	1	1	27.51819
2	StimDetailed	BAGRconnFrom3	0.413522	1	1	0.668652
3	StimDetailed	BAGRconnFrom3	1.82E-12	1	1	49.66789
4	StimDetailed	BAGRconnFrom3	0	1	1	398.2547
5	StimDetailed	BAGRconnFrom3	0	2	1	869.6359
6	StimDetailed	BAGRconnFrom3	0	1	1	141.235
7	StimDetailed	BAGRconnFrom3	0	1	1	425.5057
1	bhv	BAGRconnFromNeg	0.044429	3	3	8.077887
2	bhv	BAGRconnFromNeg	NaN	1	3	NaN
3	bhv	BAGRconnFromNeg	NaN	1	3	NaN
4	bhv	BAGRconnFromNeg	NaN	1	3	NaN
5	bhv	BAGRconnFromNeg	6.26E-12	2	3	55.18754
6	bhv	BAGRconnFromNeg	NaN	1	3	NaN
7	bhv	BAGRconnFromNeg	NaN	1	3	NaN
1	FWD	BAGRconnFromNeg	0.266248	2	1	1.235974
2	FWD	BAGRconnFromNeg	NaN	1	1	NaN
3	FWD	BAGRconnFromNeg	NaN	1	1	NaN
4	FWD	BAGRconnFromNeg	NaN	1	1	NaN
5	FWD	BAGRconnFromNeg	0.104907	2	1	2.629308
6	FWD	BAGRconnFromNeg	NaN	1	1	NaN
7	FWD	BAGRconnFromNeg	NaN	1	1	NaN
1	Stim	BAGRconnFromNeg	1.25E-07	1	1	27.93786
2	Stim	BAGRconnFromNeg	NaN	1	1	NaN
3	Stim	BAGRconnFromNeg	NaN	1	1	NaN
4	Stim	BAGRconnFromNeg	NaN	1	1	NaN
5	Stim	BAGRconnFromNeg	0.045206	1	1	4.010926
6	Stim	BAGRconnFromNeg	NaN	1	1	NaN
7	Stim	BAGRconnFromNeg	NaN	1	1	NaN
5	StimDetailed	BAGRconnFromNeg	0.247926	1	1	1.334952
7	StimDetailed	BAGRconnFromNeg	NaN	1	1	NaN
1	bhv	BAGRconnFromNeg3	3.33E-13	3	3	61.15418
2	bhv	BAGRconnFromNeg3	NaN	1	3	NaN
3	bhv	BAGRconnFromNeg3	NaN	1	3	NaN
4	bhv	BAGRconnFromNeg3	NaN	1	3	NaN
5	bhv	BAGRconnFromNeg3	NaN	1	3	NaN
6	bhv	BAGRconnFromNeg3	NaN	1	3	NaN
7	bhv	BAGRconnFromNeg3	NaN	1	3	NaN
1	FWD	BAGRconnFromNeg3	5.58E-13	2	1	51.98995
2	FWD	BAGRconnFromNeg3	NaN	1	1	NaN
3	FWD	BAGRconnFromNeg3	NaN	1	1	NaN
4	FWD	BAGRconnFromNeg3	NaN	1	1	NaN
5	FWD	BAGRconnFromNeg3	NaN	1	1	NaN
6	FWD	BAGRconnFromNeg3	NaN	1	1	NaN
7	FWD	BAGRconnFromNeg3	NaN	1	1	NaN
1	Stim	BAGRconnFromNeg3	0	1	1	116.6196
2	Stim	BAGRconnFromNeg3	NaN	1	1	NaN
3	Stim	BAGRconnFromNeg3	NaN	1	1	NaN
4	Stim	BAGRconnFromNeg3	NaN	1	1	NaN
5	Stim	BAGRconnFromNeg3	NaN	1	1	NaN

6	Stim	BAGRconnFromNeg3	NaN	1	1	NaN
7	Stim	BAGRconnFromNeg3	NaN	1	1	NaN
5	StimDetailed	BAGRconnFromNeg3	NaN	1	1	NaN
7	StimDetailed	BAGRconnFromNeg3	NaN	1	1	NaN
1	bhv	BAGRconnFromPos	0.153422	3	3	5.264503
2	bhv	BAGRconnFromPos	0.852213	1	3	0.788512
3	bhv	BAGRconnFromPos	0.86671	1	3	0.727532
4	bhv	BAGRconnFromPos	0.133764	3	3	5.582888
5	bhv	BAGRconnFromPos	6.90E-05	3	3	21.88323
6	bhv	BAGRconnFromPos	0	3	3	102.6272
7	bhv	BAGRconnFromPos	0.760397	3	3	1.169215
1	FWD	BAGRconnFromPos	0.455954	2	1	0.555808
2	FWD	BAGRconnFromPos	0.374551	1	1	0.788512
3	FWD	BAGRconnFromPos	0.393684	1	1	0.727532
4	FWD	BAGRconnFromPos	0.364824	2	1	0.821219
5	FWD	BAGRconnFromPos	0.031831	2	1	4.607581
6	FWD	BAGRconnFromPos	3.33E-10	2	1	39.46928
7	FWD	BAGRconnFromPos	0.390819	2	1	0.736392
1	Stim	BAGRconnFromPos	0.3172	2	1	1.000455
2	Stim	BAGRconnFromPos	0.316951	2	1	1.001489
3	Stim	BAGRconnFromPos	0.31698	2	1	1.001367
4	Stim	BAGRconnFromPos	0.157093	2	1	2.001984
5	Stim	BAGRconnFromPos	0.008021	2	1	7.028718
6	Stim	BAGRconnFromPos	0	2	1	111.9906
7	Stim	BAGRconnFromPos	0.31743	1	1	0.999505
1	StimDetailed	BAGRconnFromPos	0.563378	1	1	0.33389
2	StimDetailed	BAGRconnFromPos	0.56322	1	1	0.33416
3	StimDetailed	BAGRconnFromPos	0.56468	1	1	0.331666
4	StimDetailed	BAGRconnFromPos	0.413676	1	1	0.66821
5	StimDetailed	BAGRconnFromPos	0.126141	1	1	2.33936
6	StimDetailed	BAGRconnFromPos	9.79E-10	1	1	37.36721
7	StimDetailed	BAGRconnFromPos	0.563477	1	1	0.333719
1	bhv	BAGRconnFromPos3	3.60E-06	3	3	28.01632
2	bhv	BAGRconnFromPos3	0.861703	1	3	0.748663
3	bhv	BAGRconnFromPos3	0	3	3	798.0366
4	bhv	BAGRconnFromPos3	0	3	3	394.8619
5	bhv	BAGRconnFromPos3	0	1	3	292.6434
6	bhv	BAGRconnFromPos3	0	1	3	673.6905
7	bhv	BAGRconnFromPos3	0	1	3	80.29296
1	FWD	BAGRconnFromPos3	1.35E-07	2	1	27.79012
2	FWD	BAGRconnFromPos3	0.865917	1	1	0.028509
3	FWD	BAGRconnFromPos3	0	2	1	796.9195
4	FWD	BAGRconnFromPos3	0	2	1	391.6893
5	FWD	BAGRconnFromPos3	0	1	1	239.5775
6	FWD	BAGRconnFromPos3	0	1	1	330.378
7	FWD	BAGRconnFromPos3	1.07E-13	1	1	55.22841
1	Stim	BAGRconnFromPos3	1.84E-08	1	1	31.65146
2	Stim	BAGRconnFromPos3	0.156888	2	1	2.003971
3	Stim	BAGRconnFromPos3	0	1	1	83.96648
4	Stim	BAGRconnFromPos3	0	2	1	85.08102

5	Stim	BAGRconnFromPos3	0	2	1	404.9418
6	Stim	BAGRconnFromPos3	0	2	1	118.7458
7	Stim	BAGRconnFromPos3	0	2	1	573.3883
1	StimDetailed	BAGRconnFromPos3	6.48E-09	1	1	33.68641
2	StimDetailed	BAGRconnFromPos3	0.413522	1	1	0.668652
3	StimDetailed	BAGRconnFromPos3	1.82E-12	1	1	49.66789
4	StimDetailed	BAGRconnFromPos3	0	1	1	398.2547
5	StimDetailed	BAGRconnFromPos3	0	2	1	869.6359
6	StimDetailed	BAGRconnFromPos3	0	1	1	141.235
7	StimDetailed	BAGRconnFromPos3	0	1	1	425.5057
1	bhv	BAGRconnTo	0.153422	3	3	5.264503
2	bhv	BAGRconnTo	0.852213	1	3	0.788512
3	bhv	BAGRconnTo	0.86671	1	3	0.727532
4	bhv	BAGRconnTo	0.007016	3	3	12.1099
5	bhv	BAGRconnTo	0.004201	3	3	13.21129
6	bhv	BAGRconnTo	0.821141	3	3	0.917755
7	bhv	BAGRconnTo	0.760397	3	3	1.169215
1	FWD	BAGRconnTo	0.455954	2	1	0.555808
2	FWD	BAGRconnTo	0.374551	1	1	0.788512
3	FWD	BAGRconnTo	0.393684	1	1	0.727532
4	FWD	BAGRconnTo	0.521763	2	1	0.410406
5	FWD	BAGRconnTo	0.104907	2	1	2.629308
6	FWD	BAGRconnTo	0.552443	2	1	0.352958
7	FWD	BAGRconnTo	0.390819	2	1	0.736392
1	Stim	BAGRconnTo	0.3172	2	1	1.000455
2	Stim	BAGRconnTo	0.316951	2	1	1.001489
3	Stim	BAGRconnTo	0.31698	2	1	1.001367
4	Stim	BAGRconnTo	0.317191	2	1	1.000496
5	Stim	BAGRconnTo	0.045206	2	1	4.010926
6	Stim	BAGRconnTo	0.316951	2	1	1.001489
7	Stim	BAGRconnTo	0.31743	1	1	0.999505
1	StimDetailed	BAGRconnTo	0.563378	1	1	0.33389
2	StimDetailed	BAGRconnTo	0.56322	1	1	0.33416
3	StimDetailed	BAGRconnTo	0.56468	1	1	0.331666
4	StimDetailed	BAGRconnTo	0.563349	1	1	0.333939
5	StimDetailed	BAGRconnTo	0.247926	1	1	1.334952
6	StimDetailed	BAGRconnTo	0.56322	1	1	0.33416
7	StimDetailed	BAGRconnTo	0.563477	1	1	0.333719
1	bhv	BAGRconnTo3	2.37E-06	3	3	28.88709
2	bhv	BAGRconnTo3	0.852213	1	3	0.788512
3	bhv	BAGRconnTo3	0.034043	1	3	8.668266
4	bhv	BAGRconnTo3	0	3	3	815.3059
5	bhv	BAGRconnTo3	0	1	3	266.4603
6	bhv	BAGRconnTo3	0	1	3	1313.302
7	bhv	BAGRconnTo3	0	3	3	232.6008
1	FWD	BAGRconnTo3	2.15E-07	2	1	26.89487
2	FWD	BAGRconnTo3	0.374551	1	1	0.788512
3	FWD	BAGRconnTo3	0.007863	1	1	7.064456
4	FWD	BAGRconnTo3	0	2	1	805.3392
5	FWD	BAGRconnTo3	0	1	1	240.268

6	FWD	BAGRconnTo3	0	1	1	771.4798
7	FWD	BAGRconnTo3	0	2	1	232.5979
1	Stim	BAGRconnTo3	4.21E-08	1	1	30.05113
2	Stim	BAGRconnTo3	0.316951	2	1	1.001489
3	Stim	BAGRconnTo3	0.007374	1	1	7.179508
4	Stim	BAGRconnTo3	0.308309	2	1	1.037908
5	Stim	BAGRconnTo3	0	2	1	640.8911
6	Stim	BAGRconnTo3	1.96E-08	2	1	31.53523
7	Stim	BAGRconnTo3	0	2	1	174.7778
1	StimDetailed	BAGRconnTo3	1.04E-08	1	1	32.77293
2	StimDetailed	BAGRconnTo3	0.56322	1	1	0.33416
3	StimDetailed	BAGRconnTo3	0.000628	1	1	11.69025
4	StimDetailed	BAGRconnTo3	0	1	1	140.133
5	StimDetailed	BAGRconnTo3	0	2	1	599.8086
6	StimDetailed	BAGRconnTo3	0.006914	1	1	7.295128
7	StimDetailed	BAGRconnTo3	2.19E-14	1	1	58.35553
1	bhv	BAGRconnToNeg	0.000985	3	3	16.29781
2	bhv	BAGRconnToNeg	NaN	1	3	NaN
3	bhv	BAGRconnToNeg	NaN	1	3	NaN
4	bhv	BAGRconnToNeg	NaN	1	3	NaN
5	bhv	BAGRconnToNeg	1.10E-13	4	3	63.41412
6	bhv	BAGRconnToNeg	NaN	1	3	NaN
7	bhv	BAGRconnToNeg	2.41E-14	1	3	66.48456
1	FWD	BAGRconnToNeg	0.002475	2	1	9.158899
2	FWD	BAGRconnToNeg	NaN	1	1	NaN
3	FWD	BAGRconnToNeg	NaN	1	1	NaN
4	FWD	BAGRconnToNeg	NaN	1	1	NaN
5	FWD	BAGRconnToNeg	6.25E-06	2	1	20.40971
6	FWD	BAGRconnToNeg	NaN	1	1	NaN
7	FWD	BAGRconnToNeg	0.023225	1	1	5.151569
1	Stim	BAGRconnToNeg	4.60E-12	1	1	47.85242
2	Stim	BAGRconnToNeg	NaN	1	1	NaN
3	Stim	BAGRconnToNeg	NaN	1	1	NaN
4	Stim	BAGRconnToNeg	NaN	1	1	NaN
5	Stim	BAGRconnToNeg	0.004038	1	1	8.2666
6	Stim	BAGRconnToNeg	NaN	1	1	NaN
7	Stim	BAGRconnToNeg	5.66E-11	2	1	42.93477
5	StimDetailed	BAGRconnToNeg	0.711202	1	1	0.13708
5	StimDetailed	BAGRconnToNeg	0.711202	1	1	0.13708
7	StimDetailed	BAGRconnToNeg	0	2	1	128.5918
7	StimDetailed	BAGRconnToNeg	0	2	1	128.5918
1	bhv	BAGRconnToNeg3	3.59E-13	3	3	61.00187
2	bhv	BAGRconnToNeg3	NaN	1	3	NaN
3	bhv	BAGRconnToNeg3	NaN	1	3	NaN
4	bhv	BAGRconnToNeg3	NaN	1	3	NaN
5	bhv	BAGRconnToNeg3	2.48E-08	4	3	38.27155
6	bhv	BAGRconnToNeg3	NaN	1	3	NaN
7	bhv	BAGRconnToNeg3	NaN	1	3	NaN
1	FWD	BAGRconnToNeg3	4.11E-13	2	1	52.5879
2	FWD	BAGRconnToNeg3	NaN	1	1	NaN

3	FWD	BAGRconnToNeg3	NaN	1	1	NaN
4	FWD	BAGRconnToNeg3	NaN	1	1	NaN
5	FWD	BAGRconnToNeg3	0.04694	2	1	3.947556
6	FWD	BAGRconnToNeg3	NaN	1	1	NaN
7	FWD	BAGRconnToNeg3	NaN	1	1	NaN
1	Stim	BAGRconnToNeg3	0	1	1	117.7325
2	Stim	BAGRconnToNeg3	NaN	1	1	NaN
3	Stim	BAGRconnToNeg3	NaN	1	1	NaN
4	Stim	BAGRconnToNeg3	NaN	1	1	NaN
5	Stim	BAGRconnToNeg3	0.014217	2	1	6.010936
6	Stim	BAGRconnToNeg3	NaN	1	1	NaN
7	Stim	BAGRconnToNeg3	NaN	1	1	NaN
5	StimDetailed	BAGRconnToNeg3	2.14E-05	2	1	18.06014
5	StimDetailed	BAGRconnToNeg3	2.14E-05	2	1	18.06014
7	StimDetailed	BAGRconnToNeg3	NaN	1	1	NaN
7	StimDetailed	BAGRconnToNeg3	NaN	1	1	NaN
1	bhv	BAGRconnToPos	0.153422	3	3	5.264503
2	bhv	BAGRconnToPos	0.852213	1	3	0.788512
3	bhv	BAGRconnToPos	0.86671	1	3	0.727532
4	bhv	BAGRconnToPos	0.007016	3	3	12.1099
5	bhv	BAGRconnToPos	2.59E-12	3	3	56.98301
6	bhv	BAGRconnToPos	0.821141	3	3	0.917755
7	bhv	BAGRconnToPos	0.760397	3	3	1.169215
1	FWD	BAGRconnToPos	0.455954	2	1	0.555808
2	FWD	BAGRconnToPos	0.374551	1	1	0.788512
3	FWD	BAGRconnToPos	0.393684	1	1	0.727532
4	FWD	BAGRconnToPos	0.521763	2	1	0.410406
5	FWD	BAGRconnToPos	0.002105	2	1	9.45589
6	FWD	BAGRconnToPos	0.552443	2	1	0.352958
7	FWD	BAGRconnToPos	0.390819	2	1	0.736392
1	Stim	BAGRconnToPos	0.3172	2	1	1.000455
2	Stim	BAGRconnToPos	0.316951	2	1	1.001489
3	Stim	BAGRconnToPos	0.31698	2	1	1.001367
4	Stim	BAGRconnToPos	0.317191	2	1	1.000496
5	Stim	BAGRconnToPos	1.19E-05	2	1	19.18287
6	Stim	BAGRconnToPos	0.316951	2	1	1.001489
7	Stim	BAGRconnToPos	0.31743	1	1	0.999505
1	StimDetailed	BAGRconnToPos	0.563378	1	1	0.33389
2	StimDetailed	BAGRconnToPos	0.56322	1	1	0.33416
3	StimDetailed	BAGRconnToPos	0.56468	1	1	0.331666
4	StimDetailed	BAGRconnToPos	0.563349	1	1	0.333939
5	StimDetailed	BAGRconnToPos	0.011511	1	1	6.384612
6	StimDetailed	BAGRconnToPos	0.56322	1	1	0.33416
7	StimDetailed	BAGRconnToPos	0.563477	1	1	0.333719
1	bhv	BAGRconnToPos3	1.84E-08	3	3	38.87753
2	bhv	BAGRconnToPos3	0.852213	1	3	0.788512
3	bhv	BAGRconnToPos3	0.034043	1	3	8.668266
4	bhv	BAGRconnToPos3	0	3	3	815.3059
5	bhv	BAGRconnToPos3	0	1	3	266.4603
6	bhv	BAGRconnToPos3	0	1	3	1313.302

7	bhv	BAGRconnToPos3	0	3	3	232.6008
1	FWD	BAGRconnToPos3	6.32E-08	2	1	29.2641
2	FWD	BAGRconnToPos3	0.374551	1	1	0.788512
3	FWD	BAGRconnToPos3	0.007863	1	1	7.064456
4	FWD	BAGRconnToPos3	0	2	1	805.3392
5	FWD	BAGRconnToPos3	0	1	1	240.268
6	FWD	BAGRconnToPos3	0	1	1	771.4798
7	FWD	BAGRconnToPos3	0	2	1	232.5979
1	Stim	BAGRconnToPos3	0.001868	1	1	9.67507
2	Stim	BAGRconnToPos3	0.316951	2	1	1.001489
3	Stim	BAGRconnToPos3	0.007374	1	1	7.179508
4	Stim	BAGRconnToPos3	0.308309	2	1	1.037908
5	Stim	BAGRconnToPos3	0	2	1	640.8911
6	Stim	BAGRconnToPos3	1.96E-08	2	1	31.53523
7	Stim	BAGRconnToPos3	0	2	1	174.7778
1	StimDetailed	BAGRconnToPos3	9.18E-11	1	1	41.98804
2	StimDetailed	BAGRconnToPos3	0.56322	1	1	0.33416
3	StimDetailed	BAGRconnToPos3	0.000628	1	1	11.69025
4	StimDetailed	BAGRconnToPos3	0	1	1	140.133
5	StimDetailed	BAGRconnToPos3	0	2	1	599.8086
6	StimDetailed	BAGRconnToPos3	0.006914	1	1	7.295128
7	StimDetailed	BAGRconnToPos3	2.19E-14	1	1	58.35553
1	bhv	BAGRyhat	0	1	3	133.4093
2	bhv	BAGRyhat	0	3	3	571.557
3	bhv	BAGRyhat	0	3	3	1214.179
4	bhv	BAGRyhat	0	3	3	524.8399
5	bhv	BAGRyhat	3.49E-13	3	3	61.06041
6	bhv	BAGRyhat	0	3	3	120.3225
7	bhv	BAGRyhat	1.47E-09	3	3	44.04825
1	FWD	BAGRyhat	2.35E-05	2	1	17.88393
2	FWD	BAGRyhat	0	2	1	397.5158
3	FWD	BAGRyhat	0	2	1	1091.556
4	FWD	BAGRyhat	0	2	1	378.6382
5	FWD	BAGRyhat	0.094266	2	1	2.799979
6	FWD	BAGRyhat	0.00011	2	1	14.95702
7	FWD	BAGRyhat	0.271371	2	1	1.209805
1	Stim	BAGRyhat	6.00E-07	2	1	24.91174
2	Stim	BAGRyhat	0	1	1	131.4951
3	Stim	BAGRyhat	0.020047	2	1	5.407786
4	Stim	BAGRyhat	0	2	1	137.1041
5	Stim	BAGRyhat	0	2	1	419.5913
6	Stim	BAGRyhat	0	2	1	439.0087
7	Stim	BAGRyhat	0	2	1	229.6988
1	StimDetailed	BAGRyhat	0	1	1	169.0113
2	StimDetailed	BAGRyhat	0.43315	1	1	0.614361
3	StimDetailed	BAGRyhat	0	1	1	162.9758
4	StimDetailed	BAGRyhat	0	1	1	472.5759
5	StimDetailed	BAGRyhat	0	1	1	539.4291
6	StimDetailed	BAGRyhat	0	1	1	463.2034
7	StimDetailed	BAGRyhat	0	1	1	476.4153

1	bhv	BAGRyhat3	6.99E-15	1	3	68.98668
2	bhv	BAGRyhat3	NaN	1	3	NaN
3	bhv	BAGRyhat3	0	1	3	108.2079
4	bhv	BAGRyhat3	9.75E-05	3	3	21.16052
5	bhv	BAGRyhat3	0	4	3	106.5017
6	bhv	BAGRyhat3	0	1	3	115.6404
7	bhv	BAGRyhat3	0	1	3	104.023
1	FWD	BAGRyhat3	5.88E-15	1	1	60.92229
2	FWD	BAGRyhat3	NaN	1	1	NaN
3	FWD	BAGRyhat3	0.225503	1	1	1.469003
4	FWD	BAGRyhat3	0.962007	2	1	0.002269
5	FWD	BAGRyhat3	0.521478	2	1	0.410969
6	FWD	BAGRyhat3	0	1	1	103.5235
7	FWD	BAGRyhat3	9.35E-11	1	1	41.95374
1	Stim	BAGRyhat3	4.00E-15	2	1	61.68382
2	Stim	BAGRyhat3	NaN	1	1	NaN
3	Stim	BAGRyhat3	1.11E-16	2	1	67.9822
4	Stim	BAGRyhat3	0	2	1	77.89501
5	Stim	BAGRyhat3	3.61E-11	2	1	43.81698
6	Stim	BAGRyhat3	0	2	1	74.5913
7	Stim	BAGRyhat3	0	2	1	96.48785
1	StimDetailed	BAGRyhat3	0	2	1	184.8271
2	StimDetailed	BAGRyhat3	NaN	1	1	NaN
3	StimDetailed	BAGRyhat3	0	2	1	205.2519
4	StimDetailed	BAGRyhat3	0	2	1	233.3765
5	StimDetailed	BAGRyhat3	0	2	1	131.6502
6	StimDetailed	BAGRyhat3	0	2	1	223.5523
7	StimDetailed	BAGRyhat3	0	2	1	272.4734
2	bhv	RIGLconnFrom3	0	1	3	112.807
3	bhv	RIGLconnFrom3	0	1	3	285.2349
4	bhv	RIGLconnFrom3	0	3	3	160.4864
6	bhv	RIGLconnFrom3	0	3	3	199.3679
2	FWD	RIGLconnFrom3	0	1	1	112.7293
3	FWD	RIGLconnFrom3	0	1	1	240.2124
4	FWD	RIGLconnFrom3	0	2	1	76.63883
6	FWD	RIGLconnFrom3	0	2	1	102.9789
2	Stim	RIGLconnFrom3	0	1	1	141.0149
3	Stim	RIGLconnFrom3	1.54E-14	1	1	59.04495
4	Stim	RIGLconnFrom3	4.76E-07	1	1	25.35942
6	Stim	RIGLconnFrom3	0	1	1	278.0465
2	StimDetailed	RIGLconnFrom3	0.014779	1	1	5.942574
3	StimDetailed	RIGLconnFrom3	1.78E-05	1	1	18.4078
4	StimDetailed	RIGLconnFrom3	0.683721	1	1	0.165968
6	StimDetailed	RIGLconnFrom3	0	1	1	80.89194
2	bhv	RIGLconnFromNeg	NaN	1	3	NaN
3	bhv	RIGLconnFromNeg	NaN	1	3	NaN
4	bhv	RIGLconnFromNeg	NaN	1	3	NaN
6	bhv	RIGLconnFromNeg	NaN	1	3	NaN
2	FWD	RIGLconnFromNeg	NaN	1	1	NaN
3	FWD	RIGLconnFromNeg	NaN	1	1	NaN

4	FWD	RIGLconnFromNeg	NaN	1	1	NaN
6	FWD	RIGLconnFromNeg	NaN	1	1	NaN
2	Stim	RIGLconnFromNeg	NaN	1	1	NaN
3	Stim	RIGLconnFromNeg	NaN	1	1	NaN
4	Stim	RIGLconnFromNeg	NaN	1	1	NaN
6	Stim	RIGLconnFromNeg	NaN	1	1	NaN
2	bhv	RIGLconnFromNeg3	NaN	1	3	NaN
3	bhv	RIGLconnFromNeg3	NaN	1	3	NaN
4	bhv	RIGLconnFromNeg3	NaN	1	3	NaN
6	bhv	RIGLconnFromNeg3	NaN	1	3	NaN
2	FWD	RIGLconnFromNeg3	NaN	1	1	NaN
3	FWD	RIGLconnFromNeg3	NaN	1	1	NaN
4	FWD	RIGLconnFromNeg3	NaN	1	1	NaN
6	FWD	RIGLconnFromNeg3	NaN	1	1	NaN
2	Stim	RIGLconnFromNeg3	NaN	1	1	NaN
3	Stim	RIGLconnFromNeg3	NaN	1	1	NaN
4	Stim	RIGLconnFromNeg3	NaN	1	1	NaN
6	Stim	RIGLconnFromNeg3	NaN	1	1	NaN
2	bhv	RIGLconnFromPos	0.852213	1	3	0.788512
3	bhv	RIGLconnFromPos	0.010611	1	3	11.21651
4	bhv	RIGLconnFromPos	0.007016	3	3	12.1099
6	bhv	RIGLconnFromPos	0.821141	3	3	0.917755
2	FWD	RIGLconnFromPos	0.374551	1	1	0.788512
3	FWD	RIGLconnFromPos	0.820963	1	1	0.051215
4	FWD	RIGLconnFromPos	0.521763	2	1	0.410406
6	FWD	RIGLconnFromPos	0.552443	2	1	0.352958
2	Stim	RIGLconnFromPos	0.316951	2	1	1.001489
3	Stim	RIGLconnFromPos	0.156921	2	1	2.003645
4	Stim	RIGLconnFromPos	0.317191	2	1	1.000496
6	Stim	RIGLconnFromPos	0.316951	2	1	1.001489
2	StimDetailed	RIGLconnFromPos	0.56322	1	1	0.33416
3	StimDetailed	RIGLconnFromPos	0.41528	1	1	0.663634
4	StimDetailed	RIGLconnFromPos	0.563349	1	1	0.333939
6	StimDetailed	RIGLconnFromPos	0.56322	1	1	0.33416
2	bhv	RIGLconnFromPos3	0	1	3	112.807
3	bhv	RIGLconnFromPos3	0	1	3	285.2349
4	bhv	RIGLconnFromPos3	0	3	3	160.4864
6	bhv	RIGLconnFromPos3	0	3	3	199.3679
2	FWD	RIGLconnFromPos3	0	1	1	112.7293
3	FWD	RIGLconnFromPos3	0	1	1	240.2124
4	FWD	RIGLconnFromPos3	0	2	1	76.63883
6	FWD	RIGLconnFromPos3	0	2	1	102.9789
2	Stim	RIGLconnFromPos3	0	1	1	141.0149
3	Stim	RIGLconnFromPos3	1.54E-14	1	1	59.04495
4	Stim	RIGLconnFromPos3	4.76E-07	1	1	25.35942
6	Stim	RIGLconnFromPos3	0	1	1	278.0465
2	StimDetailed	RIGLconnFromPos3	0.014779	1	1	5.942574
3	StimDetailed	RIGLconnFromPos3	1.78E-05	1	1	18.4078
4	StimDetailed	RIGLconnFromPos3	0.683721	1	1	0.165968
6	StimDetailed	RIGLconnFromPos3	0	1	1	80.89194

2	bhv	RIGLconnTo3	0.852213	1	3	0.788512
3	bhv	RIGLconnTo3	0.86671	1	3	0.727532
4	bhv	RIGLconnTo3	0.007016	3	3	12.1099
6	bhv	RIGLconnTo3	1.47E-08	3	3	39.34592
2	FWD	RIGLconnTo3	0.374551	1	1	0.788512
3	FWD	RIGLconnTo3	0.393684	1	1	0.727532
4	FWD	RIGLconnTo3	0.521763	2	1	0.410406
6	FWD	RIGLconnTo3	0.0001	2	1	15.132
2	Stim	RIGLconnTo3	0.316951	2	1	1.001489
3	Stim	RIGLconnTo3	0.31698	2	1	1.001367
4	Stim	RIGLconnTo3	0.317191	2	1	1.000496
6	Stim	RIGLconnTo3	4.54E-10	1	1	38.86488
2	StimDetailed	RIGLconnTo3	0.56322	1	1	0.33416
3	StimDetailed	RIGLconnTo3	0.56468	1	1	0.331666
4	StimDetailed	RIGLconnTo3	0.563349	1	1	0.333939
6	StimDetailed	RIGLconnTo3	0.048377	1	1	3.89685
2	bhv	RIGLconnToNeg	NaN	1	3	NaN
3	bhv	RIGLconnToNeg	NaN	1	3	NaN
4	bhv	RIGLconnToNeg	NaN	1	3	NaN
6	bhv	RIGLconnToNeg	NaN	1	3	NaN
2	FWD	RIGLconnToNeg	NaN	1	1	NaN
3	FWD	RIGLconnToNeg	NaN	1	1	NaN
4	FWD	RIGLconnToNeg	NaN	1	1	NaN
6	FWD	RIGLconnToNeg	NaN	1	1	NaN
2	Stim	RIGLconnToNeg	NaN	1	1	NaN
3	Stim	RIGLconnToNeg	NaN	1	1	NaN
4	Stim	RIGLconnToNeg	NaN	1	1	NaN
6	Stim	RIGLconnToNeg	NaN	1	1	NaN
2	bhv	RIGLconnToNeg3	NaN	1	3	NaN
3	bhv	RIGLconnToNeg3	NaN	1	3	NaN
4	bhv	RIGLconnToNeg3	NaN	1	3	NaN
6	bhv	RIGLconnToNeg3	NaN	1	3	NaN
2	FWD	RIGLconnToNeg3	NaN	1	1	NaN
3	FWD	RIGLconnToNeg3	NaN	1	1	NaN
4	FWD	RIGLconnToNeg3	NaN	1	1	NaN
6	FWD	RIGLconnToNeg3	NaN	1	1	NaN
2	Stim	RIGLconnToNeg3	NaN	1	1	NaN
3	Stim	RIGLconnToNeg3	NaN	1	1	NaN
4	Stim	RIGLconnToNeg3	NaN	1	1	NaN
6	Stim	RIGLconnToNeg3	NaN	1	1	NaN
2	bhv	RIGLconnToPos	0.852213	1	3	0.788512
3	bhv	RIGLconnToPos	0.86671	1	3	0.727532
4	bhv	RIGLconnToPos	0.007016	3	3	12.1099
6	bhv	RIGLconnToPos	0.821141	3	3	0.917755
2	FWD	RIGLconnToPos	0.374551	1	1	0.788512
3	FWD	RIGLconnToPos	0.393684	1	1	0.727532
4	FWD	RIGLconnToPos	0.521763	2	1	0.410406
6	FWD	RIGLconnToPos	0.552443	2	1	0.352958
2	Stim	RIGLconnToPos	0.316951	2	1	1.001489
3	Stim	RIGLconnToPos	0.31698	2	1	1.001367

4	Stim	RIGLconnToPos	0.317191	2	1	1.000496
6	Stim	RIGLconnToPos	0.316951	2	1	1.001489
2	StimDetailed	RIGLconnToPos	0.56322	1	1	0.33416
3	StimDetailed	RIGLconnToPos	0.56468	1	1	0.331666
4	StimDetailed	RIGLconnToPos	0.563349	1	1	0.333939
6	StimDetailed	RIGLconnToPos	0.56322	1	1	0.33416
2	bhv	RIGLconnToPos3	0.852213	1	3	0.788512
3	bhv	RIGLconnToPos3	0.86671	1	3	0.727532
4	bhv	RIGLconnToPos3	0.007016	3	3	12.1099
6	bhv	RIGLconnToPos3	1.47E-08	3	3	39.34592
2	FWD	RIGLconnToPos3	0.374551	1	1	0.788512
3	FWD	RIGLconnToPos3	0.393684	1	1	0.727532
4	FWD	RIGLconnToPos3	0.521763	2	1	0.410406
6	FWD	RIGLconnToPos3	0.0001	2	1	15.132
2	Stim	RIGLconnToPos3	0.316951	2	1	1.001489
3	Stim	RIGLconnToPos3	0.31698	2	1	1.001367
4	Stim	RIGLconnToPos3	0.317191	2	1	1.000496
6	Stim	RIGLconnToPos3	4.54E-10	1	1	38.86488
2	StimDetailed	RIGLconnToPos3	0.56322	1	1	0.33416
3	StimDetailed	RIGLconnToPos3	0.56468	1	1	0.331666
4	StimDetailed	RIGLconnToPos3	0.563349	1	1	0.333939
6	StimDetailed	RIGLconnToPos3	0.048377	1	1	3.89685
2	bhv	RIGLyhat	0	1	3	264.9874
3	bhv	RIGLyhat	0	1	3	472.0281
4	bhv	RIGLyhat	0	3	3	352.085
6	bhv	RIGLyhat	0	1	3	404.9562
2	FWD	RIGLyhat	0	2	1	87.48912
3	FWD	RIGLyhat	0	1	1	363.8374
4	FWD	RIGLyhat	0.259605	2	1	1.270864
6	FWD	RIGLyhat	0	2	1	286.4555
2	Stim	RIGLyhat	0	1	1	175.521
3	Stim	RIGLyhat	0	1	1	86.12903
4	Stim	RIGLyhat	1.57E-05	1	1	18.65015
6	Stim	RIGLyhat	4.61E-05	1	1	16.60347
2	StimD	RIGLyhat	0.375292	1	1	0.786067
3	StimD	RIGLyhat	0.041838	1	1	4.141763
4	StimD	RIGLyhat	1.33E-10	1	1	41.26776
6	StimD	RIGLyhat	0.055553	1	1	3.665423
2	bhv	RIGLyhat3	NaN	1	3	NaN
3	bhv	RIGLyhat3	NaN	1	3	NaN
4	bhv	RIGLyhat3	0.00021	3	3	19.5572
6	bhv	RIGLyhat3	0	1	3	103.9001
2	FWD	RIGLyhat3	NaN	1	1	NaN
3	FWD	RIGLyhat3	NaN	1	1	NaN
4	FWD	RIGLyhat3	0.023014	2	1	5.167429
6	FWD	RIGLyhat3	0	1	1	103.9001
2	Stim	RIGLyhat3	NaN	1	1	NaN
3	Stim	RIGLyhat3	NaN	1	1	NaN
4	Stim	RIGLyhat3	1.61E-13	2	1	54.42952
6	Stim	RIGLyhat3	1.44E-09	2	1	36.61789

2	StimD	RIGLyhat3	NaN	1	1	NaN
3	StimD	RIGLyhat3	NaN	1	1	NaN
4	StimD	RIGLyhat3	0	2	1	163.073
6	StimD	RIGLyhat3	0	2	1	86.70126
1	bhv	RISconnFrom3	0.000962	3	3	16.34804
2	bhv	RISconnFrom3	0	1	3	1058.83
3	bhv	RISconnFrom3	0	1	3	1124.39
4	bhv	RISconnFrom3	0	1	3	369.8879
5	bhv	RISconnFrom3	0	1	3	1074.343
6	bhv	RISconnFrom3	0	1	3	1101.669
1	FWD	RISconnFrom3	0.000982	2	1	10.86146
2	FWD	RISconnFrom3	0	1	1	1040.901
3	FWD	RISconnFrom3	0	1	1	1004.043
4	FWD	RISconnFrom3	0	2	1	175.868
5	FWD	RISconnFrom3	0	1	1	1044.536
6	FWD	RISconnFrom3	0	1	1	785.4569
1	Stim	RISconnFrom3	1.25E-09	1	1	36.8891
2	Stim	RISconnFrom3	1.07E-14	2	1	59.77444
3	Stim	RISconnFrom3	0	2	1	125.8139
4	Stim	RISconnFrom3	0	2	1	297.7872
5	Stim	RISconnFrom3	0	2	1	744.8344
6	Stim	RISconnFrom3	1.28E-09	2	1	36.85035
1	StimDetailed	RISconnFrom3	9.00E-07	1	1	24.13013
2	StimDetailed	RISconnFrom3	0.0109	1	1	6.481579
3	StimDetailed	RISconnFrom3	2.22E-16	1	1	67.36094
4	StimDetailed	RISconnFrom3	0.014009	1	1	6.036948
5	StimDetailed	RISconnFrom3	0	1	1	294.2571
6	StimDetailed	RISconnFrom3	0.009288	1	1	6.766642
1	bhv	RISconnFromNeg	0	1	3	79.92578
2	bhv	RISconnFromNeg	NaN	1	3	NaN
3	bhv	RISconnFromNeg	NaN	1	3	NaN
4	bhv	RISconnFromNeg	NaN	1	3	NaN
5	bhv	RISconnFromNeg	0	4	3	113.7796
6	bhv	RISconnFromNeg	NaN	1	3	NaN
1	FWD	RISconnFromNeg	4.11E-15	1	1	61.62271
2	FWD	RISconnFromNeg	NaN	1	1	NaN
3	FWD	RISconnFromNeg	NaN	1	1	NaN
4	FWD	RISconnFromNeg	NaN	1	1	NaN
5	FWD	RISconnFromNeg	6.10E-05	2	1	16.07148
6	FWD	RISconnFromNeg	NaN	1	1	NaN
1	Stim	RISconnFromNeg	2.78E-10	2	1	39.82159
2	Stim	RISconnFromNeg	NaN	1	1	NaN
3	Stim	RISconnFromNeg	NaN	1	1	NaN
4	Stim	RISconnFromNeg	NaN	1	1	NaN
5	Stim	RISconnFromNeg	0.849784	1	1	0.03587
6	Stim	RISconnFromNeg	NaN	1	1	NaN
5	StimDetailed	RISconnFromNeg	0.003547	1	1	8.502054
1	bhv	RISconnFromNeg3	7.55E-11	1	3	50.11433
2	bhv	RISconnFromNeg3	NaN	1	3	NaN
3	bhv	RISconnFromNeg3	NaN	1	3	NaN

4	bhv	RISconnFromNeg3	NaN	1	3	NaN
5	bhv	RISconnFromNeg3	1.09E-09	4	3	44.6705
6	bhv	RISconnFromNeg3	NaN	1	3	NaN
1	FWD	RISconnFromNeg3	4.74E-11	1	1	43.28066
2	FWD	RISconnFromNeg3	NaN	1	1	NaN
3	FWD	RISconnFromNeg3	NaN	1	1	NaN
4	FWD	RISconnFromNeg3	NaN	1	1	NaN
5	FWD	RISconnFromNeg3	0.031831	2	1	4.607581
6	FWD	RISconnFromNeg3	NaN	1	1	NaN
1	Stim	RISconnFromNeg3	6.60E-10	2	1	38.13633
2	Stim	RISconnFromNeg3	NaN	1	1	NaN
3	Stim	RISconnFromNeg3	NaN	1	1	NaN
4	Stim	RISconnFromNeg3	NaN	1	1	NaN
5	Stim	RISconnFromNeg3	0.008079	2	1	7.015955
6	Stim	RISconnFromNeg3	NaN	1	1	NaN
5	StimDetailed	RISconnFromNeg3	4.41E-06	2	1	21.07977
1	bhv	RISconnFromPos	0.153422	3	3	5.264503
2	bhv	RISconnFromPos	0	1	3	104.5495
3	bhv	RISconnFromPos	0.077833	1	3	6.820848
4	bhv	RISconnFromPos	0.007016	3	3	12.1099
5	bhv	RISconnFromPos	0	3	3	178.7878
6	bhv	RISconnFromPos	0.821141	3	3	0.917755
1	FWD	RISconnFromPos	0.455954	2	1	0.555808
2	FWD	RISconnFromPos	1.45E-14	1	1	59.15543
3	FWD	RISconnFromPos	0.388511	1	1	0.743596
4	FWD	RISconnFromPos	0.521763	2	1	0.410406
5	FWD	RISconnFromPos	8.18E-12	2	1	46.72267
6	FWD	RISconnFromPos	0.552443	2	1	0.352958
1	Stim	RISconnFromPos	0.3172	2	1	1.000455
2	Stim	RISconnFromPos	1.66E-08	2	1	31.85334
3	Stim	RISconnFromPos	0.082914	2	1	3.006838
4	Stim	RISconnFromPos	0.317191	2	1	1.000496
5	Stim	RISconnFromPos	0	2	1	267.0984
6	Stim	RISconnFromPos	0.316951	2	1	1.001489
1	StimDetailed	RISconnFromPos	0.563378	1	1	0.33389
2	StimDetailed	RISconnFromPos	0.015251	1	1	5.88721
3	StimDetailed	RISconnFromPos	0.318303	1	1	0.995905
4	StimDetailed	RISconnFromPos	0.563349	1	1	0.333939
5	StimDetailed	RISconnFromPos	0	1	1	88.89807
6	StimDetailed	RISconnFromPos	0.56322	1	1	0.33416
1	bhv	RISconnFromPos3	0.010412	3	3	11.25754
2	bhv	RISconnFromPos3	0	1	3	1058.83
3	bhv	RISconnFromPos3	0	1	3	1124.39
4	bhv	RISconnFromPos3	0	1	3	369.8879
5	bhv	RISconnFromPos3	0	1	3	1074.343
6	bhv	RISconnFromPos3	0	1	3	1101.669
1	FWD	RISconnFromPos3	0.513743	2	1	0.426435
2	FWD	RISconnFromPos3	0	1	1	1040.901
3	FWD	RISconnFromPos3	0	1	1	1004.043
4	FWD	RISconnFromPos3	0	2	1	175.868

5	FWD	RISconnFromPos3	0	1	1	1044.536
6	FWD	RISconnFromPos3	0	1	1	785.4569
1	Stim	RISconnFromPos3	1.11E-16	1	1	69.93889
2	Stim	RISconnFromPos3	1.07E-14	2	1	59.77444
3	Stim	RISconnFromPos3	0	2	1	125.8139
4	Stim	RISconnFromPos3	0	2	1	297.7872
5	Stim	RISconnFromPos3	0	2	1	744.8344
6	Stim	RISconnFromPos3	1.28E-09	2	1	36.85035
1	StimDetailed	RISconnFromPos3	0.051391	1	1	3.795473
2	StimDetailed	RISconnFromPos3	0.0109	1	1	6.481579
3	StimDetailed	RISconnFromPos3	2.22E-16	1	1	67.36094
4	StimDetailed	RISconnFromPos3	0.014009	1	1	6.036948
5	StimDetailed	RISconnFromPos3	0	1	1	294.2571
6	StimDetailed	RISconnFromPos3	0.009288	1	1	6.766642
1	bhv	RISconnTo3	0.000469	3	3	17.86335
2	bhv	RISconnTo3	0	1	3	883.0234
3	bhv	RISconnTo3	0	1	3	152.6555
4	bhv	RISconnTo3	7.78E-05	3	3	21.63331
5	bhv	RISconnTo3	0	1	3	1081.612
6	bhv	RISconnTo3	0	1	3	1257.173
1	FWD	RISconnTo3	0.011174	2	1	6.437474
2	FWD	RISconnTo3	0	1	1	785.6922
3	FWD	RISconnTo3	0	1	1	133.6314
4	FWD	RISconnTo3	0.000132	2	1	14.6105
5	FWD	RISconnTo3	0	1	1	1049.527
6	FWD	RISconnTo3	0	2	1	610.0056
1	Stim	RISconnTo3	9.37E-11	1	1	41.94769
2	Stim	RISconnTo3	0.477601	1	1	0.504336
3	Stim	RISconnTo3	0	1	1	79.27358
4	Stim	RISconnTo3	1.83E-08	2	1	31.66345
5	Stim	RISconnTo3	0	2	1	731.444
6	Stim	RISconnTo3	0.007911	2	1	7.053413
1	StimDetailed	RISconnTo3	0.00036	1	1	12.72979
2	StimDetailed	RISconnTo3	2.66E-15	1	1	62.47534
3	StimDetailed	RISconnTo3	5.19E-09	1	1	34.11829
4	StimDetailed	RISconnTo3	0.002256	1	1	9.328616
5	StimDetailed	RISconnTo3	0	1	1	287.4945
6	StimDetailed	RISconnTo3	0.038278	1	1	4.292617
1	bhv	RISconnToNeg	9.56E-12	1	3	54.32583
2	bhv	RISconnToNeg	NaN	1	3	NaN
3	bhv	RISconnToNeg	NaN	1	3	NaN
4	bhv	RISconnToNeg	NaN	1	3	NaN
5	bhv	RISconnToNeg	3.47E-09	4	3	42.29563
6	bhv	RISconnToNeg	NaN	1	3	NaN
1	FWD	RISconnToNeg	1.18E-08	1	1	32.51581
2	FWD	RISconnToNeg	NaN	1	1	NaN
3	FWD	RISconnToNeg	NaN	1	1	NaN
4	FWD	RISconnToNeg	NaN	1	1	NaN
5	FWD	RISconnToNeg	0.066323	2	1	3.371761
6	FWD	RISconnToNeg	NaN	1	1	NaN

1	Stim	RISconnToNeg	0.000208	2	1	13.75399
2	Stim	RISconnToNeg	NaN	1	1	NaN
3	Stim	RISconnToNeg	NaN	1	1	NaN
4	Stim	RISconnToNeg	NaN	1	1	NaN
5	Stim	RISconnToNeg	3.44E-08	1	1	30.44221
6	Stim	RISconnToNeg	NaN	1	1	NaN
5	StimDetailed	RISconnToNeg	0.001457	1	1	10.13204
5	StimDetailed	RISconnToNeg	0.001457	1	1	10.13204
1	bhv	RISconnToNeg3	1.96E-07	4	3	34.02338
2	bhv	RISconnToNeg3	NaN	1	3	NaN
3	bhv	RISconnToNeg3	NaN	1	3	NaN
4	bhv	RISconnToNeg3	NaN	1	3	NaN
5	bhv	RISconnToNeg3	NaN	1	3	NaN
6	bhv	RISconnToNeg3	NaN	1	3	NaN
1	FWD	RISconnToNeg3	0.124954	2	1	2.354094
2	FWD	RISconnToNeg3	NaN	1	1	NaN
3	FWD	RISconnToNeg3	NaN	1	1	NaN
4	FWD	RISconnToNeg3	NaN	1	1	NaN
5	FWD	RISconnToNeg3	NaN	1	1	NaN
6	FWD	RISconnToNeg3	NaN	1	1	NaN
1	Stim	RISconnToNeg3	0.000299	1	1	13.07735
2	Stim	RISconnToNeg3	NaN	1	1	NaN
3	Stim	RISconnToNeg3	NaN	1	1	NaN
4	Stim	RISconnToNeg3	NaN	1	1	NaN
5	Stim	RISconnToNeg3	NaN	1	1	NaN
6	Stim	RISconnToNeg3	NaN	1	1	NaN
5	StimDetailed	RISconnToNeg3	NaN	1	1	NaN
5	StimDetailed	RISconnToNeg3	NaN	1	1	NaN
1	bhv	RISconnToPos	0.153422	3	3	5.264503
2	bhv	RISconnToPos	0.852213	1	3	0.788512
3	bhv	RISconnToPos	0.86671	1	3	0.727532
4	bhv	RISconnToPos	0.007016	3	3	12.1099
5	bhv	RISconnToPos	0.004201	3	3	13.21129
6	bhv	RISconnToPos	0.821141	3	3	0.917755
1	FWD	RISconnToPos	0.455954	2	1	0.555808
2	FWD	RISconnToPos	0.374551	1	1	0.788512
3	FWD	RISconnToPos	0.393684	1	1	0.727532
4	FWD	RISconnToPos	0.521763	2	1	0.410406
5	FWD	RISconnToPos	0.104907	2	1	2.629308
6	FWD	RISconnToPos	0.552443	2	1	0.352958
1	Stim	RISconnToPos	0.3172	2	1	1.000455
2	Stim	RISconnToPos	0.316951	2	1	1.001489
3	Stim	RISconnToPos	0.31698	2	1	1.001367
4	Stim	RISconnToPos	0.317191	2	1	1.000496
5	Stim	RISconnToPos	0.045206	2	1	4.010926
6	Stim	RISconnToPos	0.316951	2	1	1.001489
1	StimDetailed	RISconnToPos	0.563378	1	1	0.33389
2	StimDetailed	RISconnToPos	0.56322	1	1	0.33416
3	StimDetailed	RISconnToPos	0.56468	1	1	0.331666
4	StimDetailed	RISconnToPos	0.563349	1	1	0.333939

5	StimDetailed	RISconnToPos	0.247926	1	1	1.334952
6	StimDetailed	RISconnToPos	0.56322	1	1	0.33416
1	bhv	RISconnToPos3	3.46E-05	3	3	23.32004
2	bhv	RISconnToPos3	0	1	3	883.0234
3	bhv	RISconnToPos3	0	1	3	152.6555
4	bhv	RISconnToPos3	7.78E-05	3	3	21.63331
5	bhv	RISconnToPos3	0	1	3	1081.612
6	bhv	RISconnToPos3	0	1	3	1257.173
1	FWD	RISconnToPos3	0.007581	2	1	7.129898
2	FWD	RISconnToPos3	0	1	1	785.6922
3	FWD	RISconnToPos3	0	1	1	133.6314
4	FWD	RISconnToPos3	0.000132	2	1	14.6105
5	FWD	RISconnToPos3	0	1	1	1049.527
6	FWD	RISconnToPos3	0	2	1	610.0056
1	Stim	RISconnToPos3	2.80E-06	1	1	21.94659
2	Stim	RISconnToPos3	0.477601	1	1	0.504336
3	Stim	RISconnToPos3	0	1	1	79.27358
4	Stim	RISconnToPos3	1.83E-08	2	1	31.66345
5	Stim	RISconnToPos3	0	2	1	731.444
6	Stim	RISconnToPos3	0.007911	2	1	7.053413
1	StimDetailed	RISconnToPos3	6.88E-05	1	1	15.84228
2	StimDetailed	RISconnToPos3	2.66E-15	1	1	62.47534
3	StimDetailed	RISconnToPos3	5.19E-09	1	1	34.11829
4	StimDetailed	RISconnToPos3	0.002256	1	1	9.328616
5	StimDetailed	RISconnToPos3	0	1	1	287.4945
6	StimDetailed	RISconnToPos3	0.038278	1	1	4.292617
1	bhv	RISyhat	0	1	3	418.5486
2	bhv	RISyhat	0	1	3	94.02
3	bhv	RISyhat	0	1	3	1374.75
4	bhv	RISyhat	0	1	3	440.4671
5	bhv	RISyhat	0	1	3	371.1937
6	bhv	RISyhat	0	1	3	377.1536
1	FWD	RISyhat	0	1	1	395.9414
2	FWD	RISyhat	7.33E-15	1	1	60.50586
3	FWD	RISyhat	0	1	1	1340.91
4	FWD	RISyhat	0	2	1	337.836
5	FWD	RISyhat	0	1	1	370.3772
6	FWD	RISyhat	0	2	1	374.7798
1	Stim	RISyhat	0.029582	2	1	4.733394
2	Stim	RISyhat	0	2	1	439.0087
3	Stim	RISyhat	0	2	1	280.4845
4	Stim	RISyhat	0	2	1	199.1853
5	Stim	RISyhat	0	2	1	1519.873
6	Stim	RISyhat	0	2	1	541.4103
1	StimD	RISyhat	4.15E-11	1	1	43.5429
2	StimD	RISyhat	5.43E-10	1	1	38.5154
3	StimD	RISyhat	0	1	1	106.0757
4	StimD	RISyhat	0.136128	1	1	2.221196
5	StimD	RISyhat	0	1	1	431.1425
6	StimD	RISyhat	0	1	1	355.3057

1	bhv	RISyhat3	3.62E-07	1	3	32.7617
2	bhv	RISyhat3	3.33E-16	1	3	75.10756
3	bhv	RISyhat3	NaN	1	3	NaN
4	bhv	RISyhat3	0	1	3	221.6459
5	bhv	RISyhat3	0.054122	1	3	7.637764
6	bhv	RISyhat3	0	1	3	127.5039
1	FWD	RISyhat3	4.94E-06	1	1	20.85961
2	FWD	RISyhat3	0	1	1	75.10756
3	FWD	RISyhat3	NaN	1	1	NaN
4	FWD	RISyhat3	0	1	1	221.6459
5	FWD	RISyhat3	0.005716	1	1	7.637764
6	FWD	RISyhat3	0	1	1	127.5039
1	Stim	RISyhat3	0.523285	2	1	0.407414
2	Stim	RISyhat3	0	2	1	95.20514
3	Stim	RISyhat3	NaN	1	1	NaN
4	Stim	RISyhat3	0	2	1	90.91973
5	Stim	RISyhat3	0.025247	2	1	5.006833
6	Stim	RISyhat3	2.04E-11	2	1	44.93667
1	StimD	RISyhat3	9.98E-06	2	1	19.51441
2	StimD	RISyhat3	6.88E-08	1	1	29.09683
3	StimD	RISyhat3	NaN	1	1	NaN
4	StimD	RISyhat3	0.001231	1	1	10.44286
5	StimD	RISyhat3	0.000105	2	1	15.04326
6	StimD	RISyhat3	0	2	1	134.6765
1	bhv	RMEDconnFrom	0.153422	3	3	5.264503
2	bhv	RMEDconnFrom	0	1	3	458.822
3	bhv	RMEDconnFrom	0.86671	1	3	0.727532
4	bhv	RMEDconnFrom	0.007016	3	3	12.1099
5	bhv	RMEDconnFrom	0.004201	3	3	13.21129
6	bhv	RMEDconnFrom	0	1	3	857.5053
7	bhv	RMEDconnFrom	0	1	3	227.3615
1	FWD	RMEDconnFrom	0.455954	2	1	0.555808
2	FWD	RMEDconnFrom	0	1	1	453.185
3	FWD	RMEDconnFrom	0.393684	1	1	0.727532
4	FWD	RMEDconnFrom	0.521763	2	1	0.410406
5	FWD	RMEDconnFrom	0.104907	2	1	2.629308
6	FWD	RMEDconnFrom	0	2	1	382.3572
7	FWD	RMEDconnFrom	0	2	1	180.8015
1	Stim	RMEDconnFrom	0.3172	2	1	1.000455
2	Stim	RMEDconnFrom	0	2	1	380.3011
3	Stim	RMEDconnFrom	0.31698	2	1	1.001367
4	Stim	RMEDconnFrom	0.317191	2	1	1.000496
5	Stim	RMEDconnFrom	0.045206	2	1	4.010926
6	Stim	RMEDconnFrom	0.021195	2	1	5.310667
7	Stim	RMEDconnFrom	3.74E-08	2	1	30.28146
1	StimDetailed	RMEDconnFrom	0.563378	1	1	0.33389
2	StimDetailed	RMEDconnFrom	0	1	1	120.7377
3	StimDetailed	RMEDconnFrom	0.56468	1	1	0.331666
4	StimDetailed	RMEDconnFrom	0.563349	1	1	0.333939
5	StimDetailed	RMEDconnFrom	0.247926	1	1	1.334952

6	StimDetailed	RMEDconnFrom	0.027036	1	1	4.88848
7	StimDetailed	RMEDconnFrom	0.003307	1	1	8.629741
1	bhv	RMEDconnFrom3	0.153422	3	3	5.264503
2	bhv	RMEDconnFrom3	0	1	3	1685.895
3	bhv	RMEDconnFrom3	0.010611	1	3	11.21651
4	bhv	RMEDconnFrom3	0	1	3	992.8515
5	bhv	RMEDconnFrom3	0.004201	3	3	13.21129
6	bhv	RMEDconnFrom3	0	1	3	993.031
7	bhv	RMEDconnFrom3	0	1	3	1207.939
1	FWD	RMEDconnFrom3	0.455954	2	1	0.555808
2	FWD	RMEDconnFrom3	0	1	1	1647.339
3	FWD	RMEDconnFrom3	0.820963	1	1	0.051215
4	FWD	RMEDconnFrom3	0	2	1	496.936
5	FWD	RMEDconnFrom3	0.104907	2	1	2.629308
6	FWD	RMEDconnFrom3	0	1	1	617.4302
7	FWD	RMEDconnFrom3	0	1	1	1066.678
1	Stim	RMEDconnFrom3	0.3172	2	1	1.000455
2	Stim	RMEDconnFrom3	0.877386	2	1	0.023804
3	Stim	RMEDconnFrom3	0.999486	2	1	4.15E-07
4	Stim	RMEDconnFrom3	0.024262	1	1	5.075775
5	Stim	RMEDconnFrom3	0.045206	2	1	4.010926
6	Stim	RMEDconnFrom3	6.85E-07	2	1	24.65737
7	Stim	RMEDconnFrom3	2.02E-06	2	1	22.57714
1	StimDetailed	RMEDconnFrom3	0.563378	1	1	0.33389
2	StimDetailed	RMEDconnFrom3	4.80E-08	1	1	29.7958
3	StimDetailed	RMEDconnFrom3	0.41528	1	1	0.663634
4	StimDetailed	RMEDconnFrom3	0.001178	1	1	10.52442
5	StimDetailed	RMEDconnFrom3	0.247926	1	1	1.334952
6	StimDetailed	RMEDconnFrom3	0.003259	1	1	8.656482
7	StimDetailed	RMEDconnFrom3	3.34E-07	1	1	26.04279
1	bhv	RMEDconnFromNeg	4.25E-13	1	3	60.65948
2	bhv	RMEDconnFromNeg	NaN	1	3	NaN
3	bhv	RMEDconnFromNeg	NaN	1	3	NaN
4	bhv	RMEDconnFromNeg	NaN	1	3	NaN
5	bhv	RMEDconnFromNeg	2.54E-05	3	3	23.96288
6	bhv	RMEDconnFromNeg	NaN	1	3	NaN
7	bhv	RMEDconnFromNeg	NaN	1	3	NaN
1	FWD	RMEDconnFromNeg	1.96E-10	1	1	40.50183
2	FWD	RMEDconnFromNeg	NaN	1	1	NaN
3	FWD	RMEDconnFromNeg	NaN	1	1	NaN
4	FWD	RMEDconnFromNeg	NaN	1	1	NaN
5	FWD	RMEDconnFromNeg	0.000356	2	1	12.7481
6	FWD	RMEDconnFromNeg	NaN	1	1	NaN
7	FWD	RMEDconnFromNeg	NaN	1	1	NaN
1	Stim	RMEDconnFromNeg	1.43E-05	2	1	18.83403
2	Stim	RMEDconnFromNeg	NaN	1	1	NaN
3	Stim	RMEDconnFromNeg	NaN	1	1	NaN
4	Stim	RMEDconnFromNeg	NaN	1	1	NaN
5	Stim	RMEDconnFromNeg	8.30E-07	1	1	24.28664
6	Stim	RMEDconnFromNeg	NaN	1	1	NaN

7	Stim	RMEDconnFromNeg	NaN	1	1	NaN
5	StimDetailed	RMEDconnFromNeg	0.004468	1	1	8.083296
7	StimDetailed	RMEDconnFromNeg	NaN	1	1	NaN
1	bhv	RMEDconnFromNeg3	1.38E-10	1	3	48.89102
2	bhv	RMEDconnFromNeg3	NaN	1	3	NaN
3	bhv	RMEDconnFromNeg3	NaN	1	3	NaN
4	bhv	RMEDconnFromNeg3	NaN	1	3	NaN
5	bhv	RMEDconnFromNeg3	NaN	1	3	NaN
6	bhv	RMEDconnFromNeg3	NaN	1	3	NaN
7	bhv	RMEDconnFromNeg3	NaN	1	3	NaN
1	FWD	RMEDconnFromNeg3	8.20E-09	1	1	33.22673
2	FWD	RMEDconnFromNeg3	NaN	1	1	NaN
3	FWD	RMEDconnFromNeg3	NaN	1	1	NaN
4	FWD	RMEDconnFromNeg3	NaN	1	1	NaN
5	FWD	RMEDconnFromNeg3	NaN	1	1	NaN
6	FWD	RMEDconnFromNeg3	NaN	1	1	NaN
7	FWD	RMEDconnFromNeg3	NaN	1	1	NaN
1	Stim	RMEDconnFromNeg3	1.33E-05	2	1	18.96674
2	Stim	RMEDconnFromNeg3	NaN	1	1	NaN
3	Stim	RMEDconnFromNeg3	NaN	1	1	NaN
4	Stim	RMEDconnFromNeg3	NaN	1	1	NaN
5	Stim	RMEDconnFromNeg3	NaN	1	1	NaN
6	Stim	RMEDconnFromNeg3	NaN	1	1	NaN
7	Stim	RMEDconnFromNeg3	NaN	1	1	NaN
5	StimDetailed	RMEDconnFromNeg3	NaN	1	1	NaN
7	StimDetailed	RMEDconnFromNeg3	NaN	1	1	NaN
1	bhv	RMEDconnFromPos	0.153422	3	3	5.264503
2	bhv	RMEDconnFromPos	0	1	3	458.822
3	bhv	RMEDconnFromPos	0.86671	1	3	0.727532
4	bhv	RMEDconnFromPos	0.007016	3	3	12.1099
5	bhv	RMEDconnFromPos	0.004201	3	3	13.21129
6	bhv	RMEDconnFromPos	0	1	3	857.5053
7	bhv	RMEDconnFromPos	0	1	3	227.3615
1	FWD	RMEDconnFromPos	0.455954	2	1	0.555808
2	FWD	RMEDconnFromPos	0	1	1	453.185
3	FWD	RMEDconnFromPos	0.393684	1	1	0.727532
4	FWD	RMEDconnFromPos	0.521763	2	1	0.410406
5	FWD	RMEDconnFromPos	0.104907	2	1	2.629308
6	FWD	RMEDconnFromPos	0	2	1	382.3572
7	FWD	RMEDconnFromPos	0	2	1	180.8015
1	Stim	RMEDconnFromPos	0.3172	2	1	1.000455
2	Stim	RMEDconnFromPos	0	2	1	380.3011
3	Stim	RMEDconnFromPos	0.31698	2	1	1.001367
4	Stim	RMEDconnFromPos	0.317191	2	1	1.000496
5	Stim	RMEDconnFromPos	0.045206	2	1	4.010926
6	Stim	RMEDconnFromPos	0.021195	2	1	5.310667
7	Stim	RMEDconnFromPos	3.74E-08	2	1	30.28146
1	StimDetailed	RMEDconnFromPos	0.563378	1	1	0.33389
2	StimDetailed	RMEDconnFromPos	0	1	1	120.7377
3	StimDetailed	RMEDconnFromPos	0.56468	1	1	0.331666

4	StimDetailed	RMEDconnFromPos	0.563349	1	1	0.333939
5	StimDetailed	RMEDconnFromPos	0.247926	1	1	1.334952
6	StimDetailed	RMEDconnFromPos	0.027036	1	1	4.88848
7	StimDetailed	RMEDconnFromPos	0.003307	1	1	8.629741
1	bhv	RMEDconnFromPos3	0.000191	3	3	19.75565
2	bhv	RMEDconnFromPos3	0	1	3	1685.895
3	bhv	RMEDconnFromPos3	0.010611	1	3	11.21651
4	bhv	RMEDconnFromPos3	0	1	3	992.8515
5	bhv	RMEDconnFromPos3	0.004201	3	3	13.21129
6	bhv	RMEDconnFromPos3	0	1	3	993.031
7	bhv	RMEDconnFromPos3	0	1	3	1207.939
1	FWD	RMEDconnFromPos3	0.708993	2	1	0.139285
2	FWD	RMEDconnFromPos3	0	1	1	1647.339
3	FWD	RMEDconnFromPos3	0.820963	1	1	0.051215
4	FWD	RMEDconnFromPos3	0	2	1	496.936
5	FWD	RMEDconnFromPos3	0.104907	2	1	2.629308
6	FWD	RMEDconnFromPos3	0	1	1	617.4302
7	FWD	RMEDconnFromPos3	0	1	1	1066.678
1	Stim	RMEDconnFromPos3	0.051509	2	1	3.791656
2	Stim	RMEDconnFromPos3	0.877386	2	1	0.023804
3	Stim	RMEDconnFromPos3	0.999486	2	1	4.15E-07
4	Stim	RMEDconnFromPos3	0.024262	1	1	5.075775
5	Stim	RMEDconnFromPos3	0.045206	2	1	4.010926
6	Stim	RMEDconnFromPos3	6.85E-07	2	1	24.65737
7	Stim	RMEDconnFromPos3	2.02E-06	2	1	22.57714
1	StimDetailed	RMEDconnFromPos3	0.870948	1	1	0.026391
2	StimDetailed	RMEDconnFromPos3	4.80E-08	1	1	29.7958
3	StimDetailed	RMEDconnFromPos3	0.41528	1	1	0.663634
4	StimDetailed	RMEDconnFromPos3	0.001178	1	1	10.52442
5	StimDetailed	RMEDconnFromPos3	0.247926	1	1	1.334952
6	StimDetailed	RMEDconnFromPos3	0.003259	1	1	8.656482
7	StimDetailed	RMEDconnFromPos3	3.34E-07	1	1	26.04279
1	bhv	RMEDconnTo	0.153422	3	3	5.264503
2	bhv	RMEDconnTo	0.852213	1	3	0.788512
3	bhv	RMEDconnTo	0.86671	1	3	0.727532
4	bhv	RMEDconnTo	0.007016	3	3	12.1099
5	bhv	RMEDconnTo	0.004201	3	3	13.21129
6	bhv	RMEDconnTo	0	3	3	477.9279
7	bhv	RMEDconnTo	0	1	3	121.2423
1	FWD	RMEDconnTo	0.455954	2	1	0.555808
2	FWD	RMEDconnTo	0.374551	1	1	0.788512
3	FWD	RMEDconnTo	0.393684	1	1	0.727532
4	FWD	RMEDconnTo	0.521763	2	1	0.410406
5	FWD	RMEDconnTo	0.104907	2	1	2.629308
6	FWD	RMEDconnTo	0	2	1	222.2191
7	FWD	RMEDconnTo	0	2	1	88.92835
1	Stim	RMEDconnTo	0.3172	2	1	1.000455
2	Stim	RMEDconnTo	0.316951	2	1	1.001489
3	Stim	RMEDconnTo	0.31698	2	1	1.001367
4	Stim	RMEDconnTo	0.317191	2	1	1.000496

5	Stim	RMEDconnTo	0.045206	2	1	4.010926
6	Stim	RMEDconnTo	0.000856	1	1	11.11514
7	Stim	RMEDconnTo	0.034362	2	1	4.476616
1	StimDetailed	RMEDconnTo	0.563378	1	1	0.33389
2	StimDetailed	RMEDconnTo	0.56322	1	1	0.33416
3	StimDetailed	RMEDconnTo	0.56468	1	1	0.331666
4	StimDetailed	RMEDconnTo	0.563349	1	1	0.333939
5	StimDetailed	RMEDconnTo	0.247926	1	1	1.334952
6	StimDetailed	RMEDconnTo	0.287016	1	1	1.133564
7	StimDetailed	RMEDconnTo	0.433997	1	1	0.612102
1	bhv	RMEDconnTo3	0.20907	3	3	4.536361
2	bhv	RMEDconnTo3	0	1	3	1675.188
3	bhv	RMEDconnTo3	0.86671	1	3	0.727532
4	bhv	RMEDconnTo3	0	3	3	209.5953
5	bhv	RMEDconnTo3	0.004201	3	3	13.21129
6	bhv	RMEDconnTo3	0	1	3	1005.758
7	bhv	RMEDconnTo3	0	1	3	701.7116
1	FWD	RMEDconnTo3	0.583886	2	1	0.299994
2	FWD	RMEDconnTo3	0	1	1	1626.351
3	FWD	RMEDconnTo3	0.393684	1	1	0.727532
4	FWD	RMEDconnTo3	0	2	1	83.54662
5	FWD	RMEDconnTo3	0.104907	2	1	2.629308
6	FWD	RMEDconnTo3	0	2	1	607.0503
7	FWD	RMEDconnTo3	0	1	1	642.106
1	Stim	RMEDconnTo3	0.094902	1	1	2.789199
2	Stim	RMEDconnTo3	0.835944	1	1	0.042884
3	Stim	RMEDconnTo3	0.31698	2	1	1.001367
4	Stim	RMEDconnTo3	0.076017	1	1	3.148057
5	Stim	RMEDconnTo3	0.045206	2	1	4.010926
6	Stim	RMEDconnTo3	1.68E-06	2	1	22.92894
7	Stim	RMEDconnTo3	1.89E-15	2	1	63.19318
1	StimDetailed	RMEDconnTo3	0.082447	1	1	3.01599
2	StimDetailed	RMEDconnTo3	1.01E-08	1	1	32.8181
3	StimDetailed	RMEDconnTo3	0.56468	1	1	0.331666
4	StimDetailed	RMEDconnTo3	4.44E-16	1	1	66.25375
5	StimDetailed	RMEDconnTo3	0.247926	1	1	1.334952
6	StimDetailed	RMEDconnTo3	0.002324	1	1	9.273905
7	StimDetailed	RMEDconnTo3	4.05E-14	1	1	57.1444
1	bhv	RMEDconnToNeg	0.000777	1	3	16.80092
2	bhv	RMEDconnToNeg	NaN	1	3	NaN
3	bhv	RMEDconnToNeg	NaN	1	3	NaN
4	bhv	RMEDconnToNeg	NaN	1	3	NaN
5	bhv	RMEDconnToNeg	2.34E-12	4	3	57.19401
6	bhv	RMEDconnToNeg	NaN	1	3	NaN
7	bhv	RMEDconnToNeg	1.81E-11	1	3	53.02995
1	FWD	RMEDconnToNeg	0.002185	2	1	9.387521
2	FWD	RMEDconnToNeg	NaN	1	1	NaN
3	FWD	RMEDconnToNeg	NaN	1	1	NaN
4	FWD	RMEDconnToNeg	NaN	1	1	NaN
5	FWD	RMEDconnToNeg	2.52E-05	2	1	17.75105

6	FWD	RMEDconnToNeg	NaN	1	1	NaN
7	FWD	RMEDconnToNeg	2.70E-12	1	1	48.89589
1	Stim	RMEDconnToNeg	0.581952	2	1	0.303089
2	Stim	RMEDconnToNeg	NaN	1	1	NaN
3	Stim	RMEDconnToNeg	NaN	1	1	NaN
4	Stim	RMEDconnToNeg	NaN	1	1	NaN
5	Stim	RMEDconnToNeg	0.000216	1	1	13.68833
6	Stim	RMEDconnToNeg	NaN	1	1	NaN
7	Stim	RMEDconnToNeg	1.14E-11	2	1	46.07145
5	StimDetailed	RMEDconnToNeg	0.438514	1	1	0.600167
5	StimDetailed	RMEDconnToNeg	0.438514	1	1	0.600167
7	StimDetailed	RMEDconnToNeg	8.92E-05	1	1	15.35208
7	StimDetailed	RMEDconnToNeg	8.92E-05	1	1	15.35208
1	bhv	RMEDconnToNeg3	1.96E-07	4	3	34.02338
2	bhv	RMEDconnToNeg3	NaN	1	3	NaN
3	bhv	RMEDconnToNeg3	NaN	1	3	NaN
4	bhv	RMEDconnToNeg3	NaN	1	3	NaN
5	bhv	RMEDconnToNeg3	NaN	1	3	NaN
6	bhv	RMEDconnToNeg3	NaN	1	3	NaN
7	bhv	RMEDconnToNeg3	NaN	1	3	NaN
1	FWD	RMEDconnToNeg3	0.124954	2	1	2.354094
2	FWD	RMEDconnToNeg3	NaN	1	1	NaN
3	FWD	RMEDconnToNeg3	NaN	1	1	NaN
4	FWD	RMEDconnToNeg3	NaN	1	1	NaN
5	FWD	RMEDconnToNeg3	NaN	1	1	NaN
6	FWD	RMEDconnToNeg3	NaN	1	1	NaN
7	FWD	RMEDconnToNeg3	NaN	1	1	NaN
1	Stim	RMEDconnToNeg3	0.000299	1	1	13.07735
2	Stim	RMEDconnToNeg3	NaN	1	1	NaN
3	Stim	RMEDconnToNeg3	NaN	1	1	NaN
4	Stim	RMEDconnToNeg3	NaN	1	1	NaN
5	Stim	RMEDconnToNeg3	NaN	1	1	NaN
6	Stim	RMEDconnToNeg3	NaN	1	1	NaN
7	Stim	RMEDconnToNeg3	NaN	1	1	NaN
5	StimDetailed	RMEDconnToNeg3	NaN	1	1	NaN
5	StimDetailed	RMEDconnToNeg3	NaN	1	1	NaN
7	StimDetailed	RMEDconnToNeg3	NaN	1	1	NaN
7	StimDetailed	RMEDconnToNeg3	NaN	1	1	NaN
1	bhv	RMEDconnToPos	0.153422	3	3	5.264503
2	bhv	RMEDconnToPos	0.852213	1	3	0.788512
3	bhv	RMEDconnToPos	0.86671	1	3	0.727532
4	bhv	RMEDconnToPos	0.007016	3	3	12.1099
5	bhv	RMEDconnToPos	0.004201	3	3	13.21129
6	bhv	RMEDconnToPos	0	3	3	477.9279
7	bhv	RMEDconnToPos	0	1	3	121.2423
1	FWD	RMEDconnToPos	0.455954	2	1	0.555808
2	FWD	RMEDconnToPos	0.374551	1	1	0.788512
3	FWD	RMEDconnToPos	0.393684	1	1	0.727532
4	FWD	RMEDconnToPos	0.521763	2	1	0.410406
5	FWD	RMEDconnToPos	0.104907	2	1	2.629308

6	FWD	RMEDconnToPos	0	2	1	222.2191
7	FWD	RMEDconnToPos	0	2	1	88.92835
1	Stim	RMEDconnToPos	0.3172	2	1	1.000455
2	Stim	RMEDconnToPos	0.316951	2	1	1.001489
3	Stim	RMEDconnToPos	0.31698	2	1	1.001367
4	Stim	RMEDconnToPos	0.317191	2	1	1.000496
5	Stim	RMEDconnToPos	0.045206	2	1	4.010926
6	Stim	RMEDconnToPos	0.000856	1	1	11.11514
7	Stim	RMEDconnToPos	0.034362	2	1	4.476616
1	StimDetailed	RMEDconnToPos	0.563378	1	1	0.33389
2	StimDetailed	RMEDconnToPos	0.56322	1	1	0.33416
3	StimDetailed	RMEDconnToPos	0.56468	1	1	0.331666
4	StimDetailed	RMEDconnToPos	0.563349	1	1	0.333939
5	StimDetailed	RMEDconnToPos	0.247926	1	1	1.334952
6	StimDetailed	RMEDconnToPos	0.287016	1	1	1.133564
7	StimDetailed	RMEDconnToPos	0.433997	1	1	0.612102
1	bhv	RMEDconnToPos3	0.000244	3	3	19.23521
2	bhv	RMEDconnToPos3	0	1	3	1675.188
3	bhv	RMEDconnToPos3	0.86671	1	3	0.727532
4	bhv	RMEDconnToPos3	0	3	3	209.5953
5	bhv	RMEDconnToPos3	0.004201	3	3	13.21129
6	bhv	RMEDconnToPos3	0	1	3	1005.758
7	bhv	RMEDconnToPos3	0	1	3	701.7116
1	FWD	RMEDconnToPos3	0.832351	2	1	0.044811
2	FWD	RMEDconnToPos3	0	1	1	1626.351
3	FWD	RMEDconnToPos3	0.393684	1	1	0.727532
4	FWD	RMEDconnToPos3	0	2	1	83.54662
5	FWD	RMEDconnToPos3	0.104907	2	1	2.629308
6	FWD	RMEDconnToPos3	0	2	1	607.0503
7	FWD	RMEDconnToPos3	0	1	1	642.106
1	Stim	RMEDconnToPos3	0.343795	2	1	0.896228
2	Stim	RMEDconnToPos3	0.835944	1	1	0.042884
3	Stim	RMEDconnToPos3	0.31698	2	1	1.001367
4	Stim	RMEDconnToPos3	0.076017	1	1	3.148057
5	Stim	RMEDconnToPos3	0.045206	2	1	4.010926
6	Stim	RMEDconnToPos3	1.68E-06	2	1	22.92894
7	Stim	RMEDconnToPos3	1.89E-15	2	1	63.19318
1	StimDetailed	RMEDconnToPos3	0.013852	1	1	6.056883
2	StimDetailed	RMEDconnToPos3	1.01E-08	1	1	32.8181
3	StimDetailed	RMEDconnToPos3	0.56468	1	1	0.331666
4	StimDetailed	RMEDconnToPos3	4.44E-16	1	1	66.25375
5	StimDetailed	RMEDconnToPos3	0.247926	1	1	1.334952
6	StimDetailed	RMEDconnToPos3	0.002324	1	1	9.273905
7	StimDetailed	RMEDconnToPos3	4.05E-14	1	1	57.1444
1	bhv	RMEDyhat	0	1	3	1039.321
2	bhv	RMEDyhat	0	1	3	1448.827
3	bhv	RMEDyhat	0	1	3	718.4859
4	bhv	RMEDyhat	0	1	3	1189.659
5	bhv	RMEDyhat	0	1	3	1542.741
6	bhv	RMEDyhat	0	1	3	1195.449

7	bhv	RMEDyhat	0	1	3	1746.502
1	FWD	RMEDyhat	0	1	1	962.6788
2	FWD	RMEDyhat	0	1	1	1444.488
3	FWD	RMEDyhat	0	1	1	563.653
4	FWD	RMEDyhat	0	1	1	805.3795
5	FWD	RMEDyhat	0	1	1	1358.04
6	FWD	RMEDyhat	0	1	1	678.7785
7	FWD	RMEDyhat	0	1	1	1484.568
1	Stim	RMEDyhat	0	2	1	135.6306
2	Stim	RMEDyhat	0.462476	2	1	0.539895
3	Stim	RMEDyhat	3.24E-11	1	1	44.02427
4	Stim	RMEDyhat	5.96E-11	1	1	42.83251
5	Stim	RMEDyhat	0	2	1	132.9762
6	Stim	RMEDyhat	0	2	1	82.93539
7	Stim	RMEDyhat	0.000562	1	1	11.89938
1	StimD	RMEDyhat	1.57E-14	1	1	59.01426
2	StimD	RMEDyhat	8.84E-10	1	1	37.56491
3	StimD	RMEDyhat	0.720607	1	1	0.127912
4	StimD	RMEDyhat	0	1	1	117.586
5	StimD	RMEDyhat	1.67E-13	1	1	54.35565
6	StimD	RMEDyhat	1.97E-09	1	1	36.00591
7	StimD	RMEDyhat	0.002329	1	1	9.270383
1	bhv	RMEDyhat3	6.11E-08	4	3	36.41908
2	bhv	RMEDyhat3	NaN	1	3	NaN
3	bhv	RMEDyhat3	0.692525	1	3	1.455728
4	bhv	RMEDyhat3	0	1	3	96.94859
5	bhv	RMEDyhat3	0	4	3	120.4831
6	bhv	RMEDyhat3	NaN	1	3	NaN
7	bhv	RMEDyhat3	NaN	1	3	NaN
1	FWD	RMEDyhat3	0.093215	2	1	2.817949
2	FWD	RMEDyhat3	NaN	1	1	NaN
3	FWD	RMEDyhat3	0.227611	1	1	1.455728
4	FWD	RMEDyhat3	0	1	1	96.94859
5	FWD	RMEDyhat3	0.001033	2	1	10.76832
6	FWD	RMEDyhat3	NaN	1	1	NaN
7	FWD	RMEDyhat3	NaN	1	1	NaN
1	Stim	RMEDyhat3	0.000174	1	1	14.08974
2	Stim	RMEDyhat3	NaN	1	1	NaN
3	Stim	RMEDyhat3	0.999486	1	1	4.15E-07
4	Stim	RMEDyhat3	2.86E-10	1	1	39.76857
5	Stim	RMEDyhat3	4.17E-06	2	1	21.18304
6	Stim	RMEDyhat3	NaN	1	1	NaN
7	Stim	RMEDyhat3	NaN	1	1	NaN
1	StimD	RMEDyhat3	0.030123	1	1	4.702281
2	StimD	RMEDyhat3	NaN	1	1	NaN
3	StimD	RMEDyhat3	0.411453	1	1	0.674598
4	StimD	RMEDyhat3	0.000269	1	1	13.27371
5	StimD	RMEDyhat3	1.44E-15	2	1	63.64543
6	StimD	RMEDyhat3	NaN	1	1	NaN
7	StimD	RMEDyhat3	NaN	1	1	NaN

1	bhv	SABDconnFrom3	0	3	3	1273.557
1	FWD	SABDconnFrom3	0	2	1	1245.587
1	Stim	SABDconnFrom3	7.93E-14	1	1	55.82267
1	StimDetailed	SABDconnFrom3	1.10E-10	1	1	41.63502
1	bhv	SABDconnFromNeg	0	1	3	128.9231
1	FWD	SABDconnFromNeg	0	1	1	125.4333
1	Stim	SABDconnFromNeg	0	2	1	93.8425
1	bhv	SABDconnFromNeg3	0	1	3	85.67865
1	FWD	SABDconnFromNeg3	0	1	1	82.86649
1	Stim	SABDconnFromNeg3	1.33E-15	2	1	63.79963
1	bhv	SABDconnFromPos	4.11E-12	3	3	56.04617
1	FWD	SABDconnFromPos	9.09E-13	2	1	51.03212
1	Stim	SABDconnFromPos	3.24E-11	1	1	44.02653
1	StimDetailed	SABDconnFromPos	0	1	1	135.8548
1	bhv	SABDconnFromPos3	0	3	3	1449.883
1	FWD	SABDconnFromPos3	0	2	1	1416.868
1	Stim	SABDconnFromPos3	0	1	1	102.2355
1	StimDetailed	SABDconnFromPos3	0	1	1	125.0272
1	bhv	SABDconnTo3	0	3	3	1296.674
1	FWD	SABDconnTo3	0	2	1	1278.101
1	Stim	SABDconnTo3	0	1	1	83.59023
1	StimDetailed	SABDconnTo3	2.55E-15	1	1	62.61824
1	bhv	SABDconnToNeg	0	1	3	110.8257
1	FWD	SABDconnToNeg	0	1	1	107.7602
1	Stim	SABDconnToNeg	0	2	1	80.86981
1	bhv	SABDconnToNeg3	8.68E-13	1	3	59.20722
1	FWD	SABDconnToNeg3	9.24E-14	1	1	55.52343
1	Stim	SABDconnToNeg3	4.20E-12	2	1	48.02696
1	bhv	SABDconnToPos	6.53E-14	3	3	64.46438
1	FWD	SABDconnToPos	9.88E-15	2	1	59.9219
1	Stim	SABDconnToPos	2.26E-12	1	1	49.24188
1	StimDetailed	SABDconnToPos	0	1	1	151.505
1	bhv	SABDconnToPos3	0	3	3	1419.49
1	FWD	SABDconnToPos3	0	2	1	1396.352
1	Stim	SABDconnToPos3	0	1	1	123.7109
1	StimDetailed	SABDconnToPos3	0	1	1	132.1645
1	bhv	SABDyhat	0	3	3	1568.195
1	FWD	SABDyhat	0	2	1	1088.059
1	Stim	SABDyhat	0	1	1	81.02093
1	StimD	SABDyhat	0	1	1	108.9882
1	bhv	SABDyhat3	2.79E-06	4	3	28.54217
1	FWD	SABDyhat3	0.16733	2	1	1.906706
1	Stim	SABDyhat3	0.000514	1	1	12.06587
1	StimD	SABDyhat3	0.044782	1	1	4.026839
1	bhv	stimTimes	0	1	3	124.5294
2	bhv	stimTimes	0.005427	1	3	12.66214
3	bhv	stimTimes	0	1	3	93.35077
4	bhv	stimTimes	0.002228	3	3	14.56619
5	bhv	stimTimes	0	1	3	247.7468
6	bhv	stimTimes	1.55E-13	3	3	62.71312

7	bhv	stimTimes	6.01E-10	3	3	45.88311
1	FWD	stimTimes	0	2	1	117.0115
2	FWD	stimTimes	0.144226	1	1	2.132278
3	FWD	stimTimes	0	1	1	91.54593
4	FWD	stimTimes	0.00072	2	1	11.43778
5	FWD	stimTimes	0	1	1	229.4815
6	FWD	stimTimes	6.57E-13	2	1	51.66812
7	FWD	stimTimes	1.63E-11	2	1	45.37399
1	bhv	stimTimesDetailed	0	1	3	117.2001
2	bhv	stimTimesDetailed	5.05E-08	1	3	36.80785
3	bhv	stimTimesDetailed	7.11E-14	1	3	64.29177
4	bhv	stimTimesDetailed	2.38E-14	3	3	66.51937
5	bhv	stimTimesDetailed	3.97E-07	1	3	32.56672
6	bhv	stimTimesDetailed	3.49E-05	3	3	23.30617
7	bhv	stimTimesDetailed	3.38E-09	3	3	42.34827
1	FWD	stimTimesDetailed	1.11E-16	1	1	68.56674
2	FWD	stimTimesDetailed	4.49E-05	2	1	16.65269
3	FWD	stimTimesDetailed	9.01E-10	1	1	37.52745
4	FWD	stimTimesDetailed	1.55E-14	2	1	59.02509
5	FWD	stimTimesDetailed	5.63E-06	2	1	20.60837
6	FWD	stimTimesDetailed	2.14E-05	2	1	18.06051
7	FWD	stimTimesDetailed	1.89E-07	2	1	27.14673

Table 5: **Two-sided χ^2 tests for BAG and RMED activity and connectivity (inactive vs. active, defined by a threshold), behavior, and oxygen stimulation levels**. Glossary: df: degrees of freedom, Q: chi squared test statistic, bhv: behavior, [neuron]connFrom: strongest connectivity value (absolute value) from that neuron, [neuron]connTo: strongest connectivity value to that neuron,[Neuron]yhat: reconstructed activity of that neuron, [ ]3: data included only above threshold 3 standard deviations above median, [ ]Pos: only positive connections included, [ ]Neg: only negative connections included, FWD: forward crawling (value= 1) vs. all other behaviors, stimTime: first half vs. second half (value= 1), stimTimesDetailed: 21% oxygen vs. 4% (value= 1).

6.7 ANOVA and MANOVA tests

In order to test effects of categorical factors such as oxygen stimulation settings and behavior states on individual neuron activity and connectivity, we conducted ANOVA and MANOVA tests (with Roy's Largest Root, which most consistently returned non-NaN or Inf values, and which only uses the variance from the dimension of greatest separation between the groups to create the test statistic) [53; 54] for each Stim worm per-worm model (p-values in Tables 6, 7). All of the tests with connectivity to and from each neuron were found to be significant for Behavior (1-4), Stimulation (0 or 1, i.e., 21% oxygen first half vs. alternating oxygen levels second half), and interaction between the levels of Behavior and Stimulation. Most of the activity tests were also significant to varying degrees ($\alpha = 1 * 10^{-4}$ to 0.05, depending on the correction for multiple tests).

All of the neurons, including BAGL and BAGR, showed significant effects of Behavior and Stimulation levels on the connectivity to and from across all 7 Stim worms. As far as reconstructed neural activity, BAGL showed consistently significant effects of both the behavior levels, stimulation protocol, and the interaction between the two, with the exception of Worm 2's BAGR activity, despite affecting the connectivity.

Worm	variable	source	SS	df	MS	F	p
1	AVFRyhat	Bhv State	0.24934	3	0.083113	213.1895	2.53E-121
		Stim State	0.092599	1	0.092599	237.5211	5.85E-51
		Bhv State:Stim State	0.018335	3	0.006112	15.67645	4.35E-10
		Error	0.853785	2190	0.00039	NaN	NaN
		Total	1.18146	2197	NaN	NaN	NaN
1	BAGLyhat	Bhv State	0.139174	3	0.046391	19.66211	1.41E-12
		Stim State	0.044502	1	0.044502	18.86136	1.47E-05
		Bhv State:Stim State	0.113158	3	0.037719	15.98659	2.78E-10
		Error	5.167154	2190	0.002359	NaN	NaN
		Total	5.592774	2197	NaN	NaN	NaN
1	BAGRyhat	Bhv State	0.189566	3	0.063189	22.72331	1.74E-14
		Stim State	0.057059	1	0.057059	20.51888	6.22E-06
		Bhv State:Stim State	0.150531	3	0.050177	18.0442	1.44E-11
		Error	6.089929	2190	0.002781	NaN	NaN
		Total	6.648562	2197	NaN	NaN	NaN
1	RMEDyhat	Bhv State	0.36653	3	0.122177	583.1124	1.56E-278
		Stim State	0.001575	1	0.001575	7.517943	0.006158
		Bhv State:Stim State	0.013772	3	0.004591	21.90928	5.60E-14
		Error	0.458859	2190	0.00021	NaN	NaN
		Total	0.881022	2197	NaN	NaN	NaN
1	RISyhat	Bhv State	0.171073	3	0.057024	308.7481	3.71E-167
		Stim State	0.000189	1	0.000189	1.022416	0.312058
		Bhv State:Stim State	0.041543	3	0.013848	74.97549	3.68E-46
		Error	0.404483	2190	0.000185	NaN	NaN
		Total	0.667994	2197	NaN	NaN	NaN
1	SABDyhat	Bhv State	1.433296	3	0.477765	796.7039	0
		Stim State	0.006233	1	0.006233	10.39367	0.001283
		Bhv State:Stim State	0.04349	3	0.014497	24.17389	2.18E-15
		Error	1.313293	2190	0.0006	NaN	NaN
		Total	2.903239	2197	NaN	NaN	NaN
2	AVFRyhat	Bhv State	0.062716	3	0.020905	594.0314	2.31E-276
		Stim State	0.004117	1	0.004117	116.986	1.53E-26
		Bhv State:Stim State	0.009455	3	0.003152	89.55875	2.16E-54
		Error	0.070701	2009	3.52E-05	NaN	NaN
		Total	0.143094	2016	NaN	NaN	NaN
2	BAGLyhat	Bhv State	0.046611	3	0.015537	274.8257	1.88E-149
		Stim State	0.028384	1	0.028384	502.0724	1.92E-99
		Bhv State:Stim State	0.027694	3	0.009231	163.284	1.03E-94
		Error	0.113578	2009	5.65E-05	NaN	NaN
		Total	0.209056	2016	NaN	NaN	NaN
2	BAGRyhat	Bhv State	0.053041	3	0.01768	409.1915	2.02E-207
		Stim State	9.58E-05	1	9.58E-05	2.216954	0.136659
		Bhv State:Stim State	0.018352	3	0.006117	141.5774	3.22E-83
		Error	0.086805	2009	4.32E-05	NaN	NaN
		Total	0.161078	2016	NaN	NaN	NaN
2	RMEDyhat	Bhv State	4.284593	3	1.428198	974.7177	0
		Stim State	0.082105	1	0.082105	56.0349	1.06E-13
		Bhv State:Stim State	0.074121	3	0.024707	16.86202	8.10E-11
		Error	2.943672	2009	0.001465	NaN	NaN
		Total	7.333655	2016	NaN	NaN	NaN

2	RISyhat	Bhv State	0.677864	3	0.225955	207.2215	4.25E-117
		Stim State	0.325448	1	0.325448	298.4661	1.85E-62
		Bhv State:Stim State	0.586777	3	0.195592	179.3763	4.81E-103
		Error	2.190618	2009	0.00109	NaN	NaN
		Total	4.799268	2016	NaN	NaN	NaN
2	RIGLyhat	Bhv State	0.045823	3	0.015274	292.2887	1.96E-157
		Stim State	0.008737	1	0.008737	167.1939	8.53E-37
		Bhv State:Stim State	0.020971	3	0.00699	133.7663	5.23E-79
		Error	0.104985	2009	5.23E-05	NaN	NaN
		Total	0.205024	2016	NaN	NaN	NaN
3	AVFRyhat	Bhv State	0.365771	3	0.121924	366.1942	1.03E-192
		Stim State	0.069793	1	0.069793	209.6221	1.95E-45
		Bhv State:Stim State	0.013222	3	0.004407	13.23732	1.45E-08
		Error	0.728823	2189	0.000333	NaN	NaN
		Total	1.205259	2196	NaN	NaN	NaN
3	BAGLyhat	Bhv State	1.157731	3	0.38591	108.6577	1.40E-65
		Stim State	0.891979	1	0.891979	251.1473	1.25E-53
		Bhv State:Stim State	0.979026	3	0.326342	91.88558	5.24E-56
		Error	7.774485	2189	0.003552	NaN	NaN
		Total	10.63523	2196	NaN	NaN	NaN
3	BAGRyhat	Bhv State	0.789852	3	0.263284	113.761	1.86E-68
		Stim State	0.435056	1	0.435056	187.981	4.16E-41
		Bhv State:Stim State	0.673461	3	0.224487	96.99739	6.05E-59
		Error	5.066135	2189	0.002314	NaN	NaN
		Total	6.797832	2196	NaN	NaN	NaN
3	RMEDyhat	Bhv State	0.34463	3	0.114877	502.0723	3.12E-248
		Stim State	0.037059	1	0.037059	161.9688	7.57E-36
		Bhv State:Stim State	0.002323	3	0.000774	3.384947	0.017463
		Error	0.500854	2189	0.000229	NaN	NaN
		Total	0.889691	2196	NaN	NaN	NaN
3	RISyhat	Bhv State	12.26024	3	4.086748	889.8543	0
		Stim State	0.241238	1	0.241238	52.52752	5.85E-13
		Bhv State:Stim State	0.201868	3	0.067289	14.65169	1.90E-09
		Error	10.05321	2189	0.004593	NaN	NaN
		Total	24.61968	2196	NaN	NaN	NaN
3	RIGLyhat	Bhv State	0.227945	3	0.075982	390.58	3.63E-203
		Stim State	0.024267	1	0.024267	124.7434	3.30E-28
		Bhv State:Stim State	0.00095	3	0.000317	1.627242	0.180997
		Error	0.425838	2189	0.000195	NaN	NaN
		Total	0.69091	2196	NaN	NaN	NaN
4	AVFRyhat	Bhv State	0.320295	3	0.106765	687.2411	1.95E-307
		Stim State	0.126749	1	0.126749	815.8741	6.65E-151
		Bhv State:Stim State	0.010524	3	0.003508	22.58021	2.24E-14
		Error	0.31226	2010	0.000155	NaN	NaN
		Total	0.817148	2017	NaN	NaN	NaN
4	BAGLyhat	Bhv State	0.321211	3	0.10707	41.61207	4.38E-26
		Stim State	0.663805	1	0.663805	257.9829	1.03E-54
		Bhv State:Stim State	0.269192	3	0.089731	34.87316	5.74E-22
		Error	5.171845	2010	0.002573	NaN	NaN
		Total	6.500712	2017	NaN	NaN	NaN

4	BAGRyhat	Bhv State	1.029991	3	0.34333	77.41027	2.20E-47
		Stim State	1.093983	1	1.093983	246.6589	1.61E-52
		Bhv State:Stim State	0.441488	3	0.147163	33.18059	6.28E-21
		Error	8.914764	2010	0.004435	NaN	NaN
		Total	11.60492	2017	NaN	NaN	NaN
4	RMEDyhat	Bhv State	5.644404	3	1.881468	2289.303	0
		Stim State	0.532634	1	0.532634	648.0906	3.76E-124
		Bhv State:Stim State	0.400195	3	0.133398	162.3142	3.28E-94
		Error	1.651922	2010	0.000822	NaN	NaN
		Total	7.982965	2017	NaN	NaN	NaN
4	RISyhat	Bhv State	1.889158	3	0.629719	917.3913	0
		Stim State	0.150093	1	0.150093	218.6587	4.79E-47
		Bhv State:Stim State	0.572737	3	0.190912	278.126	5.53E-151
		Error	1.379712	2010	0.000686	NaN	NaN
		Total	4.425568	2017	NaN	NaN	NaN
4	RIGLyhat	Bhv State	0.112411	3	0.03747	147.4886	2.21E-86
		Stim State	0.000618	1	0.000618	2.431652	0.119065
		Bhv State:Stim State	0.010998	3	0.003666	14.42995	2.66E-09
		Error	0.510651	2010	0.000254	NaN	NaN
		Total	0.627875	2017	NaN	NaN	NaN
5	AVFRyhat	Bhv State	0.022569	3	0.007523	231.3677	2.07E-130
		Stim State	4.81E-05	1	4.81E-05	1.479604	0.223967
		Bhv State:Stim State	0.017809	3	0.005936	182.5754	1.13E-105
		Error	0.071305	2193	3.25E-05	NaN	NaN
		Total	0.105362	2200	NaN	NaN	NaN
5	BAGLyhat	Bhv State	0.790619	3	0.26354	210.1539	8.21E-120
		Stim State	0.647341	1	0.647341	516.2074	8.47E-103
		Bhv State:Stim State	0.665071	3	0.22169	176.7821	1.19E-102
		Error	2.750092	2193	0.001254	NaN	NaN
		Total	4.511179	2200	NaN	NaN	NaN
5	BAGRyhat	Bhv State	1.89202	3	0.630673	217.2061	2.32E-123
		Stim State	1.466388	1	1.466388	505.0292	7.95E-101
		Bhv State:Stim State	1.602225	3	0.534075	183.9373	2.21E-106
		Error	6.367531	2193	0.002904	NaN	NaN
		Total	10.27966	2200	NaN	NaN	NaN
5	RMEDyhat	Bhv State	0.504489	3	0.168163	1272.416	0
		Stim State	0.007017	1	0.007017	53.0975	4.41E-13
		Bhv State:Stim State	0.091989	3	0.030663	232.0131	9.93E-131
		Error	0.289828	2193	0.000132	NaN	NaN
		Total	0.871737	2200	NaN	NaN	NaN
5	RISyhat	Bhv State	1.914283	3	0.638094	672.1964	0.00E+00
		Stim State	0.826708	1	0.826708	870.8904	1.80E-161
		Bhv State:Stim State	1.572941	3	0.524314	552.3349	2.40E-267
		Error	2.081744	2193	0.000949	NaN	NaN
		Total	10.10025	2200	NaN	NaN	NaN
6	AVFRyhat	Bhv State	0.138803	3	0.046268	333.8081	7.53E-176
		Stim State	0.003932	1	0.003932	28.36787	1.12E-07
		Bhv State:Stim State	0.01241	3	0.004137	29.84459	7.11E-19
		Error	0.278458	2009	0.000139	NaN	NaN
		Total	0.440402	2016	NaN	NaN	NaN

6	BAGLyhat	Bhv State	2.358369	3	0.786123	89.97107	1.25E-54
		Stim State	2.053585	1	2.053585	235.0309	2.97E-50
		Bhv State:Stim State	1.347682	3	0.449227	51.41366	5.17E-32
		Error	17.55365	2009	0.008738	NaN	NaN
		Total	24.73945	2016	NaN	NaN	NaN
6	BAGRyhat	Bhv State	0.855305	3	0.285102	49.42099	8.18E-31
		Stim State	1.139735	1	1.139735	197.5676	7.11E-43
		Bhv State:Stim State	0.905128	3	0.301709	52.2999	1.52E-32
		Error	11.58959	2009	0.005769	NaN	NaN
		Total	14.99401	2016	NaN	NaN	NaN
6	RMEDyhat	Bhv State	14.60857	3	4.869522	2340.033	0
		Stim State	0.062202	1	0.062202	29.89074	5.14E-08
		Bhv State:Stim State	0.063655	3	0.021218	10.19647	1.16E-06
		Error	4.180654	2009	0.002081	NaN	NaN
		Total	20.06335	2016	NaN	NaN	NaN
6	RISyhat	Bhv State	0.413124	3	0.137708	307.1102	4.25E-164
		Stim State	0.083743	1	0.083743	186.7591	1.01E-40
		Bhv State:Stim State	0.105517	3	0.035172	78.44011	5.55E-48
		Error	0.900834	2009	0.000448	NaN	NaN
		Total	1.753435	2016	NaN	NaN	NaN
6	RIGLyhat	Bhv State	0.165335	3	0.055112	312.9217	1.10E-166
		Stim State	0.000191	1	0.000191	1.083657	0.298006
		Bhv State:Stim State	0.04214	3	0.014047	79.75675	9.56E-49
		Error	0.353824	2009	0.000176	NaN	NaN
		Total	0.597155	2016	NaN	NaN	NaN
7	AVFRyhat	Bhv State	0.054338	3	0.018113	102.4242	1.06E-61
		Stim State	1.53E-05	1	1.53E-05	0.086285	0.768985
		Bhv State:Stim State	0.012275	3	0.004092	23.13694	1.01E-14
		Error	0.355627	2011	0.000177	NaN	NaN
		Total	0.428958	2018	NaN	NaN	NaN
7	BAGLyhat	Bhv State	2.48278	3	0.827593	145.6931	1.98E-85
		Stim State	1.871761	1	1.871761	329.5128	2.59E-68
		Bhv State:Stim State	1.941156	3	0.647052	113.9098	3.99E-68
		Error	11.42326	2011	0.00568	NaN	NaN
		Total	19.05463	2018	NaN	NaN	NaN
7	BAGRyhat	Bhv State	2.863138	3	0.954379	98.4322	1.90E-59
		Stim State	2.934285	1	2.934285	302.6345	2.97E-63
		Bhv State:Stim State	3.193371	3	1.064457	109.7853	7.89E-66
		Error	19.49826	2011	0.009696	NaN	NaN
		Total	30.77056	2018	NaN	NaN	NaN
7	RMEDyhat	Bhv State	22.03008	3	7.34336	4028.735	0
		Stim State	0.251694	1	0.251694	138.0849	6.97E-31
		Bhv State:Stim State	0.139718	3	0.046573	25.5508	3.21E-16
		Error	3.665542	2011	0.001823	NaN	NaN
		Total	26.03246	2018	NaN	NaN	NaN

Table 6: **ANOVA tests for AVFR, BAGL, BAGR, RIGL, RIS, RMED, and SABD activity and connectivity vs. behavior and oxygen stimulation factor levels**. Glossary: [neuron]yhat: reconstructed activity, Bhv: behavior states (1-4), Stim: stim states (21 percent oxygen only first half trial, or alternating oxygen levels second half), df: degrees of freedom, SS: sum of squares, MS: mean squared, F: test statistic, p: p-value.

Worm	variable	source	df	test stat	value	F	dfN	dfD	p
1	AVFRconnTo	Bhv State	3	pillai	9.540921	NaN	30	6546	NaN
			NaN	wilks	NaN	NaN	30	6399.407	NaN
			NaN	hotelling	NaN	NaN	30	6536	NaN
			NaN	roy	3.688644	804.862	10	2182	0
		Stim State	1	pillai	0.258987	76.19194	10	2180	3.48E-134
			NaN	wilks	NaN	NaN	10	2180	NaN
			NaN	hotelling	NaN	NaN	10	2180	NaN
			NaN	roy	0.191179	41.6771	10	2180	6.15E-76
		Bhv State:Stim State	3	pillai	0.173141	13.36447	30	6546	2.97E-64
			NaN	wilks	NaN	NaN	30	6399.407	NaN
			NaN	hotelling	NaN	NaN	30	6536	NaN
			NaN	roy	2.511058	547.9128	10	2182	0
		Error	2189		NaN	NaN	NaN	NaN	NaN
		Total	2196		NaN	NaN	NaN	NaN	NaN
1	BAGLconnTo	Bhv State	3	pillai	38.13863	NaN	30	6546	NaN
			NaN	wilks	NaN	NaN	30	6399.407	NaN
			NaN	hotelling	NaN	NaN	30	6536	NaN
			NaN	roy	3.904434	851.9474	10	2182	0
		Stim State	1	pillai	-0.01884	-4.03076	10	2180	1
			NaN	wilks	NaN	NaN	10	2180	NaN
			NaN	hotelling	NaN	NaN	10	2180	NaN
			NaN	roy	0.191179	41.6771	10	2180	6.15E-76
		Bhv State:Stim State	3	pillai	1.491127	215.6337	30	6546	0
			NaN	wilks	NaN	NaN	30	6399.407	NaN
			NaN	hotelling	NaN	NaN	30	6536	NaN
			NaN	roy	2.326573	507.6582	10	2182	0
		Error	2189		NaN	NaN	NaN	NaN	NaN
		Total	2196		NaN	NaN	NaN	NaN	NaN
1	BAGRconnTo	Bhv State	3	pillai	6.912903	NaN	30	6546	NaN
			NaN	wilks	NaN	NaN	30	6399.407	NaN
			NaN	hotelling	NaN	NaN	30	6536	NaN
			NaN	roy	9.233338	2014.714	10	2182	0
		Stim State	1	pillai	0.188728	50.71384	10	2180	7.50E-92
			NaN	wilks	NaN	NaN	10	2180	NaN
			NaN	hotelling	NaN	NaN	10	2180	NaN
			NaN	roy	0.191179	41.6771	10	2180	6.15E-76
		Bhv State:Stim State	3	pillai	-0.31042	-20.4605	30	6546	1
			NaN	wilks	NaN	NaN	30	6399.407	NaN
			NaN	hotelling	NaN	NaN	30	6536	NaN
			NaN	roy	Inf	Inf	10	2182	0
		Error	2189		NaN	NaN	NaN	NaN	NaN

		Total	2196		NaN	NaN	NaN	NaN	NaN
1	RMEDconnTo	Bhv State	3	pillai	15.52548	NaN	30	6546	NaN
			NaN	wilks	NaN	NaN	30	6399.407	NaN
			NaN	hotelling	NaN	NaN	30	6536	NaN
			NaN	roy	5.416601	1181.902	10	2182	0
		Stim State	1	pillai	0.325442	105.1747	10	2180	2.87E-178
			NaN	wilks	NaN	NaN	10	2180	NaN
			NaN	hotelling	NaN	NaN	10	2180	NaN
			NaN	roy	0.395669	86.25579	10	2180	5.96E-150
		Bhv State:Stim State	3	pillai	3.905608	NaN	30	6546	NaN
			NaN	wilks	NaN	NaN	30	6399.407	NaN
			NaN	hotelling	NaN	NaN	30	6536	NaN
			NaN	roy	0.498856	108.8504	10	2182	1.30E-183
		Error	2189		NaN	NaN	NaN	NaN	NaN
		Total	2196		NaN	NaN	NaN	NaN	NaN
1	RISconnTo	Bhv State	3	pillai	Inf	NaN	30	6546	NaN
			NaN	wilks	NaN	NaN	30	6399.407	NaN
			NaN	hotelling	NaN	NaN	30	6536	NaN
			NaN	roy	3.688644	804.862	10	2182	0
		Stim State	1	pillai	-0.72455	-91.5899	10	2180	1
			NaN	wilks	NaN	NaN	10	2180	NaN
			NaN	hotelling	NaN	NaN	10	2180	NaN
			NaN	roy	0.191179	41.6771	10	2180	6.15E-76
		Bhv State:Stim State	3	pillai	1.51552	222.7626	30	6546	0
			NaN	wilks	NaN	NaN	30	6399.407	NaN
			NaN	hotelling	NaN	NaN	30	6536	NaN
			NaN	roy	0.792355	172.892	10	2182	7.47E-268
		Error	2189		NaN	NaN	NaN	NaN	NaN
		Total	2196		NaN	NaN	NaN	NaN	NaN
1	SABDconnTo	Bhv State	3	pillai	Inf	NaN	30	6546	NaN
			NaN	wilks	NaN	NaN	30	6399.407	NaN
			NaN	hotelling	NaN	NaN	30	6536	NaN
			NaN	roy	Inf	Inf	10	2182	0
		Stim State	1	pillai	0.267546	79.62975	10	2180	1.25E-139
			NaN	wilks	NaN	NaN	10	2180	NaN
			NaN	hotelling	NaN	NaN	10	2180	NaN
			NaN	roy	0.191179	41.6771	10	2180	6.15E-76
		Bhv State:Stim State	3	pillai	1.76795	313.1098	30	6546	0
			NaN	wilks	NaN	NaN	30	6399.407	NaN
			NaN	hotelling	NaN	NaN	30	6536	NaN
			NaN	roy	Inf	Inf	10	2182	0
		Error	2189		NaN	NaN	NaN	NaN	NaN
		Total	2196		NaN	NaN	NaN	NaN	NaN
1	AVFRconnFrom	Bhv State	3	pillai	11.7608	NaN	30	6546	NaN
			NaN	wilks	NaN	NaN	30	6399.407	NaN
			NaN	hotelling	NaN	NaN	30	6536	NaN
			NaN	roy	Inf	Inf	10	2182	0
		Stim State	1	pillai	0.18234	48.61463	10	2180	3.37E-88
			NaN	wilks	NaN	NaN	10	2180	NaN
			NaN	hotelling	NaN	NaN	10	2180	NaN

			NaN	roy	0.191179	41.6771	10	2180	6.15E-76
		Bhv State:Stim State	3	pillai	0.894071	92.63671	30	6546	0
			NaN	wilks	NaN	NaN	30	6399.407	NaN
			NaN	hotelling	NaN	NaN	30	6536	NaN
			NaN	roy	0.498856	108.8504	10	2182	1.30E-183
		Error	2189		NaN	NaN	NaN	NaN	NaN
		Total	2196		NaN	NaN	NaN	NaN	NaN
1	BAGLconnFrom	Bhv State	3	pillai	8.956102851	NaN	30	6546	NaN
			NaN	wilks	NaN	NaN	30	6399.407	NaN
			NaN	hotelling	NaN	NaN	30	6536	NaN
			NaN	roy	3.688644	804.862	10	2182	0
		Stim State	1	pillai	0.631617	373.7748	10	2180	0
			NaN	wilks	NaN	NaN	10	2180	NaN
			NaN	hotelling	NaN	NaN	10	2180	NaN
			NaN	roy	0.191179	41.6771	10	2180	6.15E-76
		Bhv State:Stim State	3	pillai	1.262096	158.4607	30	6546	0
			NaN	wilks	NaN	NaN	30	6399.407	NaN
			NaN	hotelling	NaN	NaN	30	6536	NaN
			NaN	roy	0.561596	122.5402	10	2182	6.58E-203
		Error	2189		NaN	NaN	NaN	NaN	NaN
		Total	2196		NaN	NaN	NaN	NaN	NaN
1	BAGRconnFrom	Bhv State	3	pillai	2.643022	1615.525	30	6546	0
			NaN	wilks	NaN	NaN	30	6399.407	NaN
			NaN	hotelling	NaN	NaN	30	6536	NaN
			NaN	roy	Inf	Inf	10	2182	0
		Stim State	1	pillai	-0.43845	-66.4477	10	2180	1
			NaN	wilks	NaN	NaN	10	2180	NaN
			NaN	hotelling	NaN	NaN	10	2180	NaN
			NaN	roy	0.191179	41.6771	10	2180	6.15E-76
		Bhv State:Stim State	3	pillai	1.485479	214.0157	30	6546	0
			NaN	wilks	NaN	NaN	30	6399.407	NaN
			NaN	hotelling	NaN	NaN	30	6536	NaN
			NaN	roy	0.498856	108.8504	10	2182	1.30E-183
		Error	2189		NaN	NaN	NaN	NaN	NaN
		Total	2196		NaN	NaN	NaN	NaN	NaN
1	RMEDconnFrom	Bhv State	3	pillai	0.972019	104.584	30	6546	0
			NaN	wilks	NaN	NaN	30	6399.407	NaN
			NaN	hotelling	NaN	NaN	30	6536	NaN
			NaN	roy	Inf	Inf	10	2182	0
		Stim State	1	pillai	0.289151	88.67555	10	2180	1.15E-153
			NaN	wilks	NaN	NaN	10	2180	NaN
			NaN	hotelling	NaN	NaN	10	2180	NaN
			NaN	roy	0.191179	41.6771	10	2180	6.15E-76
		Bhv State:Stim State	3	pillai	-0.5458	-33.5874	30	6546	1
			NaN	wilks	NaN	NaN	30	6399.407	NaN
			NaN	hotelling	NaN	NaN	30	6536	NaN
			NaN	roy	0.498856	108.8504	10	2182	1.30E-183
		Error	2189		NaN	NaN	NaN	NaN	NaN
		Total	2196		NaN	NaN	NaN	NaN	NaN
1	RISconnFrom	Bhv State	3	pillai	3.091754	NaN	30	6546	NaN

			NaN	wilks	NaN	NaN	30	6399.407	NaN
			NaN	hotelling	NaN	NaN	30	6536	NaN
			NaN	roy	Inf	Inf	10	2182	0
		Stim State	1	pillai	0.161072	41.85552	10	2180	2.95E-76
			NaN	wilks	NaN	NaN	10	2180	NaN
			NaN	hotelling	NaN	NaN	10	2180	NaN
			NaN	roy	0.191179	41.6771	10	2180	6.15E-76
		Bhv State:Stim State	3	pillai	Inf	NaN	30	6546	NaN
			NaN	wilks	NaN	NaN	30	6399.407	NaN
			NaN	hotelling	NaN	NaN	30	6536	NaN
			NaN	roy	1.497624	326.7815	10	2182	0
		Error	2189		NaN	NaN	NaN	NaN	NaN
		Total	2196		NaN	NaN	NaN	NaN	NaN
1	SABDconnFrom	Bhv State	3	pillai	3.843016	NaN	30	6546	NaN
			NaN	wilks	NaN	NaN	30	6399.407	NaN
			NaN	hotelling	NaN	NaN	30	6536	NaN
			NaN	roy	3.688644	804.862	10	2182	0
		Stim State	1	pillai	0.419079	157.2664	10	2180	1.42E-248
			NaN	wilks	NaN	NaN	10	2180	NaN
			NaN	hotelling	NaN	NaN	10	2180	NaN
			NaN	roy	0.191179	41.6771	10	2180	6.15E-76
		Bhv State:Stim State	3	pillai	0.995657	108.3908	30	6546	0
			NaN	wilks	NaN	NaN	30	6399.407	NaN
			NaN	hotelling	NaN	NaN	30	6536	NaN
			NaN	roy	0.498856	108.8504	10	2182	1.30E-183
		Error	2189		NaN	NaN	NaN	NaN	NaN
		Total	2196		NaN	NaN	NaN	NaN	NaN
2	AVFRconnTo	Bhv State	3	pillai	1.418663	179.5155	30	6003	0
			NaN	wilks	NaN	NaN	30	5868.136	NaN
			NaN	hotelling	NaN	NaN	30	5993	NaN
			NaN	roy	Inf	Inf	10	2001	0
		Stim State	1	pillai	-0.20132	-33.4992	10	1999	1
			NaN	wilks	NaN	NaN	10	1999	NaN
			NaN	hotelling	NaN	NaN	10	1999	NaN
			NaN	roy	3.635291	726.6948	10	1999	0
		Bhv State:Stim State	3	pillai	4.724728	NaN	30	6003	NaN
			NaN	wilks	NaN	NaN	30	5868.136	NaN
			NaN	hotelling	NaN	NaN	30	5993	NaN
			NaN	roy	2.607103	521.6814	10	2001	0
		Error	2008		NaN	NaN	NaN	NaN	NaN
		Total	2015		NaN	NaN	NaN	NaN	NaN
2	BAGLconnTo	Bhv State	3	pillai	2.074213	448.3214	30	6003	0
			NaN	wilks	NaN	NaN	30	5868.136	NaN
			NaN	hotelling	NaN	NaN	30	5993	NaN
			NaN	roy	7.165604	1433.837	10	2001	0
		Stim State	1	pillai	0.735164	554.9059	10	1999	0
			NaN	wilks	NaN	NaN	10	1999	NaN
			NaN	hotelling	NaN	NaN	10	1999	NaN
			NaN	roy	3.635291	726.6948	10	1999	0
		Bhv State:Stim State	3	pillai	7.303966	NaN	30	6003	NaN

			NaN	wilks	NaN	NaN	30	5868.136	NaN
			NaN	hotelling	NaN	NaN	30	5993	NaN
			NaN	roy	3.79062	758.5031	10	2001	0
		Error	2008		NaN	NaN	NaN	NaN	NaN
		Total	2015		NaN	NaN	NaN	NaN	NaN
2	BAGRconnTo	Bhv State	3	pillai	Inf	NaN	30	6003	NaN
			NaN	wilks	NaN	NaN	30	5868.136	NaN
			NaN	hotelling	NaN	NaN	30	5993	NaN
			NaN	roy	13.42021	2685.383	10	2001	0
		Stim State	1	pillai	0.567904	262.7284	10	1999	0
			NaN	wilks	NaN	NaN	10	1999	NaN
			NaN	hotelling	NaN	NaN	10	1999	NaN
			NaN	roy	3.635291	726.6948	10	1999	0
		Bhv State:Stim State	3	pillai	5.554439	NaN	30	6003	NaN
			NaN	wilks	NaN	NaN	30	5868.136	NaN
			NaN	hotelling	NaN	NaN	30	5993	NaN
			NaN	roy	Inf	Inf	10	2001	0
		Error	2008		NaN	NaN	NaN	NaN	NaN
		Total	2015		NaN	NaN	NaN	NaN	NaN
2	RMEDconnTo	Bhv State	3	pillai	12.48272	NaN	30	6003	NaN
			NaN	wilks	NaN	NaN	30	5868.136	NaN
			NaN	hotelling	NaN	NaN	30	5993	NaN
			NaN	roy	7.165604	1433.837	10	2001	0
		Stim State	1	pillai	6.473308	NaN	10	1999	NaN
			NaN	wilks	NaN	NaN	10	1999	NaN
			NaN	hotelling	NaN	NaN	10	1999	NaN
			NaN	roy	3.635291	726.6948	10	1999	0
		Bhv State:Stim State	3	pillai	19.49274	NaN	30	6003	NaN
			NaN	wilks	NaN	NaN	30	5868.136	NaN
			NaN	hotelling	NaN	NaN	30	5993	NaN
			NaN	roy	10.38253	2077.544	10	2001	0
		Error	2008		NaN	NaN	NaN	NaN	NaN
		Total	2015		NaN	NaN	NaN	NaN	NaN
2	RISconnTo	Bhv State	3	pillai	22.19098	NaN	30	6003	NaN
			NaN	wilks	NaN	NaN	30	5868.136	NaN
			NaN	hotelling	NaN	NaN	30	5993	NaN
			NaN	roy	Inf	Inf	10	2001	0
		Stim State	1	pillai	5.540859	NaN	10	1999	NaN
			NaN	wilks	NaN	NaN	10	1999	NaN
			NaN	hotelling	NaN	NaN	10	1999	NaN
			NaN	roy	6.057822	1210.959	10	1999	0
		Bhv State:Stim State	3	pillai	-5.06838	-125.698	30	6003	1
			NaN	wilks	NaN	NaN	30	5868.136	NaN
			NaN	hotelling	NaN	NaN	30	5993	NaN
			NaN	roy	Inf	Inf	10	2001	0
		Error	2008		NaN	NaN	NaN	NaN	NaN
		Total	2015		NaN	NaN	NaN	NaN	NaN
2	RIGLconnTo	Bhv State	3	pillai	7.094907	NaN	30	6003	NaN
			NaN	wilks	NaN	NaN	30	5868.136	NaN
			NaN	hotelling	NaN	NaN	30	5993	NaN

			NaN	roy	7.165604	1433.837	10	2001	0
		Stim State	1	pillai	0.695073	455.6659	10	1999	0
			NaN	wilks	NaN	NaN	10	1999	NaN
			NaN	hotelling	NaN	NaN	10	1999	NaN
			NaN	roy	3.635291	726.6948	10	1999	0
		Bhv State:Stim State	3	pillai	5.711106	NaN	30	6003	NaN
			NaN	wilks	NaN	NaN	30	5868.136	NaN
			NaN	hotelling	NaN	NaN	30	5993	NaN
			NaN	roy	2.607103	521.6814	10	2001	0
		Error	2008		NaN	NaN	NaN	NaN	NaN
		Total	2015		NaN	NaN	NaN	NaN	NaN
2	AVFRconnFrom	Bhv State	3	pillai	16.55175	NaN	30	6003	NaN
			NaN	wilks	NaN	NaN	30	5868.136	NaN
			NaN	hotelling	NaN	NaN	30	5993	NaN
			NaN	roy	Inf	Inf	10	2001	0
		Stim State	1	pillai	7.930625	NaN	10	1999	NaN
			NaN	wilks	NaN	NaN	10	1999	NaN
			NaN	hotelling	NaN	NaN	10	1999	NaN
			NaN	roy	3.635291	726.6948	10	1999	0
		Bhv State:Stim State	3	pillai	Inf	NaN	30	6003	NaN
			NaN	wilks	NaN	NaN	30	5868.136	NaN
			NaN	hotelling	NaN	NaN	30	5993	NaN
			NaN	roy	Inf	Inf	10	2001	0
		Error	2008		NaN	NaN	NaN	NaN	NaN
		Total	2015		NaN	NaN	NaN	NaN	NaN
2	BAGLconnFrom	Bhv State	3	pillai	9.292581	NaN	30	6003	NaN
			NaN	wilks	NaN	NaN	30	5868.136	NaN
			NaN	hotelling	NaN	NaN	30	5993	NaN
			NaN	roy	Inf	Inf	10	2001	0
		Stim State	1	pillai	0.558362	252.7334	10	1999	0
			NaN	wilks	NaN	NaN	10	1999	NaN
			NaN	hotelling	NaN	NaN	10	1999	NaN
			NaN	roy	3.635291	726.6948	10	1999	0
		Bhv State:Stim State	3	pillai	Inf	NaN	30	6003	NaN
			NaN	wilks	NaN	NaN	30	5868.136	NaN
			NaN	hotelling	NaN	NaN	30	5993	NaN
			NaN	roy	Inf	Inf	10	2001	0
		Error	2008		NaN	NaN	NaN	NaN	NaN
		Total	2015		NaN	NaN	NaN	NaN	NaN
2	BAGRconnFrom	Bhv State	3	pillai	3.774569	NaN	30	6003	NaN
			NaN	wilks	NaN	NaN	30	5868.136	NaN
			NaN	hotelling	NaN	NaN	30	5993	NaN
			NaN	roy	7.165604	1433.837	10	2001	0
		Stim State	1	pillai	1.739933	NaN	10	1999	NaN
			NaN	wilks	NaN	NaN	10	1999	NaN
			NaN	hotelling	NaN	NaN	10	1999	NaN
			NaN	roy	3.635291	726.6948	10	1999	0
		Bhv State:Stim State	3	pillai	5.264125	NaN	30	6003	NaN
			NaN	wilks	NaN	NaN	30	5868.136	NaN
			NaN	hotelling	NaN	NaN	30	5993	NaN

			NaN	roy	3.02664	605.6306	10	2001	0
		Error	2008		NaN	NaN	NaN	NaN	NaN
		Total	2015		NaN	NaN	NaN	NaN	NaN
2	RMEDconnFrom	Bhv State	3	pillai	4.521005	NaN	30	6003	NaN
			NaN	wilks	NaN	NaN	30	5868.136	NaN
			NaN	hotelling	NaN	NaN	30	5993	NaN
			NaN	roy	7.165604	1433.837	10	2001	0
		Stim State	1	pillai	2.799158	NaN	10	1999	NaN
			NaN	wilks	NaN	NaN	10	1999	NaN
			NaN	hotelling	NaN	NaN	10	1999	NaN
			NaN	roy	3.635291	726.6948	10	1999	0
		Bhv State:Stim State	3	pillai	11.6236	NaN	30	6003	NaN
			NaN	wilks	NaN	NaN	30	5868.136	NaN
			NaN	hotelling	NaN	NaN	30	5993	NaN
			NaN	roy	Inf	Inf	10	2001	0
		Error	2008		NaN	NaN	NaN	NaN	NaN
		Total	2015		NaN	NaN	NaN	NaN	NaN
2	RISconnFrom	Bhv State	3	pillai	Inf	NaN	30	6003	NaN
			NaN	wilks	NaN	NaN	30	5868.136	NaN
			NaN	hotelling	NaN	NaN	30	5993	NaN
			NaN	roy	7.165604	1433.837	10	2001	0
		Stim State	1	pillai	-2.35667	-140.347	10	1999	1
			NaN	wilks	NaN	NaN	10	1999	NaN
			NaN	hotelling	NaN	NaN	10	1999	NaN
			NaN	roy	3.635291	726.6948	10	1999	0
		Bhv State:Stim State	3	pillai	Inf	NaN	30	6003	NaN
			NaN	wilks	NaN	NaN	30	5868.136	NaN
			NaN	hotelling	NaN	NaN	30	5993	NaN
			NaN	roy	2.607103	521.6814	10	2001	0
		Error	2008		NaN	NaN	NaN	NaN	NaN
		Total	2015		NaN	NaN	NaN	NaN	NaN
2	RIGLconnFrom	Bhv State	3	pillai	Inf	NaN	30	6003	NaN
			NaN	wilks	NaN	NaN	30	5868.136	NaN
			NaN	hotelling	NaN	NaN	30	5993	NaN
			NaN	roy	8.969872	1794.871	10	2001	0
		Stim State	1	pillai	2.953883	NaN	10	1999	NaN
			NaN	wilks	NaN	NaN	10	1999	NaN
			NaN	hotelling	NaN	NaN	10	1999	NaN
			NaN	roy	3.635291	726.6948	10	1999	0
		Bhv State:Stim State	3	pillai	7.360898	NaN	30	6003	NaN
			NaN	wilks	NaN	NaN	30	5868.136	NaN
			NaN	hotelling	NaN	NaN	30	5993	NaN
			NaN	roy	2.607103	521.6814	10	2001	0
		Error	2008		NaN	NaN	NaN	NaN	NaN
		Total	2015		NaN	NaN	NaN	NaN	NaN
3	AVFRconnTo	Bhv State	3	pillai	5.436535	NaN	30	6543	NaN
			NaN	wilks	NaN	NaN	30	6396.471	NaN
			NaN	hotelling	NaN	NaN	30	6533	NaN
			NaN	roy	Inf	Inf	10	2181	0
		Stim State	1	pillai	0.256133	75.02875	10	2179	2.54E-132

			NaN	wilks	NaN	NaN	10	2179	NaN
			NaN	hotelling	NaN	NaN	10	2179	NaN
			NaN	roy	0.372163	81.09426	10	2179	6.41E-142
		Bhv State:Stim State	3	pillai	0.758778	73.83901	30	6543	0
			NaN	wilks	NaN	NaN	30	6396.471	NaN
			NaN	hotelling	NaN	NaN	30	6533	NaN
			NaN	roy	0.675456	147.317	10	2181	6.05E-236
		Error	2188		NaN	NaN	NaN	NaN	NaN
		Total	2195		NaN	NaN	NaN	NaN	NaN
3	BAGLconnTo	Bhv State	3	pillai	2.093326	503.5487	30	6543	0
			NaN	wilks	NaN	NaN	30	6396.471	NaN
			NaN	hotelling	NaN	NaN	30	6533	NaN
			NaN	roy	8.460378	1845.208	10	2181	0
		Stim State	1	pillai	0.337662	111.086	10	2179	9.04E-187
			NaN	wilks	NaN	NaN	10	2179	NaN
			NaN	hotelling	NaN	NaN	10	2179	NaN
			NaN	roy	0.372163	81.09426	10	2179	6.41E-142
		Bhv State:Stim State	3	pillai	1.143403	134.3189	30	6543	0
			NaN	wilks	NaN	NaN	30	6396.471	NaN
			NaN	hotelling	NaN	NaN	30	6533	NaN
			NaN	roy	1.025491	223.6595	10	2181	0
		Error	2188		NaN	NaN	NaN	NaN	NaN
		Total	2195		NaN	NaN	NaN	NaN	NaN
3	BAGRconnTo	Bhv State	3	pillai	1.917996	386.6114	30	6543	0
			NaN	wilks	NaN	NaN	30	6396.471	NaN
			NaN	hotelling	NaN	NaN	30	6533	NaN
			NaN	roy	8.460378	1845.208	10	2181	0
		Stim State	1	pillai	0.243887	70.28456	10	2179	1.11E-124
			NaN	wilks	NaN	NaN	10	2179	NaN
			NaN	hotelling	NaN	NaN	10	2179	NaN
			NaN	roy	0.372163	81.09426	10	2179	6.41E-142
		Bhv State:Stim State	3	pillai	Inf	NaN	30	6543	NaN
			NaN	wilks	NaN	NaN	30	6396.471	NaN
			NaN	hotelling	NaN	NaN	30	6533	NaN
			NaN	roy	0.675456	147.317	10	2181	6.05E-236
		Error	2188		NaN	NaN	NaN	NaN	NaN
		Total	2195		NaN	NaN	NaN	NaN	NaN
3	RMEDconnTo	Bhv State	3	pillai	4.696826	NaN	30	6543	NaN
			NaN	wilks	NaN	NaN	30	6396.471	NaN
			NaN	hotelling	NaN	NaN	30	6533	NaN
			NaN	roy	8.460378	1845.208	10	2181	0
		Stim State	1	pillai	0.076766	18.11825	10	2179	3.47E-32
			NaN	wilks	NaN	NaN	10	2179	NaN
			NaN	hotelling	NaN	NaN	10	2179	NaN
			NaN	roy	0.372163	81.09426	10	2179	6.41E-142
		Bhv State:Stim State	3	pillai	0.61223	55.92137	30	6543	2.11E-296
			NaN	wilks	NaN	NaN	30	6396.471	NaN
			NaN	hotelling	NaN	NaN	30	6533	NaN
			NaN	roy	0.675456	147.317	10	2181	6.05E-236
		Error	2188		NaN	NaN	NaN	NaN	NaN

		Total	2195		NaN	NaN	NaN	NaN	NaN
3	RISconnTo	Bhv State	3	pillai	Inf	NaN	30	6543	NaN
			NaN	wilks	NaN	NaN	30	6396.471	NaN
			NaN	hotelling	NaN	NaN	30	6533	NaN
			NaN	roy	8.460378	1845.208	10	2181	0
		Stim State	1	pillai	0.402413	146.7332	10	2179	3.82E-235
			NaN	wilks	NaN	NaN	10	2179	NaN
			NaN	hotelling	NaN	NaN	10	2179	NaN
			NaN	roy	0.372163	81.09426	10	2179	6.41E-142
		Bhv State:Stim State	3	pillai	0.684342	64.4547	30	6543	0
			NaN	wilks	NaN	NaN	30	6396.471	NaN
			NaN	hotelling	NaN	NaN	30	6533	NaN
			NaN	roy	0.675456	147.317	10	2181	6.05E-236
		Error	2188		NaN	NaN	NaN	NaN	NaN
		Total	2195		NaN	NaN	NaN	NaN	NaN
3	RIGLconnTo	Bhv State	3	pillai	2.988541	56882.41	30	6543	0
			NaN	wilks	NaN	NaN	30	6396.471	NaN
			NaN	hotelling	NaN	NaN	30	6533	NaN
			NaN	roy	8.460378	1845.208	10	2181	0
		Stim State	1	pillai	0.299912	93.34644	10	2179	9.51E-161
			NaN	wilks	NaN	NaN	10	2179	NaN
			NaN	hotelling	NaN	NaN	10	2179	NaN
			NaN	roy	0.372163	81.09426	10	2179	6.41E-142
		Bhv State:Stim State	3	pillai	Inf	NaN	30	6543	NaN
			NaN	wilks	NaN	NaN	30	6396.471	NaN
			NaN	hotelling	NaN	NaN	30	6533	NaN
			NaN	roy	0.675456	147.317	10	2181	6.05E-236
		Error	2188		NaN	NaN	NaN	NaN	NaN
		Total	2195		NaN	NaN	NaN	NaN	NaN
3	AVFRconnFrom	Bhv State	3	pillai	3.008799	NaN	30	6543	NaN
			NaN	wilks	NaN	NaN	30	6396.471	NaN
			NaN	hotelling	NaN	NaN	30	6533	NaN
			NaN	roy	8.460378	1845.208	10	2181	0
		Stim State	1	pillai	0.047243	10.80469	10	2179	4.02E-18
			NaN	wilks	NaN	NaN	10	2179	NaN
			NaN	hotelling	NaN	NaN	10	2179	NaN
			NaN	roy	0.372163	81.09426	10	2179	6.41E-142
		Bhv State:Stim State	3	pillai	Inf	NaN	30	6543	NaN
			NaN	wilks	NaN	NaN	30	6396.471	NaN
			NaN	hotelling	NaN	NaN	30	6533	NaN
			NaN	roy	Inf	Inf	10	2181	0
		Error	2188		NaN	NaN	NaN	NaN	NaN
		Total	2195		NaN	NaN	NaN	NaN	NaN
3	BAGLconnFrom	Bhv State	3	pillai	3.445535	NaN	30	6543	NaN
			NaN	wilks	NaN	NaN	30	6396.471	NaN
			NaN	hotelling	NaN	NaN	30	6533	NaN
			NaN	roy	8.460378	1845.208	10	2181	0
		Stim State	1	pillai	-2.54424	-156.42	10	2179	1
			NaN	wilks	NaN	NaN	10	2179	NaN
			NaN	hotelling	NaN	NaN	10	2179	NaN

			NaN	roy	0.482507	105.1382	10	2179	3.35E-178
		Bhv State:Stim State	3	pillai	3.99122	NaN	30	6543	NaN
			NaN	wilks	NaN	NaN	30	6396.471	NaN
			NaN	hotelling	NaN	NaN	30	6533	NaN
			NaN	roy	2.552385	556.6751	10	2181	0
		Error	2188		NaN	NaN	NaN	NaN	NaN
		Total	2195		NaN	NaN	NaN	NaN	NaN
3	BAGRconnFrom	Bhv State	3	pillai	3.73884	NaN	30	6543	NaN
			NaN	wilks	NaN	NaN	30	6396.471	NaN
			NaN	hotelling	NaN	NaN	30	6533	NaN
			NaN	roy	8.460378	1845.208	10	2181	0
		Stim State	1	pillai	0.786657	803.4623	10	2179	0
			NaN	wilks	NaN	NaN	10	2179	NaN
			NaN	hotelling	NaN	NaN	10	2179	NaN
			NaN	roy	0.528555	115.1721	10	2179	1.43E-192
		Bhv State:Stim State	3	pillai	1.880698	366.4609	30	6543	0
			NaN	wilks	NaN	NaN	30	6396.471	NaN
			NaN	hotelling	NaN	NaN	30	6533	NaN
			NaN	roy	0.675456	147.317	10	2181	6.05E-236
		Error	2188		NaN	NaN	NaN	NaN	NaN
		Total	2195		NaN	NaN	NaN	NaN	NaN
3	RMEDconnFrom	Bhv State	3	pillai	2.868298	4749.936	30	6543	0
			NaN	wilks	NaN	NaN	30	6396.471	NaN
			NaN	hotelling	NaN	NaN	30	6533	NaN
			NaN	roy	8.460378	1845.208	10	2181	0
		Stim State	1	pillai	-0.81273	-97.6943	10	2179	1
			NaN	wilks	NaN	NaN	10	2179	NaN
			NaN	hotelling	NaN	NaN	10	2179	NaN
			NaN	roy	0.562984	122.6742	10	2179	4.88E-203
		Bhv State:Stim State	3	pillai	0.712167	67.89113	30	6543	0
			NaN	wilks	NaN	NaN	30	6396.471	NaN
			NaN	hotelling	NaN	NaN	30	6533	NaN
			NaN	roy	0.675456	147.317	10	2181	6.05E-236
		Error	2188		NaN	NaN	NaN	NaN	NaN
		Total	2195		NaN	NaN	NaN	NaN	NaN
3	RISconnFrom	Bhv State	3	pillai	5.05797	NaN	30	6543	NaN
			NaN	wilks	NaN	NaN	30	6396.471	NaN
			NaN	hotelling	NaN	NaN	30	6533	NaN
			NaN	roy	8.460378	1845.208	10	2181	0
		Stim State	1	pillai	0.31697	101.1198	10	2179	2.52E-172
			NaN	wilks	NaN	NaN	10	2179	NaN
			NaN	hotelling	NaN	NaN	10	2179	NaN
			NaN	roy	0.372163	81.09426	10	2179	6.41E-142
		Bhv State:Stim State	3	pillai	0.692917	65.50482	30	6543	0
			NaN	wilks	NaN	NaN	30	6396.471	NaN
			NaN	hotelling	NaN	NaN	30	6533	NaN
			NaN	roy	Inf	Inf	10	2181	0
		Error	2188		NaN	NaN	NaN	NaN	NaN
		Total	2195		NaN	NaN	NaN	NaN	NaN
3	RIGLconnFrom	Bhv State	3	pillai	Inf	NaN	30	6543	NaN

			NaN	wilks	NaN	NaN	30	6396.471	NaN
			NaN	hotelling	NaN	NaN	30	6533	NaN
			NaN	roy	Inf	Inf	10	2181	0
		Stim State	1	pillai	0.150116	38.48789	10	2179	3.35E-70
			NaN	wilks	NaN	NaN	10	2179	NaN
			NaN	hotelling	NaN	NaN	10	2179	NaN
			NaN	roy	0.372163	81.09426	10	2179	6.41E-142
		Bhv State:Stim State	3	pillai	1.022565	112.7832	30	6543	0
			NaN	wilks	NaN	NaN	30	6396.471	NaN
			NaN	hotelling	NaN	NaN	30	6533	NaN
			NaN	roy	0.675456	147.317	10	2181	6.05E-236
		Error	2188		NaN	NaN	NaN	NaN	NaN
		Total	2195		NaN	NaN	NaN	NaN	NaN
4	AVFRconnTo	Bhv State	3	pillai	Inf	NaN	30	6006	NaN
			NaN	wilks	NaN	NaN	30	5871.071	NaN
			NaN	hotelling	NaN	NaN	30	5996	NaN
			NaN	roy	Inf	Inf	10	2002	0
		Stim State	1	pillai	0.988793	17645.57	10	2000	0
			NaN	wilks	NaN	NaN	10	2000	NaN
			NaN	hotelling	NaN	NaN	10	2000	NaN
			NaN	roy	0.676766	135.3532	10	2000	3.79E-216
		Bhv State:Stim State	3	pillai	2.261981	613.6004	30	6006	0
			NaN	wilks	NaN	NaN	30	5871.071	NaN
			NaN	hotelling	NaN	NaN	30	5996	NaN
			NaN	roy	Inf	Inf	10	2002	0
		Error	2009		NaN	NaN	NaN	NaN	NaN
		Total	2016		NaN	NaN	NaN	NaN	NaN
4	BAGLconnTo	Bhv State	3	pillai	7.164019	NaN	30	6006	NaN
			NaN	wilks	NaN	NaN	30	5871.071	NaN
			NaN	hotelling	NaN	NaN	30	5996	NaN
			NaN	roy	5.107653	1022.552	10	2002	0
		Stim State	1	pillai	-0.70637	-82.7923	10	2000	1
			NaN	wilks	NaN	NaN	10	2000	NaN
			NaN	hotelling	NaN	NaN	10	2000	NaN
			NaN	roy	1.760714	352.1429	10	2000	0
		Bhv State:Stim State	3	pillai	11.83314	NaN	30	6006	NaN
			NaN	wilks	NaN	NaN	30	5871.071	NaN
			NaN	hotelling	NaN	NaN	30	5996	NaN
			NaN	roy	5.445769	1090.243	10	2002	0
		Error	2009		NaN	NaN	NaN	NaN	NaN
		Total	2016		NaN	NaN	NaN	NaN	NaN
4	BAGRconnTo	Bhv State	3	pillai	0.357376	27.07414	30	6006	2.61E-141
			NaN	wilks	NaN	NaN	30	5871.071	NaN
			NaN	hotelling	NaN	NaN	30	5996	NaN
			NaN	roy	4.981182	997.2327	10	2002	0
		Stim State	1	pillai	-0.42517	-59.6655	10	2000	1
			NaN	wilks	NaN	NaN	10	2000	NaN
			NaN	hotelling	NaN	NaN	10	2000	NaN
			NaN	roy	2.128611	425.7222	10	2000	0
		Bhv State:Stim State	3	pillai	7.432339	NaN	30	6006	NaN

			NaN	wilks	NaN	NaN	30	5871.071	NaN
			NaN	hotelling	NaN	NaN	30	5996	NaN
			NaN	roy	4.64093	929.1142	10	2002	0
		Error	2009		NaN	NaN	NaN	NaN	NaN
		Total	2016		NaN	NaN	NaN	NaN	NaN
4	RMEDconnTo	Bhv State	3	pillai	Inf	NaN	30	6006	NaN
			NaN	wilks	NaN	NaN	30	5871.071	NaN
			NaN	hotelling	NaN	NaN	30	5996	NaN
			NaN	roy	10.8506	2172.291	10	2002	0
		Stim State	1	pillai	1.08889	NaN	10	2000	NaN
			NaN	wilks	NaN	NaN	10	2000	NaN
			NaN	hotelling	NaN	NaN	10	2000	NaN
			NaN	roy	1.288698	257.7397	10	2000	0
		Bhv State:Stim State	3	pillai	Inf	NaN	30	6006	NaN
			NaN	wilks	NaN	NaN	30	5871.071	NaN
			NaN	hotelling	NaN	NaN	30	5996	NaN
			NaN	roy	0.910127	182.2074	10	2002	9.92E-273
		Error	2009		NaN	NaN	NaN	NaN	NaN
		Total	2016		NaN	NaN	NaN	NaN	NaN
4	RISconnTo	Bhv State	3	pillai	Inf	NaN	30	6006	NaN
			NaN	wilks	NaN	NaN	30	5871.071	NaN
			NaN	hotelling	NaN	NaN	30	5996	NaN
			NaN	roy	4.981182	997.2327	10	2002	0
		Stim State	1	pillai	3.640791	NaN	10	2000	NaN
			NaN	wilks	NaN	NaN	10	2000	NaN
			NaN	hotelling	NaN	NaN	10	2000	NaN
			NaN	roy	0.98479	196.958	10	2000	4.94E-289
		Bhv State:Stim State	3	pillai	3.642977	NaN	30	6006	NaN
			NaN	wilks	NaN	NaN	30	5871.071	NaN
			NaN	hotelling	NaN	NaN	30	5996	NaN
			NaN	roy	1.04049	208.306	10	2002	2.59E-301
		Error	2009		NaN	NaN	NaN	NaN	NaN
		Total	2016		NaN	NaN	NaN	NaN	NaN
4	RIGLconnTo	Bhv State	3	pillai	Inf	NaN	30	6006	NaN
			NaN	wilks	NaN	NaN	30	5871.071	NaN
			NaN	hotelling	NaN	NaN	30	5996	NaN
			NaN	roy	4.981182	997.2327	10	2002	0
		Stim State	1	pillai	0.865044	1281.961	10	2000	0
			NaN	wilks	NaN	NaN	10	2000	NaN
			NaN	hotelling	NaN	NaN	10	2000	NaN
			NaN	roy	0.676766	135.3532	10	2000	3.79E-216
		Bhv State:Stim State	3	pillai	-0.11174	-7.18909	30	6006	1
			NaN	wilks	NaN	NaN	30	5871.071	NaN
			NaN	hotelling	NaN	NaN	30	5996	NaN
			NaN	roy	Inf	Inf	10	2002	0
		Error	2009		NaN	NaN	NaN	NaN	NaN
		Total	2016		NaN	NaN	NaN	NaN	NaN
4	AVFRconnFrom	Bhv State	3	pillai	5.097954	NaN	30	6006	NaN
			NaN	wilks	NaN	NaN	30	5871.071	NaN
			NaN	hotelling	NaN	NaN	30	5996	NaN

			NaN	roy	4.981182	997.2327	10	2002	0
		Stim State	1	pillai	0.64557	364.2861	10	2000	0
			NaN	wilks	NaN	NaN	10	2000	NaN
			NaN	hotelling	NaN	NaN	10	2000	NaN
			NaN	roy	0.676766	135.3532	10	2000	3.79E-216
		Bhv State:Stim State	3	pillai	3.702773	NaN	30	6006	NaN
			NaN	wilks	NaN	NaN	30	5871.071	NaN
			NaN	hotelling	NaN	NaN	30	5996	NaN
			NaN	roy	1.381701	276.6166	10	2002	0
		Error	2009		NaN	NaN	NaN	NaN	NaN
		Total	2016		NaN	NaN	NaN	NaN	NaN
4	BAGLconnFrom	Bhv State	3	pillai	21.68129031	NaN	30	6006	NaN
			NaN	wilks	NaN	NaN	30	5871.071	NaN
			NaN	hotelling	NaN	NaN	30	5996	NaN
			NaN	roy	4.981182	997.2327	10	2002	0
		Stim State	1	pillai	0.843296	1076.295	10	2000	0
			NaN	wilks	NaN	NaN	10	2000	NaN
			NaN	hotelling	NaN	NaN	10	2000	NaN
			NaN	roy	0.790001	158.0001	10	2000	2.25E-244
		Bhv State:Stim State	3	pillai	-6.18659	-134.822	30	6006	1
			NaN	wilks	NaN	NaN	30	5871.071	NaN
			NaN	hotelling	NaN	NaN	30	5996	NaN
			NaN	roy	Inf	Inf	10	2002	0
		Error	2009		NaN	NaN	NaN	NaN	NaN
		Total	2016		NaN	NaN	NaN	NaN	NaN
4	BAGRconnFrom	Bhv State	3	pillai	7.688177	NaN	30	6006	NaN
			NaN	wilks	NaN	NaN	30	5871.071	NaN
			NaN	hotelling	NaN	NaN	30	5996	NaN
			NaN	roy	Inf	Inf	10	2002	0
		Stim State	1	pillai	0.093517	20.63281	10	2000	7.67E-37
			NaN	wilks	NaN	NaN	10	2000	NaN
			NaN	hotelling	NaN	NaN	10	2000	NaN
			NaN	roy	2.496726	499.3451	10	2000	0
		Bhv State:Stim State	3	pillai	-7.39599	-142.428	30	6006	1
			NaN	wilks	NaN	NaN	30	5871.071	NaN
			NaN	hotelling	NaN	NaN	30	5996	NaN
			NaN	roy	2.369641	474.4022	10	2002	0
		Error	2009		NaN	NaN	NaN	NaN	NaN
		Total	2016		NaN	NaN	NaN	NaN	NaN
4	RMEDconnFrom	Bhv State	3	pillai	Inf	NaN	30	6006	NaN
			NaN	wilks	NaN	NaN	30	5871.071	NaN
			NaN	hotelling	NaN	NaN	30	5996	NaN
			NaN	roy	5.509721	1103.046	10	2002	0
		Stim State	1	pillai	7.644877	NaN	10	2000	NaN
			NaN	wilks	NaN	NaN	10	2000	NaN
			NaN	hotelling	NaN	NaN	10	2000	NaN
			NaN	roy	0.676766	135.3532	10	2000	3.79E-216
		Bhv State:Stim State	3	pillai	0.981588	97.36066	30	6006	0
			NaN	wilks	NaN	NaN	30	5871.071	NaN
			NaN	hotelling	NaN	NaN	30	5996	NaN

			NaN	roy	3.459415	692.5749	10	2002	0
		Error	2009		NaN	NaN	NaN	NaN	NaN
		Total	2016		NaN	NaN	NaN	NaN	NaN
4	RISconnFrom	Bhv State	3	pillai	13.93709	NaN	30	6006	NaN
			NaN	wilks	NaN	NaN	30	5871.071	NaN
			NaN	hotelling	NaN	NaN	30	5996	NaN
			NaN	roy	Inf	Inf	10	2002	0
		Stim State	1	pillai	2.385488	NaN	10	2000	NaN
			NaN	wilks	NaN	NaN	10	2000	NaN
			NaN	hotelling	NaN	NaN	10	2000	NaN
			NaN	roy	3.586237	717.2475	10	2000	0
		Bhv State:Stim State	3	pillai	Inf	NaN	30	6006	NaN
			NaN	wilks	NaN	NaN	30	5871.071	NaN
			NaN	hotelling	NaN	NaN	30	5996	NaN
			NaN	roy	Inf	Inf	10	2002	0
		Error	2009		NaN	NaN	NaN	NaN	NaN
		Total	2016		NaN	NaN	NaN	NaN	NaN
4	RIGLconnFrom	Bhv State	3	pillai	9.798042	NaN	30	6006	NaN
			NaN	wilks	NaN	NaN	30	5871.071	NaN
			NaN	hotelling	NaN	NaN	30	5996	NaN
			NaN	roy	Inf	Inf	10	2002	0
		Stim State	1	pillai	-0.72977	-84.378	10	2000	1
			NaN	wilks	NaN	NaN	10	2000	NaN
			NaN	hotelling	NaN	NaN	10	2000	NaN
			NaN	roy	2.88145	576.2901	10	2000	0
		Bhv State:Stim State	3	pillai	7.017622	NaN	30	6006	NaN
			NaN	wilks	NaN	NaN	30	5871.071	NaN
			NaN	hotelling	NaN	NaN	30	5996	NaN
			NaN	roy	Inf	Inf	10	2002	0
		Error	2009		NaN	NaN	NaN	NaN	NaN
		Total	2016		NaN	NaN	NaN	NaN	NaN
5	AVFRconnTo	Bhv State	3	pillai	16.99549	NaN	30	6546	NaN
			NaN	wilks	NaN	NaN	30	6399.407	NaN
			NaN	hotelling	NaN	NaN	30	6536	NaN
			NaN	roy	3.002281	655.0977	10	2182	0
		Stim State	1	pillai	5.279827	NaN	10	2180	NaN
			NaN	wilks	NaN	NaN	10	2180	NaN
			NaN	hotelling	NaN	NaN	10	2180	NaN
			NaN	roy	1.383692	301.6448	10	2180	0
		Bhv State:Stim State	3	pillai	Inf	NaN	30	6546	NaN
			NaN	wilks	NaN	NaN	30	6399.407	NaN
			NaN	hotelling	NaN	NaN	30	6536	NaN
			NaN	roy	Inf	Inf	10	2182	0
		Error	2189		NaN	NaN	NaN	NaN	NaN
		Total	2196		NaN	NaN	NaN	NaN	NaN
5	BAGLconnTo	Bhv State	3	pillai	NaN	NaN	30	6546	NaN
			NaN	wilks	NaN	NaN	30	6399.407	NaN
			NaN	hotelling	NaN	NaN	30	6536	NaN
			NaN	roy	30.85556	6732.683	10	2182	0
		Stim State	1	pillai	1.561908	NaN	10	2180	NaN

			NaN	wilks	NaN	NaN	10	2180	NaN
			NaN	hotelling	NaN	NaN	10	2180	NaN
			NaN	roy	1.383692	301.6448	10	2180	0
		Bhv State:Stim State	3	pillai	NaN	NaN	30	6546	NaN
			NaN	wilks	NaN	NaN	30	6399.407	NaN
			NaN	hotelling	NaN	NaN	30	6536	NaN
			NaN	roy	2.869226	626.0652	10	2182	0
		Error	2189		NaN	NaN	NaN	NaN	NaN
		Total	2196		NaN	NaN	NaN	NaN	NaN
5	BAGRconnTo	Bhv State	3	pillai	Inf	NaN	30	6546	NaN
			NaN	wilks	NaN	NaN	30	6399.407	NaN
			NaN	hotelling	NaN	NaN	30	6536	NaN
			NaN	roy	7.105358	1550.389	10	2182	0
		Stim State	1	pillai	1.391508	NaN	10	2180	NaN
			NaN	wilks	NaN	NaN	10	2180	NaN
			NaN	hotelling	NaN	NaN	10	2180	NaN
			NaN	roy	1.383692	301.6448	10	2180	0
		Bhv State:Stim State	3	pillai	9.010978	NaN	30	6546	NaN
			NaN	wilks	NaN	NaN	30	6399.407	NaN
			NaN	hotelling	NaN	NaN	30	6536	NaN
			NaN	roy	1.318831	287.769	10	2182	0
		Error	2189		NaN	NaN	NaN	NaN	NaN
		Total	2196		NaN	NaN	NaN	NaN	NaN
5	RMEDconnTo	Bhv State	3	pillai	-13.4659	-178.445	30	6546	1
			NaN	wilks	NaN	NaN	30	6399.407	NaN
			NaN	hotelling	NaN	NaN	30	6536	NaN
			NaN	roy	3.002269	655.0951	10	2182	0
		Stim State	1	pillai	4.881581	NaN	10	2180	NaN
			NaN	wilks	NaN	NaN	10	2180	NaN
			NaN	hotelling	NaN	NaN	10	2180	NaN
			NaN	roy	2.757386	601.1102	10	2180	0
		Bhv State:Stim State	3	pillai	-Inf	NaN	30	6546	NaN
			NaN	wilks	NaN	NaN	30	6399.407	NaN
			NaN	hotelling	NaN	NaN	30	6536	NaN
			NaN	roy	1.179258	257.3141	10	2182	0
		Error	2189		NaN	NaN	NaN	NaN	NaN
		Total	2196		NaN	NaN	NaN	NaN	NaN
5	RISconnTo	Bhv State	3	pillai	-5.6087	-142.161	30	6546	1
			NaN	wilks	NaN	NaN	30	6399.407	NaN
			NaN	hotelling	NaN	NaN	30	6536	NaN
			NaN	roy	5.696891	1243.062	10	2182	0
		Stim State	1	pillai	0.181777	48.4309	10	2180	7.07E-88
			NaN	wilks	NaN	NaN	10	2180	NaN
			NaN	hotelling	NaN	NaN	10	2180	NaN
			NaN	roy	1.383692	301.6448	10	2180	0
		Bhv State:Stim State	3	pillai	5.731466	NaN	30	6546	NaN
			NaN	wilks	NaN	NaN	30	6399.407	NaN
			NaN	hotelling	NaN	NaN	30	6536	NaN
			NaN	roy	1.179262	257.315	10	2182	0
		Error	2189		NaN	NaN	NaN	NaN	NaN

		Total	2196		NaN	NaN	NaN	NaN	NaN
5	AVFRconnFrom	Bhv State	3	pillai	-15.3432	-182.514	30	6546	1
			NaN	wilks	NaN	NaN	30	6399.407	NaN
			NaN	hotelling	NaN	NaN	30	6536	NaN
			NaN	roy	Inf	Inf	10	2182	0
		Stim State	1	pillai	1.939526	NaN	10	2180	NaN
			NaN	wilks	NaN	NaN	10	2180	NaN
			NaN	hotelling	NaN	NaN	10	2180	NaN
			NaN	roy	2.79325	608.9286	10	2180	0
		Bhv State:Stim State	3	pillai	-4.24803	-127.886	30	6546	1
			NaN	wilks	NaN	NaN	30	6399.407	NaN
			NaN	hotelling	NaN	NaN	30	6536	NaN
			NaN	roy	8.463852	1846.813	10	2182	0
		Error	2189		NaN	NaN	NaN	NaN	NaN
		Total	2196		NaN	NaN	NaN	NaN	NaN
5	BAGLconnFrom	Bhv State	3	pillai	9.916235	NaN	30	6546	NaN
			NaN	wilks	NaN	NaN	30	6399.407	NaN
			NaN	hotelling	NaN	NaN	30	6536	NaN
			NaN	roy	7.223471	1576.161	10	2182	0
		Stim State	1	pillai	2.00242	NaN	10	2180	NaN
			NaN	wilks	NaN	NaN	10	2180	NaN
			NaN	hotelling	NaN	NaN	10	2180	NaN
			NaN	roy	1.683645	367.0347	10	2180	0
		Bhv State:Stim State	3	pillai	8.12102	NaN	30	6546	NaN
			NaN	wilks	NaN	NaN	30	6399.407	NaN
			NaN	hotelling	NaN	NaN	30	6536	NaN
			NaN	roy	1.17926	257.3146	10	2182	0
		Error	2189		NaN	NaN	NaN	NaN	NaN
		Total	2196		NaN	NaN	NaN	NaN	NaN
5	BAGRconnFrom	Bhv State	3	pillai	13.5854	NaN	30	6546	NaN
			NaN	wilks	NaN	NaN	30	6399.407	NaN
			NaN	hotelling	NaN	NaN	30	6536	NaN
			NaN	roy	7.154367	1561.083	10	2182	0
		Stim State	1	pillai	-10.9598	-199.772	10	2180	1
			NaN	wilks	NaN	NaN	10	2180	NaN
			NaN	hotelling	NaN	NaN	10	2180	NaN
			NaN	roy	5.87354	1280.432	10	2180	0
		Bhv State:Stim State	3	pillai	2295.522	NaN	30	6546	NaN
			NaN	wilks	NaN	NaN	30	6399.407	NaN
			NaN	hotelling	NaN	NaN	30	6536	NaN
			NaN	roy	1.17926	257.3145	10	2182	0
		Error	2189		NaN	NaN	NaN	NaN	NaN
		Total	2196		NaN	NaN	NaN	NaN	NaN
5	RMEDconnFrom	Bhv State	3	pillai	Inf	NaN	30	6546	NaN
			NaN	wilks	NaN	NaN	30	6399.407	NaN
			NaN	hotelling	NaN	NaN	30	6536	NaN
			NaN	roy	5.625032	1227.382	10	2182	0
		Stim State	1	pillai	-6.90431	-190.42	10	2180	1
			NaN	wilks	NaN	NaN	10	2180	NaN
			NaN	hotelling	NaN	NaN	10	2180	NaN

			NaN	roy	12.77507	2784.965	10	2180	0
		Bhv State:Stim State	3	pillai	5.238716	NaN	30	6546	NaN
			NaN	wilks	NaN	NaN	30	6399.407	NaN
			NaN	hotelling	NaN	NaN	30	6536	NaN
			NaN	roy	1.702784	371.5475	10	2182	0
		Error	2189		NaN	NaN	NaN	NaN	NaN
		Total	2196		NaN	NaN	NaN	NaN	NaN
5	RISconnFrom	Bhv State	3	pillai	-37.9097	-202.199	30	6546	1
			NaN	wilks	NaN	NaN	30	6399.407	NaN
			NaN	hotelling	NaN	NaN	30	6536	NaN
			NaN	roy	16.89769	3687.076	10	2182	0
		Stim State	1	pillai	7.056771	NaN	10	2180	NaN
			NaN	wilks	NaN	NaN	10	2180	NaN
			NaN	hotelling	NaN	NaN	10	2180	NaN
			NaN	roy	3.337371	727.547	10	2180	0
		Bhv State:Stim State	3	pillai	1.681033	278.0975	30	6546	0
			NaN	wilks	NaN	NaN	30	6399.407	NaN
			NaN	hotelling	NaN	NaN	30	6536	NaN
			NaN	roy	3.333998	727.4783	10	2182	0
		Error	2189		NaN	NaN	NaN	NaN	NaN
		Total	2196		NaN	NaN	NaN	NaN	NaN
6	AVFRconnTo	Bhv State	3	pillai	8.826785	NaN	30	6003	NaN
			NaN	wilks	NaN	NaN	30	5868.136	NaN
			NaN	hotelling	NaN	NaN	30	5993	NaN
			NaN	roy	4.942005	988.8951	10	2001	0
		Stim State	1	pillai	0.741408	573.1339	10	1999	0
			NaN	wilks	NaN	NaN	10	1999	NaN
			NaN	hotelling	NaN	NaN	10	1999	NaN
			NaN	roy	0.919442	183.7964	10	1999	2.06E-274
		Bhv State:Stim State	3	pillai	7.463102	NaN	30	6003	NaN
			NaN	wilks	NaN	NaN	30	5868.136	NaN
			NaN	hotelling	NaN	NaN	30	5993	NaN
			NaN	roy	Inf	Inf	10	2001	0
		Error	2008		NaN	NaN	NaN	NaN	NaN
		Total	2015		NaN	NaN	NaN	NaN	NaN
6	BAGLconnTo	Bhv State	3	pillai	-24.139	-177.981	30	6003	1
			NaN	wilks	NaN	NaN	30	5868.136	NaN
			NaN	hotelling	NaN	NaN	30	5993	NaN
			NaN	roy	5.382651	1077.068	10	2001	0
		Stim State	1	pillai	-6.35067	-172.705	10	1999	1
			NaN	wilks	NaN	NaN	10	1999	NaN
			NaN	hotelling	NaN	NaN	10	1999	NaN
			NaN	roy	3.979493	795.5007	10	1999	0
		Bhv State:Stim State	3	pillai	-34.8366	-184.234	30	6003	1
			NaN	wilks	NaN	NaN	30	5868.136	NaN
			NaN	hotelling	NaN	NaN	30	5993	NaN
			NaN	roy	46.23934	9252.492	10	2001	0
		Error	2008		NaN	NaN	NaN	NaN	NaN
		Total	2015		NaN	NaN	NaN	NaN	NaN
6	BAGRconnTo	Bhv State	3	pillai	8.261621	NaN	30	6003	NaN

			NaN	wilks	NaN	NaN	30	5868.136	NaN
			NaN	hotelling	NaN	NaN	30	5993	NaN
			NaN	roy	Inf	Inf	10	2001	0
		Stim State	1	pillai	-5.85772	-170.75	10	1999	1
			NaN	wilks	NaN	NaN	10	1999	NaN
			NaN	hotelling	NaN	NaN	10	1999	NaN
			NaN	roy	1.177303	235.3428	10	1999	0
		Bhv State:Stim State	3	pillai	-13.7052	-164.165	30	6003	1
			NaN	wilks	NaN	NaN	30	5868.136	NaN
			NaN	hotelling	NaN	NaN	30	5993	NaN
			NaN	roy	6.161402	1232.897	10	2001	0
		Error	2008		NaN	NaN	NaN	NaN	NaN
		Total	2015		NaN	NaN	NaN	NaN	NaN
6	RMEDconnTo	Bhv State	3	pillai	Inf	NaN	30	6003	NaN
			NaN	wilks	NaN	NaN	30	5868.136	NaN
			NaN	hotelling	NaN	NaN	30	5993	NaN
			NaN	roy	3.053005	610.9063	10	2001	0
		Stim State	1	pillai	2.435717	NaN	10	1999	NaN
			NaN	wilks	NaN	NaN	10	1999	NaN
			NaN	hotelling	NaN	NaN	10	1999	NaN
			NaN	roy	0.919442	183.7964	10	1999	2.06E-274
		Bhv State:Stim State	3	pillai	8.408283	NaN	30	6003	NaN
			NaN	wilks	NaN	NaN	30	5868.136	NaN
			NaN	hotelling	NaN	NaN	30	5993	NaN
			NaN	roy	2.084351	417.0786	10	2001	0
		Error	2008		NaN	NaN	NaN	NaN	NaN
		Total	2015		NaN	NaN	NaN	NaN	NaN
6	RISconnTo	Bhv State	3	pillai	-6.91855	-139.577	30	6003	1
			NaN	wilks	NaN	NaN	30	5868.136	NaN
			NaN	hotelling	NaN	NaN	30	5993	NaN
			NaN	roy	3.053005	610.9063	10	2001	0
		Stim State	1	pillai	0.980359	9977.658	10	1999	0
			NaN	wilks	NaN	NaN	10	1999	NaN
			NaN	hotelling	NaN	NaN	10	1999	NaN
			NaN	roy	0.92788	185.4832	10	1999	2.61E-276
		Bhv State:Stim State	3	pillai	-40.1053	-186.174	30	6003	1
			NaN	wilks	NaN	NaN	30	5868.136	NaN
			NaN	hotelling	NaN	NaN	30	5993	NaN
			NaN	roy	Inf	Inf	10	2001	0
		Error	2008		NaN	NaN	NaN	NaN	NaN
		Total	2015		NaN	NaN	NaN	NaN	NaN
6	RIGLconnTo	Bhv State	3	pillai	Inf	NaN	30	6003	NaN
			NaN	wilks	NaN	NaN	30	5868.136	NaN
			NaN	hotelling	NaN	NaN	30	5993	NaN
			NaN	roy	3.053005	610.9063	10	2001	0
		Stim State	1	pillai	1.088109	NaN	10	1999	NaN
			NaN	wilks	NaN	NaN	10	1999	NaN
			NaN	hotelling	NaN	NaN	10	1999	NaN
			NaN	roy	0.919442	183.7964	10	1999	2.06E-274
		Bhv State:Stim State	3	pillai	2.874338	4576.982	30	6003	0

			NaN	wilks	NaN	NaN	30	5868.136	NaN
			NaN	hotelling	NaN	NaN	30	5993	NaN
			NaN	roy	Inf	Inf	10	2001	0
		Error	2008		NaN	NaN	NaN	NaN	NaN
		Total	2015		NaN	NaN	NaN	NaN	NaN
6	AVFRconnFrom	Bhv State	3	pillai	18.95035	NaN	30	6003	NaN
			NaN	wilks	NaN	NaN	30	5868.136	NaN
			NaN	hotelling	NaN	NaN	30	5993	NaN
			NaN	roy	3.053005	610.9063	10	2001	0
		Stim State	1	pillai	1.945632	NaN	10	1999	NaN
			NaN	wilks	NaN	NaN	10	1999	NaN
			NaN	hotelling	NaN	NaN	10	1999	NaN
			NaN	roy	0.919442	183.7964	10	1999	2.06E-274
		Bhv State:Stim State	3	pillai	-Inf	NaN	30	6003	NaN
			NaN	wilks	NaN	NaN	30	5868.136	NaN
			NaN	hotelling	NaN	NaN	30	5993	NaN
			NaN	roy	3.770027	754.3823	10	2001	0
		Error	2008		NaN	NaN	NaN	NaN	NaN
		Total	2015		NaN	NaN	NaN	NaN	NaN
6	BAGLconnFrom	Bhv State	3	pillai	Inf	NaN	30	6003	NaN
			NaN	wilks	NaN	NaN	30	5868.136	NaN
			NaN	hotelling	NaN	NaN	30	5993	NaN
			NaN	roy	Inf	Inf	10	2001	0
		Stim State	1	pillai	-16.6902	-188.6	10	1999	1
			NaN	wilks	NaN	NaN	10	1999	NaN
			NaN	hotelling	NaN	NaN	10	1999	NaN
			NaN	roy	10.5508	2109.104	10	1999	0
		Bhv State:Stim State	3	pillai	-1.17146	-56.1934	30	6003	1
			NaN	wilks	NaN	NaN	30	5868.136	NaN
			NaN	hotelling	NaN	NaN	30	5993	NaN
			NaN	roy	18.65075	3732.015	10	2001	0
		Error	2008		NaN	NaN	NaN	NaN	NaN
		Total	2015		NaN	NaN	NaN	NaN	NaN
6	BAGRconnFrom	Bhv State	3	pillai	-7.66123	-143.793	30	6003	1
			NaN	wilks	NaN	NaN	30	5868.136	NaN
			NaN	hotelling	NaN	NaN	30	5993	NaN
			NaN	roy	19.15906	3833.727	10	2001	0
		Stim State	1	pillai	-1.76815	-127.686	10	1999	1
			NaN	wilks	NaN	NaN	10	1999	NaN
			NaN	hotelling	NaN	NaN	10	1999	NaN
			NaN	roy	2.970505	593.804	10	1999	0
		Bhv State:Stim State	3	pillai	33.32944	NaN	30	6003	NaN
			NaN	wilks	NaN	NaN	30	5868.136	NaN
			NaN	hotelling	NaN	NaN	30	5993	NaN
			NaN	roy	77.37948	15483.63	10	2001	0
		Error	2008		NaN	NaN	NaN	NaN	NaN
		Total	2015		NaN	NaN	NaN	NaN	NaN
6	RMEDconnFrom	Bhv State	3	pillai	14.45374	NaN	30	6003	NaN
			NaN	wilks	NaN	NaN	30	5868.136	NaN
			NaN	hotelling	NaN	NaN	30	5993	NaN

			NaN	roy	Inf	Inf	10	2001	0
		Stim State	1	pillai	0.845385	1092.993	10	1999	0
			NaN	wilks	NaN	NaN	10	1999	NaN
			NaN	hotelling	NaN	NaN	10	1999	NaN
			NaN	roy	4.581661	915.8741	10	1999	0
		Bhv State:Stim State	3	pillai	8.753248	NaN	30	6003	NaN
			NaN	wilks	NaN	NaN	30	5868.136	NaN
			NaN	hotelling	NaN	NaN	30	5993	NaN
			NaN	roy	Inf	Inf	10	2001	0
		Error	2008		NaN	NaN	NaN	NaN	NaN
		Total	2015		NaN	NaN	NaN	NaN	NaN
6	RISconnFrom	Bhv State	3	pillai	Inf	NaN	30	6003	NaN
			NaN	wilks	NaN	NaN	30	5868.136	NaN
			NaN	hotelling	NaN	NaN	30	5993	NaN
			NaN	roy	Inf	Inf	10	2001	0
		Stim State	1	pillai	0.067012	14.35791	10	1999	6.97E-25
			NaN	wilks	NaN	NaN	10	1999	NaN
			NaN	hotelling	NaN	NaN	10	1999	NaN
			NaN	roy	0.919442	183.7964	10	1999	2.06E-274
		Bhv State:Stim State	3	pillai	689.0754	NaN	30	6003	NaN
			NaN	wilks	NaN	NaN	30	5868.136	NaN
			NaN	hotelling	NaN	NaN	30	5993	NaN
			NaN	roy	Inf	Inf	10	2001	0
		Error	2008		NaN	NaN	NaN	NaN	NaN
		Total	2015		NaN	NaN	NaN	NaN	NaN
6	RIGLconnFrom	Bhv State	3	pillai	15.97938	NaN	30	6003	NaN
			NaN	wilks	NaN	NaN	30	5868.136	NaN
			NaN	hotelling	NaN	NaN	30	5993	NaN
			NaN	roy	3.053005	610.9063	10	2001	0
		Stim State	1	pillai	-0.53597	-69.7545	10	1999	1
			NaN	wilks	NaN	NaN	10	1999	NaN
			NaN	hotelling	NaN	NaN	10	1999	NaN
			NaN	roy	0.919442	183.7964	10	1999	2.06E-274
		Bhv State:Stim State	3	pillai	37.41194	NaN	30	6003	NaN
			NaN	wilks	NaN	NaN	30	5868.136	NaN
			NaN	hotelling	NaN	NaN	30	5993	NaN
			NaN	roy	6.492054	1299.06	10	2001	0
		Error	2008		NaN	NaN	NaN	NaN	NaN
		Total	2015		NaN	NaN	NaN	NaN	NaN
7	AVFRconnTo	Bhv State	3	pillai	Inf	NaN	30	6009	NaN
			NaN	wilks	NaN	NaN	30	5874.006	NaN
			NaN	hotelling	NaN	NaN	30	5999	NaN
			NaN	roy	Inf	Inf	10	2003	0
		Stim State	1	pillai	-0.01671	-3.28846	10	2001	1
			NaN	wilks	NaN	NaN	10	2001	NaN
			NaN	hotelling	NaN	NaN	10	2001	NaN
			NaN	roy	0.877247	175.5371	10	2001	4.44E-265
		Bhv State:Stim State	3	pillai	0.675101	58.16286	30	6009	1.13E-304
			NaN	wilks	NaN	NaN	30	5874.006	NaN
			NaN	hotelling	NaN	NaN	30	5999	NaN

			NaN	roy	1.859382	372.4343	10	2003	0
		Error	2010		NaN	NaN	NaN	NaN	NaN
		Total	2017		NaN	NaN	NaN	NaN	NaN
7	BAGLconnTo	Bhv State	3	pillai	30.08855	NaN	30	6009	NaN
			NaN	wilks	NaN	NaN	30	5874.006	NaN
			NaN	hotelling	NaN	NaN	30	5999	NaN
			NaN	roy	8.483433	1699.232	10	2003	0
		Stim State	1	pillai	-2.19332	-137.438	10	2001	1
			NaN	wilks	NaN	NaN	10	2001	NaN
			NaN	hotelling	NaN	NaN	10	2001	NaN
			NaN	roy	0.888936	177.8761	10	2001	9.17E-268
		Bhv State:Stim State	3	pillai	5.035505	NaN	30	6009	NaN
			NaN	wilks	NaN	NaN	30	5874.006	NaN
			NaN	hotelling	NaN	NaN	30	5999	NaN
			NaN	roy	1.112134	222.7604	10	2003	2.020790200289
		Error	2010		NaN	NaN	NaN	NaN	NaN
		Total	2017		NaN	NaN	NaN	NaN	NaN
7	BAGRconnTo	Bhv State	3	pillai	Inf	NaN	30	6009	NaN
			NaN	wilks	NaN	NaN	30	5874.006	NaN
			NaN	hotelling	NaN	NaN	30	5999	NaN
			NaN	roy	Inf	Inf	10	2003	0
		Stim State	1	pillai	0.100571	22.37439	10	2001	3.93E-40
			NaN	wilks	NaN	NaN	10	2001	NaN
			NaN	hotelling	NaN	NaN	10	2001	NaN
			NaN	roy	0.877247	175.5371	10	2001	4.44E-265
		Bhv State:Stim State	3	pillai	2.935479	9112.973	30	6009	0
			NaN	wilks	NaN	NaN	30	5874.006	NaN
			NaN	hotelling	NaN	NaN	30	5999	NaN
			NaN	roy	1.016636	203.6322	10	2003	2.26E-296
		Error	2010		NaN	NaN	NaN	NaN	NaN
		Total	2017		NaN	NaN	NaN	NaN	NaN
7	RMEDconnTo	Bhv State	3	pillai	9.720703	NaN	30	6009	NaN
			NaN	wilks	NaN	NaN	30	5874.006	NaN
			NaN	hotelling	NaN	NaN	30	5999	NaN
			NaN	roy	Inf	Inf	10	2003	0
		Stim State	1	pillai	-0.1848	-31.211	10	2001	1
			NaN	wilks	NaN	NaN	10	2001	NaN
			NaN	hotelling	NaN	NaN	10	2001	NaN
			NaN	roy	0.877247	175.5371	10	2001	4.44E-265
		Bhv State:Stim State	3	pillai	Inf	NaN	30	6009	NaN
			NaN	wilks	NaN	NaN	30	5874.006	NaN
			NaN	hotelling	NaN	NaN	30	5999	NaN
			NaN	roy	Inf	Inf	10	2003	0
		Error	2010		NaN	NaN	NaN	NaN	NaN
		Total	2017		NaN	NaN	NaN	NaN	NaN
7	AVFRconnFrom	Bhv State	3	pillai	21.77719	NaN	30	6009	NaN
			NaN	wilks	NaN	NaN	30	5874.006	NaN
			NaN	hotelling	NaN	NaN	30	5999	NaN
			NaN	roy	Inf	Inf	10	2003	0
		Stim State	1	pillai	0.868348	1319.819	10	2001	0

			NaN	wilks	NaN	NaN	10	2001	NaN
			NaN	hotelling	NaN	NaN	10	2001	NaN
			NaN	roy	0.877247	175.5371	10	2001	4.44E-265
		Bhv State:Stim State	3	pillai	Inf	NaN	30	6009	NaN
			NaN	wilks	NaN	NaN	30	5874.006	NaN
			NaN	hotelling	NaN	NaN	30	5999	NaN
			NaN	roy	Inf	Inf	10	2003	0
		Error	2010		NaN	NaN	NaN	NaN	NaN
		Total	2017		NaN	NaN	NaN	NaN	NaN
7	BAGLconnFrom	Bhv State	3	pillai	7.398395	NaN	30	6009	NaN
			NaN	wilks	NaN	NaN	30	5874.006	NaN
			NaN	hotelling	NaN	NaN	30	5999	NaN
			NaN	roy	14.16715	2837.679	10	2003	0
		Stim State	1	pillai	-1.01454	-100.772	10	2001	1
			NaN	wilks	NaN	NaN	10	2001	NaN
			NaN	hotelling	NaN	NaN	10	2001	NaN
			NaN	roy	0.877247	175.5371	10	2001	4.44E-265
		Bhv State:Stim State	3	pillai	4.812528	NaN	30	6009	NaN
			NaN	wilks	NaN	NaN	30	5874.006	NaN
			NaN	hotelling	NaN	NaN	30	5999	NaN
			NaN	roy	Inf	Inf	10	2003	0
		Error	2010		NaN	NaN	NaN	NaN	NaN
		Total	2017		NaN	NaN	NaN	NaN	NaN
7	BAGRconnFrom	Bhv State	3	pillai	Inf	NaN	30	6009	NaN
			NaN	wilks	NaN	NaN	30	5874.006	NaN
			NaN	hotelling	NaN	NaN	30	5999	NaN
			NaN	roy	Inf	Inf	10	2003	0
		Stim State	1	pillai	0.500317	200.3539	10	2001	9.28E-293
			NaN	wilks	NaN	NaN	10	2001	NaN
			NaN	hotelling	NaN	NaN	10	2001	NaN
			NaN	roy	1.339435	268.0209	10	2001	0
		Bhv State:Stim State	3	pillai	-0.7837	-41.4874	30	6009	1
			NaN	wilks	NaN	NaN	30	5874.006	NaN
			NaN	hotelling	NaN	NaN	30	5999	NaN
			NaN	roy	9.657142	1934.325	10	2003	0
		Error	2010		NaN	NaN	NaN	NaN	NaN
		Total	2017		NaN	NaN	NaN	NaN	NaN
7	RMEDconnFrom	Bhv State	3	pillai	8.534169	NaN	30	6009	NaN
			NaN	wilks	NaN	NaN	30	5874.006	NaN
			NaN	hotelling	NaN	NaN	30	5999	NaN
			NaN	roy	9.593546	1921.587	10	2003	0
		Stim State	1	pillai	0.013388	2.715372	10	2001	0.002581
			NaN	wilks	NaN	NaN	10	2001	NaN
			NaN	hotelling	NaN	NaN	10	2001	NaN
			NaN	roy	1.013987	202.8988	10	2001	1.68E-295
		Bhv State:Stim State	3	pillai	980.8036	NaN	30	6009	NaN
			NaN	wilks	NaN	NaN	30	5874.006	NaN
			NaN	hotelling	NaN	NaN	30	5999	NaN
			NaN	roy	1.016636	203.6322	10	2003	2.26E-296
		Error	2010		NaN	NaN	NaN	NaN	NaN

Total	2017	NaN	NaN	NaN	NaN	NaN

Table 7: **MANOVA tests for AVFR, BAGL, BAGR, RIGL, RIS, RMED, and SABD activity and connectivity vs. behavior and oxygen stimulation factor levels**. Glossary: [neuron]connFrom: strongest connectivity value (absolute value) from that neuron, [neuron]connTo: strongest connectivity value to that neuron, Bhv: behavior states (1-4), Stim: stim states (21 percent oxygen only first half trial, or alternating oxygen levels second half), Bhv:Stim: Behavior: Stimulus interaction term, df: degrees of freedom, test stat: test statistic, value: value of test statistic, F: corresponding F value, dfN: degrees of freedom of numerator, dfD: degrees of freedom of denominator, p: p-value.

6.8 RMED dynamic connectivity tally

Table 8 is a tally of strong connectivity with or activity in RMED across the worms' dynamic connectivity maps for each DO.

RMED was utilized in 22/31 forward crawling DOs and during forward crawling in 6/7 Stim worms, but only in 4/36 reverse sustained crawling DOs and during reverse sustained crawling in 3/7 worms (Supplementary Figs. 27, 30, Table 8). RMED-featuring DOs were not at all present in the small number of DOs exclusively active in the first half of the experiments and were present in DOs exclusively active in the second half in 4/7 worms, but otherwise they were utilized in a more balanced way between halves of the experiment (Supplementary Figs. 16, 19, 21, 24). Notably, this relationship between RMED and forward crawling was even stronger in the NoStim worms, which were not exposed to hypoxia. It would seem that RMED should have shown the opposite bias (toward the first half of the Stim experiment) if its nonstationarity were being affected by the oxygenation levels; this observed bias toward the second half of the experiment could be a result of the corresponding bias in the base rates of the forward crawling state(s).

subset	per-worm DOs	worms	aligned DOs	worms
Stim FWD	22/31	6/7	35/46	7/7
Stim REVSUS	4/36	3/7	8/54	3/7
Stim only 1st half	0/3	0/7	1/6	1/7
Stim mostly 1st half	3/11	2/7	4/8	2/7
Stim mostly 2nd half	4/8	2/7	6/9	3/7
Stim only 2nd half	8/9	4/7	12/20	7/7
Stim sign flip between halves	2/3	2/7	0/1	0/7
NoStim FWD	17/21	5/5		
NoStim SLOW	20/27	5/5		
NoStim REVSUS	3/23	3/5		

Table 8: **Tally of RMED presence in dynamic connectivity maps across conditions.**

References

[1] Steven W. Flavell and Andrew Gordus. Dynamic functional connectivity in the static connectome of Caenorhabditis elegans, 4 2022. doi:10.1016/j.conb.2021.12.002.

[2] Shreya Saxena and John P Cunningham. Towards the neural population doctrine. *Current opinion in neurobiology*, 55:103–111, 2019.

[3] Saul Kato, Harris S. Kaplan, Tina Schrödel, Susanne Skora, Theodore H. Lindsay, Eviatar Yemini, Shawn Lockery, and Manuel Zimmer. Global Brain Dynamics Embed the Motor Command Sequence of Caenorhabditis elegans. *Cell*, 163(3):656–669, 2015. doi:10.1016/j.cell.2015.09.034.

[4] Eleni Gourgou, Kavya Adiga, Anne Goettemoeller, Chieh Chen, and Ao Lin Hsu. Caenorhabditis elegans learning in a structured maze is a multisensory behavior. *iScience*, 24, 4 2021. doi:10.1016/j.isci.2021.102284.

[5] Manuel Zimmer, Jesse M. Gray, Navin Pokala, Andy J. Chang, David S. Karow, Michael A. Marletta, Martin L. Hudson, David B. Morton, Nikos Chronis, and Cornelia I. Bargmann. Neurons detect increases and decreases in oxygen levels using distinct guanylate cyclases. *Neuron*, 61:865–879, 3 2009. doi:10.1016/j.neuron.2009.02.013.

[6] Geneva M. Stein and Coleen T. Murphy. C. elegans positive olfactory associative memory is a molecularly conserved behavioral paradigm. *Neurobiology of Learning and Memory*, 115:86–94, 11 2014. doi:10.1016/j.nlm.2014.07.011.

[7] Neuronal Wiring. URL: https://www.wormatlas.org/neuronalwiring.html#NeuronalconnectivityII.

[8] J. G. White, E. Southgate, J. N. Thomson, and S. Brenner. The structure of the nervous system of the nematode Caenorhabditis elegans. *Philosophical Transactions of the Royal Society of London*, 314, 1986. URL: https://royalsocietypublishing.org/.

[9] Steven J. Cook, Travis A. Jarrell, Christopher A. Brittin, Yi Wang, Adam E. Bloniarz, Maksim A. Yakovlev, Ken C.Q. Nguyen, Leo T.H. Tang, Emily A. Bayer, Janet S. Duerr, Hannes E. Bülow, Oliver Hobert, David H. Hall, and Scott W. Emmons. Whole-animal connectomes of both Caenorhabditis elegans sexes. *Nature*, 571:63–71, 7 2019. doi:10.1038/s41586-019-1352-7.

[10] Daniel Witvliet, Ben Mulcahy, James K. Mitchell, Yaron Meirovitch, Daniel R. Berger, Yuelong Wu, Yufang Liu, Wan Xian Koh, Rajeev Parvathala, Douglas Holmyard, Richard L. Schalek, Nir Shavit, Andrew D. Chisholm, Jeff W. Lichtman, Aravinthan D.T. Samuel, and Mei Zhen. Connectomes across development reveal principles of brain maturation. *Nature*, 596:257–261, 8 2021. doi:10.1038/s41586-021-03778-8.

[11] Francesco Randi, Anuj K. Sharma, Sophie Dvali, and Andrew M. Leifer. Neural signal propagation atlas of Caenorhabditis elegans. *Nature*, 623:406–414, 11 2023. doi:10.1038/s41586-023-06683-4.

[12] Reemy Ali Nasser, Yuval Harel, and Shay Stern. Early-life experience reorganizes neuromodulatory regulation of stage-specific behavioral responses and individuality dimensions during development. *eLife*, 12, 5 2023. doi:10.7554/eLife.84312.

[13] Shay Stern, Christoph Kirst, and Cornelia I. Bargmann. Neuromodulatory control of long-term behavioral patterns and individuality across development. *Cell*, 171:1649–1662.e10, 12 2017. doi:10.1016/j.cell.2017.10.041.

[14] Connor Brennan and Alexander Proekt. A quantitative model of conserved macroscopic dynamics predicts future motor commands. 2019. doi:10.7554/eLife.46814.001.

[15] Isabel Beets, Sven Zels, Elke Vandewyer, Jonas Demeulemeester, Jelle Caers, Esra Baytemur, William R Schafer, Petra E Vértes, Olivier Mirabeau, and Liliane Schoofs. System-wide mapping of neuropeptide-gpcr interactions in C. elegans. *bioRxiv*, 2022. doi:10.1101/2022.10.30.514428.

[16] Lidia Ripoll-Sánchez, Jan Watteyne, Haosheng Sun, Robert Fernandez, Seth R Taylor, Alexis Weinreb, Mark Hammarlund, David M Miller Iii, Oliver Hobert, Isabel Beets, Petra E Vértes, and William R Schafer. The neuropeptidergic connectome of C. elegans. *bioRxiv*, page 2022.10.30.514396, 11 2022. URL: https://www.biorxiv.org/content/10.1101/2022.10.30.514396v2https://www.biorxiv.org/content/10.1101/2022.10.30.514396v2.abstract, doi:10.1101/2022.10.30.514396.

[17] Keertana Venkatesh, Lidia Ripoll-Sánchez, Isabel Beets, and William R Schafer. C. elegans wired and wireless connectome: insights into principles of nervous system structure and function. *Journal of Biosciences*, 50:16, 3 2025. URL: https://link.springer.com/10.1007/s12038-025-00513-7, doi:10.1007/s12038-025-00513-7.

[18] Theodore H. Lindsay, Tod R. Thiele, and Shawn R. Lockery. Optogenetic analysis of synaptic transmission in the central nervous system of the nematode Caenorhabditis elegans. *Nature Communications*, 2, 2011. doi:10.1038/ncomms1304.

[19] Jingyuan Jiang, Yifan Su, Ruilin Zhang, Haiwen Li, Louis Tao, and Qiang Liu. C. elegans enteric motor neurons fire synchronized action potentials underlying the defecation motor program. *Nature Communications*, 13, 12 2022. doi:10.1038/s41467-022-30452-y.

[20] Han Wang, Kelly Girskis, Tom Janssen, Jason P. Chan, Krishnakali Dasgupta, James A. Knowles, Liliane Schoofs, and Derek Sieburth. Neuropeptide secreted from a pacemaker activates neurons to control a rhythmic behavior. *Current Biology*, 23:746–754, 5 2013. doi:10.1016/j.cub.2013.03.049.

[21] Dennis H. Kim and Steven W. Flavell. Host-microbe interactions and the behavior of Caenorhabditis elegans, 2020. doi:10.1080/01677063.2020.1802724.

[22] Kelsey M. Hallinen, Ross Dempsey, Monika Scholz, Xinwei Yu, Ashley Linder, Francesco Randi, Anuj Sharma, Joshua W. Shaevitz, and Andrew M. Leifer. Decoding locomotion from population neural activity in moving c. elegans. *eLife*, 10, 7 2021. doi:10.7554/eLife.66135.

[23] Adam A. Atanas, Jungsoo Kim, Ziyu Wang, Eric Bueno, McCoy Becker, Di Kang, Jungyeon Park, Talya S. Kramer, Flossie K. Wan, Saba Baskoylu, Ugur Dag, Elpiniki Kalogeropoulou, Matthew A. Gomes, Cassi Estrem, Netta Cohen, Vikash K. Mansinghka, and Steven W. Flavell. Brain-wide representations of behavior spanning multiple timescales and states in C. elegans. *Cell*, 8 2023. URL: https://linkinghub.elsevier.com/retrieve/pii/S0092867423008504, doi:10.1016/j.cell.2023.07.035.

[24] Ni Ji, Gurrein K Madan, Guadalupe I Fabre, Alyssa Dayan, Casey M Baker, Talya S Kramer, Ijeoma Nwabudike, and Steven W Flavell. A neural circuit for flexible control of persistent behavioral states, 2021.

[25] Julia Riedl, Charles Fieseler, and Manuel Zimmer. Tyraminergic corollary discharge filters reafferent perception in a chemosensory neuron. *Current Biology*, 32:3048–3058.e6, 7 2022. doi:10.1016/j.cub.2022.05.051.

[26] Sandeep Kumar, Anuj K. Sharma, and Andrew M. Leifer. An inhibitory acetylcholine receptor gates context dependent mechanosensory processing in C. elegans. *iScience*, page 110776, 10 2024. doi:10.1016/j.isci.2024.110776.

[27] Munzareen Khan, Anna H. Hartmann, Michael P. O'Donnell, Madeline Piccione, Pin-Hao Chao, Noelle D. Dwyer, Cornelia I. Bargmann, and Piali Sengupta. Context-dependent inversion of the response in a single sensory neuron type reverses olfactory preference behavior, 11 2021. URL: http://biorxiv.org/lookup/doi/10.1101/2021.11.08.467792, doi:10.1101/2021.11.08.467792.

[28] Vladislav Susoy, Wesley Hung, Daniel Witvliet, Joshua E. Whitener, Min Wu, Core Francisco Park, Brett J. Graham, Mei Zhen, Vivek Venkatachalam, and Aravinthan D.T. Samuel. Natural sensory context drives diverse brain-wide activity during c. elegans mating. *Cell*, 184:5122–5137.e17, 9 2021. doi:10.1016/j.cell.2021.08.024.

[29] Steven W. Flavell, David M. Raizen, and Young Jai You. Behavioral states, 10 2020. doi:10.1534/genetics.120.303539.

[30] Catharine H Rankin and Brett S Broster. Factors affecting habituation and recovery from habituation in the nematode Caenorhabditis elegans, 1992.

[31] Aelon Rahmani and Yee Lian Chew. Investigating the molecular mechanisms of learning and memory using Caenorhabditis elegans, 11 2021. doi:10.1111/jnc.15510.

[32] Catherine H Rankin, Christine D O Beck, Catherine M Chiba, and C H Rankin. Caenorhabditis elegans: a new model system for the study of learning and memory, 1990.

[33] J. K. Rose and C. H. Rankin. Analyses of habituation in Caenorhabditis elegans, 2001. doi:10.1101/lm.37801.

[34] Evan L. Ardiel and Catharine H. Rankin. An elegant mind: Learning and memory in Caenorhabditis elegans, 4 2010. doi:10.1101/lm.960510.

[35] Kerem Uzel, Saul Kato, and Manuel Zimmer. A set of hub neurons and non-local connectivity features support global brain dynamics in C. elegans. *Current Biology*, 32:3443–3459.e8, 8 2022. doi:10.1016/J.CUB.2022.06.039.

[36] Charles Fieseler, Itamar Lev, Ulises Rey, Lukas Hille, Hannah Brenner, and Manuel Zimmer. An intrinsic neuronal manifold underlies brain-wide hierarchical organization of behavior in c. elegans, 3 2025. URL: http://biorxiv.org/lookup/doi/10.1101/2025.03.09.642241, doi:10.1101/2025.03.09.642241.

[37] Scott W. Linderman, Annika L. A. Nichols, David M. Blei, Manuel Zimmer, and Liam Paninski. Hierarchical recurrent state space models reveal discrete and continuous dynamics of neural activity in C. elegans. *bioRxiv*, page 621540, 2019. URL: https://www.biorxiv.org/content/10.1101/621540v1.abstract?%3Fcollection=, doi:10.1101/621540.

[38] Antonio C. Costa, Tosif Ahamed, and Greg J. Stephens. Adaptive, locally linear models of complex dynamics. *Proceedings of the National Academy of Sciences of the United States of America*, 116:1501–1510, 1 2019. doi:10.1073/pnas.1813476116.

[39] Francesco Randi and Andrew M. Leifer. Measuring and modeling whole-brain neural dynamics in Caenorhabditis elegans. *Current Opinion in Neurobiology*, 65:167–175, 12 2020. doi:10.1016/j.conb.2020.11.001.

[40] Bingni W. Brunton, Lise A. Johnson, Jeffrey G. Ojemann, and J. Nathan Kutz. Extracting spatial-temporal coherent patterns in large-scale neural recordings using dynamic mode decomposition. *Journal of Neuroscience Methods*, 258:1–15, 1 2016. doi:10.1016/j.jneumeth.2015.10.010.

[41] Matthew S. Creamer, Andrew M. Leifer, and Jonathan W. Pillow. Bridging the gap between the connectome and whole-brain activity in c. elegans, 9 2024. URL: http://biorxiv.org/lookup/doi/10.1101/2024.09.22.614271, doi:10.1101/2024.09.22.614271.

[42] Noga Mudrik, Yenho Chen, Eva Yezerets, Christopher J Rozell, and Adam S Charles. Decomposed linear dynamical systems (dlds) for learning the latent components of neural dynamics. *Journal of Machine Learning Research*, 25(59):1–44, 2024.

[43] Jiaming Ji, Tianyi Qiu, Boyuan Chen, Borong Zhang, Hantao Lou, Kaile Wang, Yawen Duan, Zhonghao He, Jiayi Zhou, Zhaowei Zhang, Fanzhi Zeng, Kwan Yee Ng, Juntao Dai, Xuehai Pan, Aidan O'Gara, Yingshan Lei, Hua Xu, Brian Tse, Jie Fu, Stephen McAleer, Yaodong Yang, Yizhou Wang, Song-Chun Zhu, Yike Guo, and Wen Gao. Ai alignment: A comprehensive survey. 10 2023. URL: http://arxiv.org/abs/2310.19852.

[44] Z. Altun. WormAtlas individual neurons, 2014. URL: https://www.wormatlas.org/neurons/Individual%20Neurons/Neuronframeset.html.

[45] Annika L.A. Nichols, Tomáš Eichler, Richard Latham, and Manuel Zimmer. A global brain state underlies c. elegans sleep behavior. *Science*, 356:1247–1256, 2017. doi:10.1126/science.aam6851.

[46] Yu Shen, Quan Wen, He Liu, Connie Zhong, Yuqi Qin, Gareth Harris, Taizo Kawano, Min Wu, Tianqi Xu, Aravinthan DT Samuel, and Yun Zhang. An extrasynaptic gabaergic signal modulates a pattern of forward movement in Caenorhabditis elegans. 2016. doi:10.7554/eLife.14197.001.

[47] Kaeser M. Sabrin, Yongbin Wei, Martijn Pieter van den Heuvel, and Constantine Dovrolis. The hourglass organization of the Caenorhabditis elegans connectome. *PLoS Computational Biology*, 16, 2020. doi:10.1371/journal.pcbi.1007526.

[48] Kevin M. Anderson, Meghan A. Collins, Rowena Chin, Tian Ge, Monica D. Rosenberg, and Avram J. Holmes. Transcriptional and imaging-genetic association of cortical interneurons, brain function, and schizophrenia risk. *Nature Communications*, 11, 12 2020. doi:10.1038/s41467-020-16710-x.

[49] Manuel Zimmer. Kato2015 whole brain imaging data, January 2021. URL: osf.io/2395t, doi:10.17605/OSF.IO/2395T.

[50] Scott Linderman, Benjamin Antin, David Zoltowski, and Joshua Glaser. SSM: Bayesian Learning and Inference for State Space Models (version 0.0.1, 10 2020. URL: https://github.com/lindermanlab/ssm.

[51] Paul Kassebaum. circularGraph. GitHub, 2025. URL: https://www.mathworks.com/matlabcentral/fileexchange/48576-circulargraph.

[52] Peder Axensten. chi2test, 2007. URL: https://www.mathworks.com/matlabcentral/fileexchange/16177-chi2test.

[53] Analysis of variance (ANOVA) results - MATLAB. URL: https://www.mathworks.com/help/stats/anova.html.

[54] Multivariate analysis of variance (MANOVA) results - MATLAB. URL: https://www.mathworks.com/help/stats/manova.html.